Epigenetic control of O-antigen length in *Salmonella enterica*

Memoria elaborada por Ignacio Cota García para optar al grado de Doctor en Biología

Tesis realizada bajo la dirección del Dr. Josep Casadesús Pursals en el Departamento de Genética de la Facultad de Biología de la Universidad de Sevilla

Josep Casadesús Pursals

Ignacio Cota García

Sevilla, 12 de enero de 2016

INDEX

RESUMEN

El locus *STM2209-STM2208* (*opvAB*) es exclusivo de *Salmonella enterica* y presenta características típicas de genes adquiridos por transferencia horizontal. Fue descrito inicialmente como un locus reprimido por metilación Dam. Sin embargo, durante el desarrollo de esta tesis se ha establecido que la metilación Dam no reprime simplemente la expresión de *opvAB*, sino que forma parte de un mecanismo complejo de regulación que da lugar a dos subpoblaciones genéticamente iguales pero con distinto nivel de expresión de *opvAB*. Otro factor fundamental para la formación de estas subpoblaciones es OxyR, un factor de transcripción de tipo LysR.

La regulación de la expresión de *opvAB* es transcripcional y se ejerce a través de una secuencia reguladora situada en la región 5' previa al promotor de *opvAB*, en la cual se incluyen cuatro sitios GATC y sitios de unión de OxyR que solapan con ellos.

La eliminación de los sitios GATC de esta secuencia reguladora elimina la variación de fase y permite la expresión constitutiva de *opvAB*. La síntesis de OpvA y OpvB modifica la estructura del lipopolisacárido, reduciendo la longitud predominante del antígeno O a 3-8 unidades de repetición.

La expresión de *opvAB* y la consecuente alteración del la estructura del antígeno O divide las poblaciones de *Salmonella enterica* en dos subpoblaciones: la subpoblación mayoritaria $OpvAB^{OFF}$ es virulenta y sensible a bacteriófagos que usan el antígeno O como receptor. La subpoblación minoritaria $OpvAB^{ON}$ es resistente a dichos bacteriófagos y avirulenta. La expresión variable de *opvAB* constituye un mecanismo epigenético y reversible de resistencia a bacteriófagos que utilizan el antígeno O como receptor. En presencia del bacteriófago, la subpoblación $OpvAB^{OFF}$ es eliminada y se seleccionan las células $OpvAB^{ON}$. Cuando el bacteriófago desaparece, la alta tasa de transición ON→OFF permite la rápida regeneración de la subpoblación $OpvAB^{OFF}$.

La formación de subpoblaciones $OpvAB^{OFF}$ y $OpvAB^{ON}$ depende de la formación de patrones de metilación específicos en los cuatro sitios GATC situados en la región reguladora de *opvAB*. En fase OFF, los sitios $GATC_1$ y $GATC_3$ están protegidos por la proteína OxyR y se encuentran desmetilados, mientras que $GATC_2$ y $GATC_4$ son metilados. En fase ON, el patrón es el contrario: OxyR protege los sitios $GATC_2$ y $GATC_4$ de ser metilados, mientras que $GATC_1$ y $GATC_3$ son metilados.

Se han identificado factores auxiliares que participan en la formación de las subpoblaciones $OpvAB^{OFF}$ y $OpvAB^{ON}$. SeqA es una proteína de unión a sitios GATC que reprime específicamente la tasa de transición OFF→ON. La proteína asociada al nucleoide HU es fundamental para la formación de la subpoblación $OpvAB^{ON}$.

INTRODUCTION

The genus *Salmonella*

The genus *Salmonella* includes facultative, anaerobic, rod-shaped Gram-negative bacteria that are able to infect a wide variety of animal hosts including amphibians, reptiles, mammals, and birds. *Salmonella* belongs to the family Enterobacteriaceae and is phylogenetically close to the genera *Escherichia*, *Shigella*, and *Citrobacter*.

The genus *Salmonella* is currently divided into two species, known as *Salmonella enterica* and *Salmonella bongori* [1]. *Salmonella enterica* includes six subspecies [2]: *enterica* (I), *salamae* (II), *arizonae* (IIIa), *diarizonae* (IIIb), *houtenae* (IV) and *indica* (VI). Historically, *Salmonella enterica* subsp. V was *bongori*, which is now considered a different species.

Salmonella isolates from the same subspecies are further classified into serovars based on the White-Kauffman classification scheme [3], which relies on specific patterns of agglutination reactions based on antisera against two highly variable surface antigens, O (lipopolysaccharide O-antigen) and H (flagellar proteins) [2,4]. There are more than 2,500 *Salmonella* serovars, most of which belong to the subsp. *enterica* [5]. Only serovars of this subspecies regularly colonize warm-blooded vertebrates [6], and so they account for 99% of human infections by *Salmonella*, while serovars of *Salmonella bongori* and the rest of *Salmonella enterica* subspecies are usually associated to cold-blooded vertebrates or to the environment [7].

Serovars belonging to subsp. *enterica* differ in their host specificity and in the types of diseases they produce. Some serovars are host-restricted, while others can infect a wide variety of animal hosts [8]. The diseases caused by subsp. *enterica* serovars vary from self-limiting gastroenteritis to life-threatening systemic infection, and the outcome of the disease depends on the specific serovar-host combination. For example, the specialist human-restricted serovar Typhi produces typhoid fever, whereas the generalist serovar Typhimurium produces mild gastroenteritis in humans but causes a systemic infection similar to human typhoid fever when infecting mice [9]. For this reason, the interaction between serovar Typhimurium and mice has been extensively used as a model for typhoid fever in humans [10], and most studies in *Salmonella* have employed this serovar. In this work, we have used the mouse-virulent strain *Salmonella enterica* subsp. *enterica* serovar Typhimurium ATCC 14028 [11]. For simplicity, it will be often abbreviated as *Salmonella enterica*.

Evolution of *Salmonella*

Salmonella and *Escherichia* are close relatives, and diverged 120-160 million years ago [12]. Almost 25% of the *Salmonella* genome consists of genetic material that is absent in *Escherichia coli* [6,13]. The evolution of *Salmonella* pathogenicity (**Figure I1**) has involved the sequential acquisition of genetic elements, each contributing to different aspects of its lifestyle [14,15]. Amongst those elements are the *Salmonella* pathogenicity islands (SPIs), which are clusters of virulence genes in the chromosome. More than 10 SPIs have been described [16], including some which are serotype-specific. These regions are absent in the chromosome of other Enterobacteriaceae, and usually have different G+C content than the average of the *Salmonella* chromosome, suggesting that they have been acquired by horizontal gene transfer [13,15].

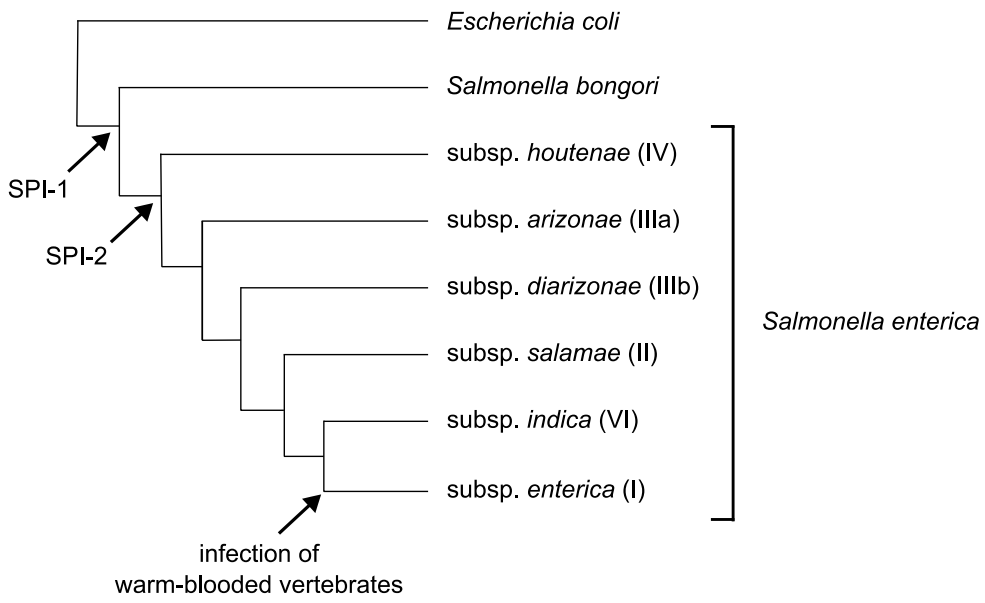

Figure I1. Phylogeny of the genus *Salmonella*. The acquisition of SPI-1, SPI-2, and the ability to infect warm-blooded vertebrates is indicated. Modified from [17].

The best characterized SPIs are *Salmonella* pathogenicity island 1 (SPI-1) and *Salmonella* pathogenicity island 2 (SPI-2). SPI-1 was acquired first by the common ancestor of the two *Salmonella* species, and is involved in the invasion of intestinal epithelial cells in the animal host [18]. SPI-1 acquisition likely allowed *Salmonella* to become an intracellular pathogen associated with cold-blooded vertebrates [17]. SPI-2

allows *Salmonella* to survive in macrophages and colonize deeper tissues [19], and its acquisition marked the split of the two *Salmonella* species [17]. Hence, only members of *Salmonella enterica* have the ability to reach deep tissues and organs to produce systemic infections.

The ancestor of subsp. *enterica* acquired the capacity to infect warm-blooded vertebrates, and different strains subsequently evolved to colonize a variety of hosts. Even though the mechanisms of host specificity are not fully understood, the presence of a virulence plasmid in some serovars of subsp. *enterica* has suggested the potential involvement of plasmid functions [7]. Another factor that may be involved in host specificity is the presence of different sets of fimbrial operons in different serovars [7,20].

Salmonella infection

Infection with *Salmonella enterica* is usually caused by ingestion of contaminated food or water. Along the digestive track, *Salmonella* must endure adverse conditions that serve as protective mechanisms against bacterial infections.

In the stomach, acid pH destroys the majority of microorganisms [21]. Activation of the acid tolerance response enables *Salmonella* to endure periods of severe acid stress [22,23].

In the small intestine, *Salmonella* finds high concentrations of bile, secreted in the duodenum during digestion. Bile has two main antibacterial activities: as a detergent that disrupts the cell envelope [24] and as a DNA damaging agent [25]. However, *Salmonella* and other enterobacteria are intrinsically resistant to high concentrations of bile [24], partly through activation of the general stress response [26] and by modification of the peptidoglycan structure [27].

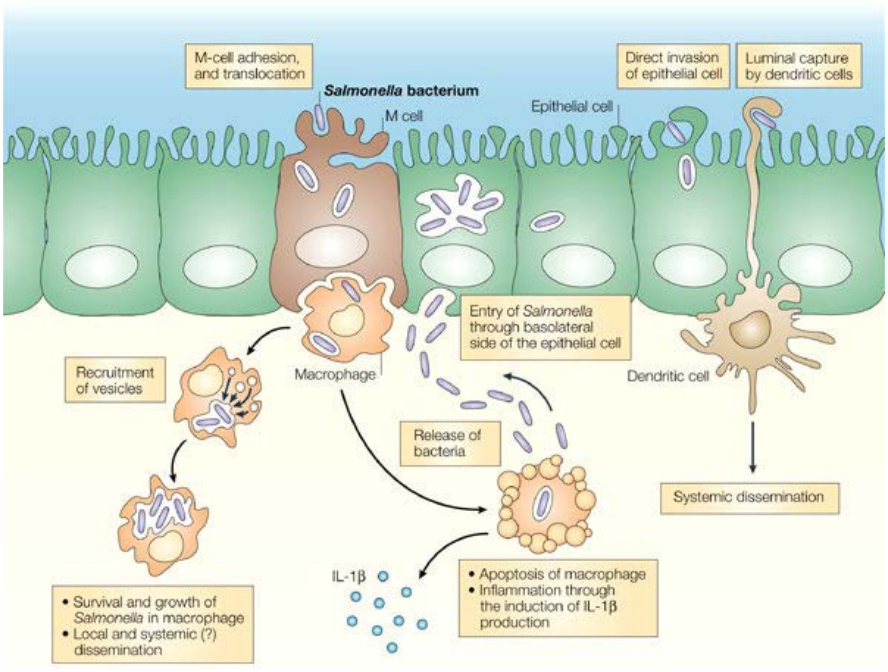

Figure I2. Diagram of *Salmonella* infection. The three main routes of *Salmonella* invasion of the intestinal epithelium are represented: adhesion and translocation through M cells, direct invasion of intestinal epithelial cells, and capture by dendritic cells. Reproduced from [28].

When *Salmonella* reaches the distal small intestine, a large array of adhesins and fimbriae allow the pathogen to adhere to the intestinal epithelium [29]. *Salmonella* is able to invade the intestinal epithelium through three different routes (**Figure I2**): (i) by inducing a phagocytosis-like process in non-phagocytic enterocytes, (ii) through specialized epithelial M cells, and (iii) through dendritic cells that intercalate epithelial cells by extending protrusions into the gut lumen [30,31]. The two first routes are mediated by the virulence-associated type 3 secretion system encoded on *Salmonella* pathogenicity island 1 (SPI-1) [32], with invasion of M cells being the predominant route of intestinal traversal [33].

After invasion, and depending on the host-serovar combination, *Salmonella* can cause two main kinds of infection outcomes: gastroenteritis and systemic infection.

In gastroenteritis, the infection is localized in the intestine, and induces an inflammatory reaction in the intestinal mucosa. Accumulation of liquid in the intestinal lumen leads to diarrhea [34,35]. The inflammatory response creates a novel luminal niche, which favors growth of *Salmonella* over the resident microbiota of the intestine. Remarkably,

the cascade of events that takes place as consequence of inflammation produces the accumulation of tetrathionate ($S_4O_6^{2-}$) in the intestinal lumen [36]. *Salmonella* can use tetrathionate as electron acceptor for respiration to obtain energy for growth in the inflamed gut lumen, taking advantage over the resident microbiota, which must rely on less efficient fermentation processes.

In systemic infection, *Salmonella* crosses the epithelial barrier and can survive inside phagocytes due to the possession of a second type 3 secretion system encoded on *Salmonella* pathogenicity island 2 (SPI-2), and disseminates through the lymphatic system reaching deep tissues. *Salmonella* can colonize multiple target organs, particularly the spleen, the liver, the gall bladder and the bone marrow, where bacteria can proliferate, potentially resulting in a fatal outcome [37].

A fraction of individuals recovering from systemic infection become asymptomatic, life-long carriers of *Salmonella*, acting as reservoirs for future infections. In humans, serovar Typhi can establish chronic carriage in the gall bladder [37].

Lipopolysaccharide (LPS)

The cell envelope of Gram negative bacteria can be divided in three layers: the cytoplasmic or inner membrane, the peptidoglycan cell wall, and the outer membrane. The outer membrane is highly asymmetrical: its inner leaflet consists mainly of phospholipids, while the outer leaflet is almost entirely composed of a particular kind of glycolipid known as lipopolysaccharide (LPS) [38].

The LPS is essential for many aspects of the lifestyle of *Salmonella*, including swarming motility [39]; intestinal colonization [40]; invasion and intracellular replication [41–43]; and resistance to serum [44,45], bile [46], and cationic peptides [43]. LPS is also a common receptor for bacteriophages, including P22 [47].

The LPS can be divided in three structural regions: lipid A (endotoxin), a highly conserved hydrophobic molecule which serves as an anchor to the membrane; the core saccharide, a genus-conserved short oligosaccharide; and the O-antigen, an immunogenic molecule made up by a number of repeats of the same saccharide unit composed of three to five sugars [48,49] **(Figure I3A**). Most of the structural diversity

of LPS is found in the O-antigen. Altered sugar composition, linkage, and number of O-antigen repeats lead to the production of many different kinds of O-antigen molecules both between and within bacterial strains.

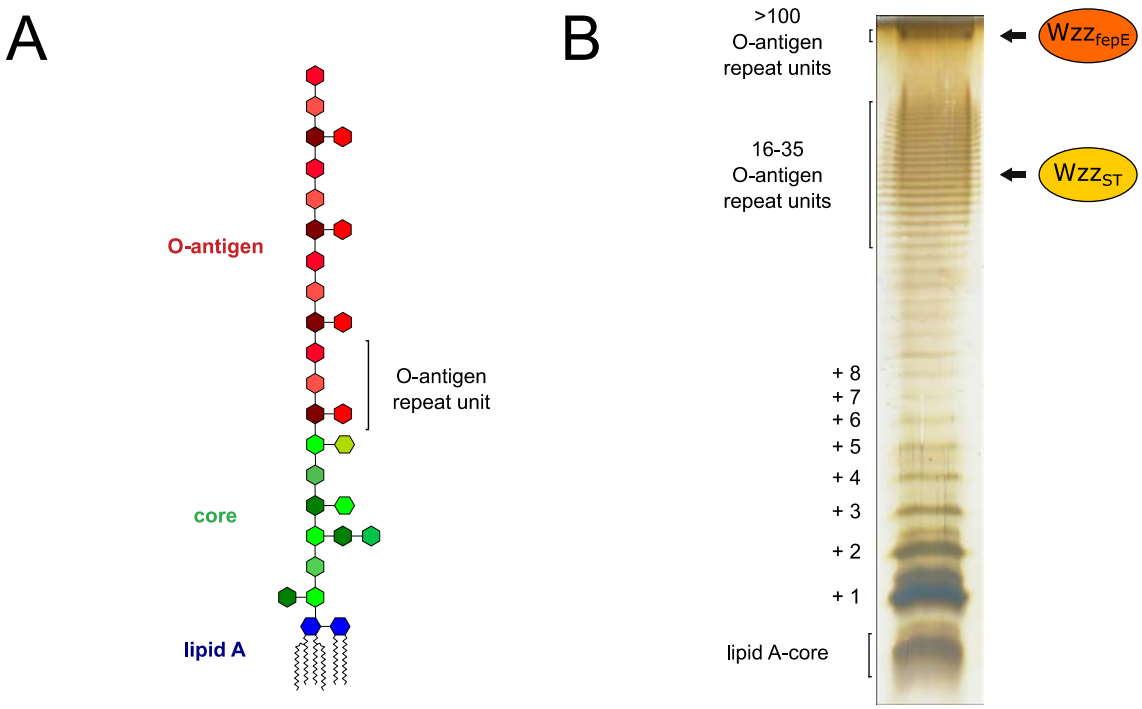

Figure I3. A. Idealized structure of an LPS molecule. For simplicity, only four O-antigen repeat units are represented, but individual LPS molecules can have more than 100 O-antigen repeat units. **B.** Visualization in SDS-PAGE gel of a typical LPS structure from *Salmonella enterica*. The O-antigen chain modal lengths imposed by the regulators Wzz_{ST} and Wzz_{fepE} are indicated.

Synthesis of the O-antigen is complex and involves a large number of inner membrane proteins [50]. First, synthesis of a single O-antigen repeat unit linked to the lipid carrier undecaprenyl pyrophosphate takes place in the cytoplasmic leaflet of the inner membrane. The lipid-linked O-antigen unit is then flipped to the periplasmic leaflet of the inner membrane by the O-antigen flippase Wzx. In the periplasm, the O-antigen polymerase Wzy (also called Rfc in *Salmonella*) combines O-antigen repeat units in a growing O-antigen chain until preferred modal lengths conferred by O-antigen chain length regulators (also known as polysaccharide copolymerases or PCPs and commonly designated Wzz) are produced. Once the O-antigen chain is complete, it is ligated to the

lipid A-core by the O-antigen ligase WaaL and tranported to the outer membrane (**Figure I4**).

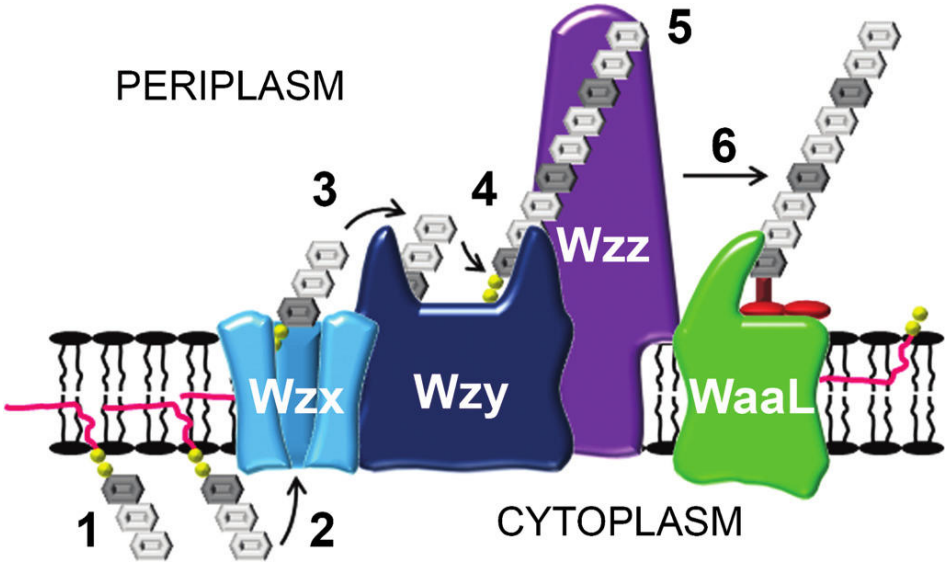

Figure I4. Diagram of the synthesis of the O-antigen. 1. O-antigen repeat unit synthesis on the undecaprenyl pyrophosphate-lipid carrier in the cytoplasmic leaflet of the inner membrane. **2.** Flipping of the lipid-linked O-antigen subunit to the perisplasmic leaflet by the O-antigen flippase Wzx. **3.** Transfer to the O-antigen polymerase Wzy. **4.** Addition of single lipid-linked O-antigen subunits to the growing O-antigen chain. **5.** Length regulation of the O-antigen chain by O-antigen chain regulators Wzz. **6.** Ligation of the polymerized O-antigen chain to a lipid A-core molecule by the O-antigen ligase WaaL. Reproduced from [51].

Visualization of LPS in SDS-PAGE gels results in a typical “ladder” structure in which every step reflects the addition of a single O-antigen repeat unit (**Figure I3B**). Different O-antigen chain modal lengths are easily identified within the same bacterial strain by increased intensity of bands of a particular size range. As already stated, O-antigen chain modal lengths depend on O-antigen chain length regulators. As many other species in the Enterobacteriaceae family [52], *Salmonella enterica* displays two modal lengths (**Figure I3B**): long O-antigen (16-35 repeat units) is conferred by Wzz_{ST} (also known as Rol, Cld or WzzB) [53], and very long O-antigen (>100 repeat units) by Wzz_{fepE} (FepE) [52]. In the absence of both Wzz regulators, *Salmonella* LPS displays a stochastic distribution, with bands decreasing in intensity as the O-antigen chain grows longer.

Albeit with remarkable variations in amino acid sequence, Wzz regulators share several structural properties: nearly all harbor transmembrane segments near the N and C termini and a hydrophilic α-helical periplasmic domain containing a coiled-coil region [54] and display a particular set of conserved amino acid residues near the N terminus [55]. Wzz regulators are known to form oligomers in a characteristic bell shape [56].

The mechanism for regulation of O-antigen chain length by Wzz regulators is not established, and has been the subject to considerable debate. Depending on the model, Wzz regulators have been proposed to act as molecular timers that modulate the ability of Wzy to elongate the O-antigen chain [57], as chaperones that assemble O-antigen synthesis machinery proteins in particular ratios [58], as scaffolds in which O-antigen chain lengths are conferred by the number of Wzz subunits in a given oligomer [55] or as rulers that set O-antigen chain length by direct interaction to the O-antigen chain [59]. Later on, the role of changes in the structure of the growing O-antigen in the interaction with the Wzz regulators has been incorporated into a chain-feedback model [60]. A hybrid model combining ruler and chain-feedback elements has been recently proposed and is supported by a large body of evidence [50]. According to this model, the interaction between Wzy and Wzz favors the formation of a longer O-antigen chain by direct binding of the growing O-antigen chain to the Wzz protein. However, when the O-antigen chain attains a particular length, higher-order structures begin to destabilize the interaction with Wzz. When the O-antigen chain reaches the tip of the bell-shaped Wzz oligomer, the lipid-linked O-antigen is freed from the O-antigen synthesis complex rendering it susceptible to ligation by WaaL to form a mature LPS molecule.

The LPS molecule is subsequently exported to the outer membrane at a limited number of sites, in a ribbon-like shape that is largely immobile [61–63], probably due to strong lateral interactions between LPS molecules [64,65]. These interactions induce the assembly of a mechanically stable network in which the structure of the lipid A-core is rigid and well-defined [66] but the O-antigen is flexible and can adopt many conformations [67].

Ribbon-like dispositions have also been described for many inner and outer membrane proteins, suggesting that the whole cell envelope might be organized in a helical fashion [63,68].

OxyR

The OxyR protein belongs to the LysR-type family of transcriptional regulators (LTTRs) [69], the largest family of prokaryotic DNA-binding proteins [70]. A typical LTTR is made of approximately 330 amino acid residues with an N-terminal helix-turn-helix DNA-binding motif. Members of this family can act as transcriptional repressors or activators, and regulate the expression of genes involved in variety of cellular processes such as amino acid metabolism, oxidative stress, nitrogen fixation, degradation of aromatic compounds, and bacterial virulence [71]. The presence of a co-inducer is usually necessary for LTTR function, but no inducer has been described for OxyR. Most LTTRs, including OxyR, are able to induce DNA bending [70].

OxyR functions as a tetramer (dimer of dimers) [72,73], which is the preferred structure for most LTTRs [74–78]. Others are known to form simple dimers in solution, which could be their active form [79][80]. Exceptionally, octamers [81] and hexamers [82] have also been described.

OxyR controls a regulon of almost 40 genes in *Escherichia coli* and *Salmonella* [83], and OxyR homologs are present and play a role in hydrogen peroxide resistance in many different bacteria. The products of upregulated genes protect the cell from oxidative stress damage [84] and include enzymes such as catalases and alkylhydroperoxide reductases. The OxyR regulon has also a role in protection against heat stress [85], response to near-UV light [86], singlet oxygen [87], lipid-peroxidation-mediated cell damage [88] and neutrophil-mediated killing [89].

OxyR is both the sensor and the transducer of the oxidative stress signal, and undergoes a conformational change upon oxidation. In the presence of hydrogen peroxide, the sulphur residue of a particular cystein in the OxyR protein, Cys199, is oxidized and forms a reversible disulfide bond with Cys208. An $oxyR^{C199S}$ mutation produces an altered form of OxyR which cannot be oxidized but retains all the properties of the reduced form [90,91], and has been useful in a number of studies [92,93].

Oxidation of the OxyR tetramer causes a conformational change which results in the rearrangement of the dimers [72] and relaxes the DNA bending induced in the majority of the promoters of OxyR-regulated genes. In the oxidized conformation, OxyR induces

cooperative binding of the RNA polymerase [91] and promotes transcription of genes in the OxyR regulon.

A general LTTR-binding DNA sequence has been defined as a palindromic sequence containing a T-X_{11}-A consensus (where X is any nucleotide), based on a comparison of binding sites for LysR-type regulators in several species [94]. A single OxyR dimer recognizes the palindromic sequence ATAGxAxxxTxCTAT (where x is any nucleotide). The distance between two consecutive OxyR binding sites is 10 base pairs for the oxidized OxyR tetramer (which contacts four adjacent major grooves in the DNA) and 17 base pairs for the reduced OxyR tetramer (which binds two pairs of adjacent major grooves separated by a helical turn) [90].

Although originally described as the main regulator of the oxidative stress response, OxyR also controls transcription of certain genes irrespective of its oxidation state. Examples include the *mom* gene of bacteriophage Mu [95], the *agn43* gene of *Escherichia coli* [96] and the *gtr* operon of *Salmonella enterica* [93]. The two latter systems have also been shown to be subject to phase variation, and will be discussed in more detail due to their relevant relationship to our own results.

Dam methylation

Base methylation is a DNA modification present in all kingdoms of life. C^5-methyl-cytosine and N^6-methyl-adenine are found in bacterial, archaeal and eukaryotic genomes, whereas N^4-methyl-cytosine is found only in bacteria [97,98]. The methyl group of modified bases protrudes from the major groove of the double DNA helix, which is a typical place for recognition of DNA motifs by DNA-binding proteins [99]. Consequently, the methylation state of critical adenosine or cytosine moieties can regulate the interaction between DNA-binding proteins and their cognate DNA sequences [99,100]. The formation of N^6-methyl-adenine also lowers the thermodynamic stability of DNA [101] and alters DNA curvature [102], which could further influence DNA-protein interactions.

Base modification in bacterial genomes is performed by two kinds of methyltransferases: most are associated with restriction-modification systems that protect the cell from foreign unmethylated DNA [103,104], but some are solitary

methyltransferases that do not have a restriction enzyme partner [100]. One of this solitary methyltransferases is the Dam methylase of Gamma-proteobacteria.

Dam is only found in a particular clade of bacteria consisting of the orders Enterobacteriales, Vibrionales, Aeromonadales, Pasteurellales, and Alteromonadales [105]. It is essential for viability in *Vibrio cholerae* and certain strains of *Yersinia* [106]. In *Escherichia coli* and *Salmonella enterica* a *dam* mutation causes pleiotropic defects but is not lethal [107,108].

Dam shares significant sequence identity with DNA methyltransferases such as MboI and DpnII, both of which have a restriction enzyme counterpart [105,109]. This relatedness suggests that Dam has evolved from an ancestral restriction-modification system. A crucial difference, however, is that the Dam methylase is highly processive, able to perform multiple methylation reactions before dissociating from the DNA molecule, whereas restriction-modification DNA methylases are distributive [110].

Dam methylation involves transfer of a methyl group from S-adenosyl-methyonine to the N^6 amino group of the adenosine moiety of 5'GATC3' sites [107]. Methylation occurs shortly after DNA replication, which means that hemimethylated GATC sites are the natural substrate of the Dam methylase. However, Dam methylates both hemimethylated and unmethylated GATC sites with similar efficiency [107]. DNA binding and/or methyl transfer are influenced by the flanking sequences of the GATC sites [111].

N^6-methyl-adenine can be used as a signal for genome defense, DNA replication and repair, nucleoid segregation, regulation of gene expression, control of transposition, and host-pathogen interactions [105,107,109,112] (**Figure I5**).

Dam plays a crucial role in the correction of replication errors by providing a way to identify the template DNA strand [113]. The formation of a mismatched base pair results in recognition by the MutS protein and the recruitment and assembly of the MutHLS complex. Methyl-directed mismatch repair is regulated by MutH, which nicks the nonmethylated (newly replicated) DNA strand at the nearest hemimethylated GATC site, ensuring that the parental template strand is not altered [114]. Degradation and resynthesis of the mismatched daughter strand eventually result in correction of the mismatched sequence.

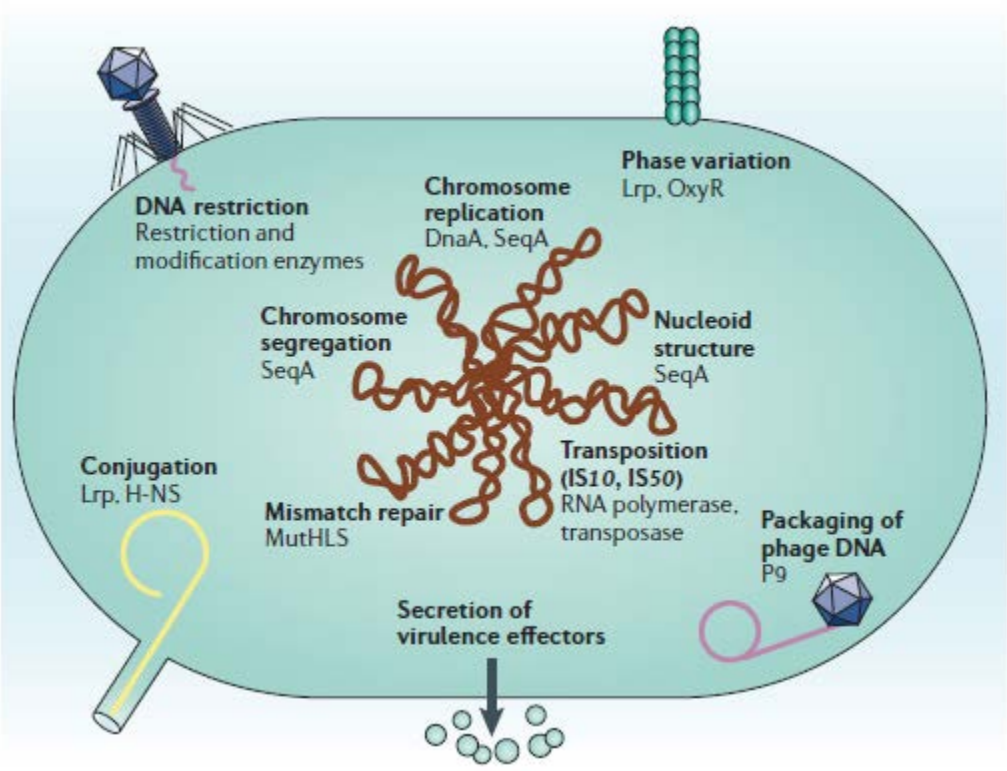

Figure I5. Examples of roles of N^6-methyl-adenine in enteric bacteria. Where known, the methylation-sensitive DNA-binding proteins involved in each process are indicated. Reproduced from [100].

Initiation of chromosome replication in *E. coli* requires binding of an ATP-bound form of the initiator protein DnaA to the replication origin (*oriC*), followed by separation of the two strands of the double helix and loading of DNA helicase. However, binding of DnaA at the *oriC* region is only possible if the GATCs located in the region are methylated; a hemimethylated origin is inactive [115]. Interestingly, the density of GATC sites in the *oriC* region is roughly tenfold higher than the average in the *E. coli* chromosome (11 GATC sites within 245 base pairs) [116].

Dam-dependent timing of DNA replication and nucleoid organization are controlled by a protein known as SeqA, which binds hemimethylated GATC sites in the *oriC* region, inhibiting further rounds of replication [117], and also to newly generated hemimethylated GATC sites along the chromosome, organizing the daughter chromosomes into nucleoid domains [118,119]. This will be discussed in the section dedicated to SeqA.

The involvement of Dam methylation in virulence was first described in *Salmonella*: the 50% lethal dose (LD_{50}) of a *dam* mutant is 10,000 fold higher than that of the wild type upon oral inoculation[120][121]. Pleiotropic effects caused by absence of Dam methylation might explain this extreme phenotype: *dam* mutants display a lower colonization capacity, reduced mobility, envelope instability, ectopic expression of fimbriae, sensitivity to bile salts, lower expression of virulence genes, and altered LPS O-antigen chain length [122–124].

Dam methylation-dependent transcriptional control of gene expression can be classified into two main types [125]:

(i) Clock-like controls that use the methylation state of the DNA as a signal to couple gene expression to a particular stage of the cell cycle. Examples of activation by hemimethylation include the conjugal transfer gene *traJ* and the IS*10* transposase gene [126,127]. Repression by hemimethylation include the chromosome replication gene *dnaA* [128].

(ii) Switch-like controls that turn on and off gene expression based on differential methylation patterns of GATC sites typically found around the promoters of phase variation systems [129]. Because active methylation is not known to occur in bacteria, competition of DNA-binding proteins and Dam methylase is the only mechanism known to generate nonmethylation [130]. The decrease in processivity caused by certain DNA sequences around the GATC sites in some of these systems plays a role in the generation of nonmethylated DNA [111]. Several examples of this kind of epigenetic control will be discussed in the section dedicated to Dam-regulated phase variation systems.

SeqA

The *seqA* gene is found only in a subset of Gram negative bacteria together with *dam* and *mutH* [105,131]. The SeqA protein was first described as a factor inhibiting reinitiation of DNA replication at the chromosomal replication origin *oriC* in *Escherichia coli* [132]. SeqA keeps the origin inactivated for about one third of the cell cycle by a process known as sequestration [133]. Sequestration depends on the high

concentration of GATC sites in this region [132], which provides multiple binding sites for SeqA.

Although SeqA was initially believed to be a tetramer based on size-exclusion chromatographic experiments [134], current evidence suggest that the basic structural and functional SeqA unit is a dimer [119,135]. SeqA dimers preferentially bind to pairs of GATC sites less than 31 base pairs apart *in vitro*, especially if the two GATC sites are on the same face of the DNA helix [136,137]. SeqA shows much higher affinity for hemimethylated over fully methylated DNA and no binding to unmethylated DNA [138–140]. However, SeqA has been shown to bind a fully methylated *oriC*, probably due to the extraordinary concentration of GATC sites [139,141].

The main role of SeqA in the cells is the delay of primary and secondary replication initiations. SeqA delays the primary replication initiation event by binding to the fully methylated *oriC* until the cell reaches its critical mass, counteracting the DnaA protein that activates replication initiation [133,142–144]. After replication is initiated, preferential binding of SeqA over Dam [140] means that SeqA binds the newly generated hemimethylated GATC sites and sequesters *oriC* from Dam methylase and DnaA, thus preventing secondary replication initiation within a single cell cycle [132,133]

During sequestration, re-initiation is further inhibited by three mechanisms: (i) inactivation of DnaA by hydrolysis of the ATP-form of DnaA to the ADP-form [145], (ii) titration of DnaA to the new DnaA binding sites generated by DNA replicaton [146], and (iii) repression of *dnaA* transcription by *dnaA* gene sequestration [133,147].

SeqA also forms foci which appear to track replication forks [148,149] and consist of several hundred SeqA molecules and about 100 kb of DNA [150]. The formation of these foci seems to be related to the organization, cohesion and final segregation of the newly formed chromosomes [136,151,152].

SeqA is also involved in gene regulation [153]. Because SeqA binding delays Dam methylation, deletion of *seqA* results in an expression profile almost identical to Dam overproduction [153]. Interestingly, in *Escherichia coli*, the *agn43* was one of the few genes that showed different expression in a *dam*-overproducing and in a *seqA* background. This suggests that SeqA plays a different role in this case, possibly altering

the competition between Dam methylation and OxyR binding at the *agn43* upstream regulatory element [154]. SeqA binding could favor Dam methylation over OxyR binding. The same could be true for the Dam-methylated fimbrial operon *std*, where SeqA could favor Dam methylation over binding of the LysR-type transcription factor HdfR [155].

HU

HU is a small, basic, dimeric DNA-binding protein that belongs to the DNABII family [156]. Together with other bacterial histone-like or nucleoid-associated proteins such as IHF, Fis, and H-NS, it is a major structural component of the nucleoid. HU is conserved among the majority of bacteria and is also present in archaea and in plant chloroplasts [157,158].

In most bacteria, HU is encoded by a single gene, but members of the families Enterobacteriaceae and Vibrionaceae possess two unlinked and non-identical HU-encoding genes, *hupA* and *hupB* [159]. HU can exist in three forms: the HU αβ heterodimer and the HU α_2 and β_2 homodimers. The αβ heterodimer is the dominant form throughout most of the cell cycle, except very early in exponential phase when the α_2 homodimer is more abundant. The β_2 homodimer is minoritary and only detected in late stationary phase [160]. Synthesis of *hupB*, however, is preferentially stimulated during cold shock [161].

Whereas single *hupA* and *hupB* mutations do not result in a significant growth defect, double *hupA hupB* mutants of *E. coli* and *S. enterica* are highly pleiotropic and grow slowly, but remain viable [162,163]. Interestingly, the HU mutation is lethal in *Bacillus subtilis*, which has no other histone-like protein [164].

The αβ heterodimer and the α_2 and β_2 homodimers have different DNA binding properties towards particular DNA structures [165]. As a whole, HU binds with relative non-specificity to DNA, albeit with a bias for AT-rich sequences [166,167], but shows a strong preference for binding to unusual DNA conformations such as cruciforms, single-stranded breaks, mismatches, gaps and loops [168–171]. This is also consistent with its role in recombination and DNA repair [172–174].

Histone-like proteins such as HU are able to alter DNA topology by bending, supercoiling and compacting it [175], leading to multiple effects in the cell including transcriptional regulation [176]. DNA supercoiling, bending and loop formation by binding of HU has also been shown *in vitro* [177–179], although a possible dual role in compaction and stiffening of the DNA has also been suggested [180].

HU is capable of inducing or stabilizing very different DNA bend angles [181,182]. In fact, HU creates a more flexible bend that other DNA-bending proteins, and might often stabilize previously bent DNA rather than bend DNA itself [183]. The ability of HU to form flexible bends instead of a rigid structure might be important for its biological function, facilitating the formation of higher-order protein-DNA complexes.

In *E. coli*, the HU regulon includes genes responding to anaerobiosis, acid and osmotic stress, and SOS induction [184]. It has also recently been shown to be involved in biofilm formation by uropathogenic *E. coli* [185]. In *Salmonella*, HU regulates expression of a large number of genes related to virulence, motility, stress response and general physiology of the cell [163]. Several studies have shown that both the *E. coli* and *Salmonella* HU regulons show different degrees of overlap between genes regulated by the heterodimer and the two homodimers, although the *hupA hupB* mutation usually has the strongest effect on gene expression, followed by the *hupA* mutation, with the *hupB* mutation having the smallest effect [158,163].

The involvement of HU in direct interaction with a promoter has been studied in most detail in the *gal* promoter of *E. coli*. HU has a crucial role in the assembly of the Gal repressosome, a nucleoprotein complex that represses transcription of the partially overlapping *gal* promoters P1 and P2. The formation of the repressosome involves the formation of a DNA loop encompassing the promoter region and also requires binding of the LysR-type transcription factor GalR. GalR dimers interact with two spatially separated operators O_E and O_I and transiently form a DNA loop by tetramerization [186]. This creates a distorted region which can be now be bound by HU, which is already recruited by association with GalR [187] and can now be trasferred to the distorted locus, resulting in a highly stable repressosome [188].

Formation of bacterial lineages

The study of differentiation in bacterial species that undergo developmental programs has played a historic role in biology [189–191]. In addition, phenotypic differences between colonies [192] and within colonies [193,194] were described many years ago in bacterial species that do not undergo development. Despite their technical limitations, these early studies contributed to bring about the idea that phenotypic heterogeneity might be a common phenomenon in the bacterial world [195]. This view has been confirmed by single cell analysis technologies [196–200]. Furthermore, theoretical analysis has provided evidence that phenotypic heterogeneity can have adaptive value, especially in hostile or changing environments [201–203]. In certain cases, the adaptive value of subpopulation formation is illustrated by experimental evidence [26,204,205].

In general, the evolutionary significance of the formation of bacterial subpopulations can be interpreted as the result of two different strategies: division of labor and bet-hedging [199][206][207]. Division of labor, also known as cooperation, implies that there is an interaction between different phenotypes, and in a given environment both subpopulations together are fitter than any of them separately. Bet-hedging or risk-spreading occurs when each subpopulation is fitter than the other in a particular environment, so that the population as a whole is fitter in a variety of conditions and prepared to adapt to an environmental change.

Formation of bacterial lineages is governed by diverse mechanisms, including programmed genetic rearrangement [208] and contraction or expansion of DNA repeats at genome regions known as contingency loci [209,210]. In other cases, however, lineage formation is controlled by epigenetic mechanisms [130,200]. Although the known examples of non-genetic heterogeneity show disparate levels of complexity, epigenetic formation of bacterial subpopulations typically fits in the following, simplified model: certain cell-to-cell differences can serve as physiological signals, and signal propagation by a feedback loop generates an inheritable phenotype [200,211]. Cell-to-cell differences can be a consequence of environmental inputs or result from the noise intrinsical to many cellular processes [198,200,203]. An important factor that contributes to gene expression noise is the finite number effect: noise is more prevalent if the number of molecules involved in a process is limited [212–214]. This is relevant in gene expression since transcription and translation events are relatively infrequent

events, and also because transcription factors are often present in small numbers [215]. In turn, the feedback loops that propagate the initial state beyond can be relatively simple (e. g., the perpetuation of autogenous control beyond cell division) or involve complex mechanisms like the formation of inheritable DNA adenine methylation patterns in the genome [130,200,216]. Some feedback loops are stable enough to cause bistability, the bifurcation of a bacterial population into two distinct phenotypic states [211].

If a feedback loop is metastable, reversion of the epigenetic state will occur after a certain number of cell divisions. Reversible bistability is usually known as phase variation, and typically involves reversible switching of gene expression from OFF to ON or from low to high expression [129,217,218]. Examples of phase variation have been described mostly in bacterial pathogens, and subpopulation formation is frequently viewed as a strategy that may facilitate evasion of the immune system during infection of animals [129,217]. This view is supported by the observation that phase-variable loci often encode envelope components or proteins involved in modification of the bacterial envelope [129,217].

Some phase-variable envelope modifications controlled by DNA adenine methylation play roles in bacteriophage resistance. For instance, phase variation in the *gtrABC1* cluster protects *S. enterica* against the T5-like phage SPC35, probably by an indirect mechanism [219]. In *Haemophilus influenzae*, DNA adenine methylation controls phase-variable resistance to bacteriophage HP1c1 but the underlying mechanism remains hypothetical [220]. Phase variation can also contribute to phage resistance without alteration of the bacterial surface. For instance, certain genes encoding restriction-modification systems show phase variation [221,222].

Phase variation systems regulated by Dam methylation

Dam-dependent gene regulation often controls the synthesis or modification of envelope structures such as fimbriae or the LPS O-antigen [223]. Several of these systems show phase variation and are under epigenetic control. Binding of certain transcriptional regulators hinders Dam methylation, and creates heritable DNA methylation patterns (combinations of methylated and nonmethylated GATC sites). We will briefly discuss

three of them: *pap* and *agn43* from *Escherichia coli* and *gtr* from *Salmonella enterica* and the bacteriophage P22.

pap

The *pap* operon of uropathogenic *Escherichia coli* encodes pyelonephritis-associated pili that mediate adhesion to the urinary mucosa and facilitate colonization of the kidneys [224]. Pap pili expression is subject to phase variation, and switching between ON and OFF states is controlled by Dam methylation [225] (**Figure I6**).

The biological role of *pap* phase variation is not well established, but could be related to evasion of the immune system, the establishment of a bind-release-bind mechanism that allows succesive generations of bacteria to ascend the urinary tract, and/or modulation of growth by contact-dependent inhibition [130].

The upstream regulatory sequence of the *pap* operon contains six binding sites for the leucine-responsive regulatory protein (Lrp). Two of these sites contain GATC motifs, which are called $GATC^{dist}$ (site 5) and $GATC^{prox}$ (site 2). In the OFF state, Lrp binds cooperatively and with high affinity to sites 1-3 and prevents RNA polymerase binding and transcription of *pap*. Lrp binding at sites 1-3 reduces the affinity of Lrp for sites 4-6 and prevents methylation of $GATC^{prox}$. Lack of protection by Lrp means that $GATC^{dist}$ is methylated. The high affinity of Lrp for the nonmethylated $GATC^{prox}$ and its inability to bind a methylated $GATC^{dist}$ create a feedback loop that propagates the OFF state.

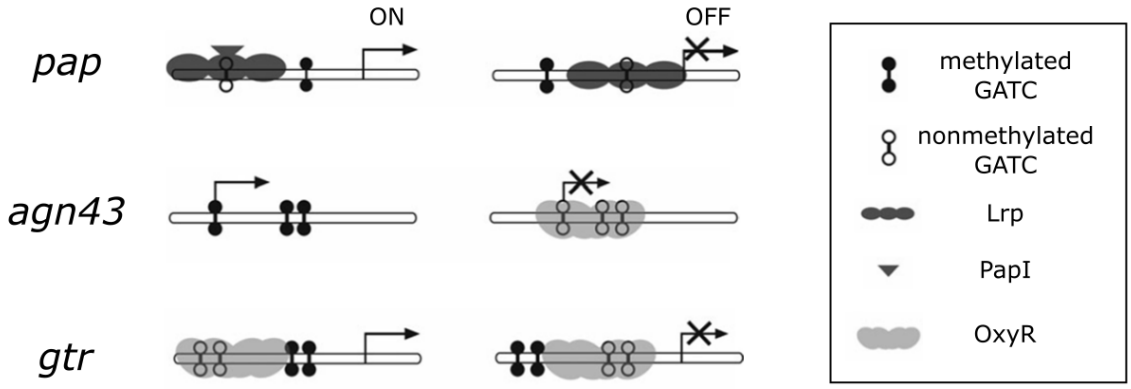

Figure I6. Diagrams for Dam methylation-dependent regulation of *pap*, *agn43* and *gtr* phase variation. For simplicity, binding sites, Dam methylase and RNA polymerase are not represented. Cartoons not to scale. Modified from [93].

Switching to the ON state requires that Lrp is translocated to sites 4-6. Translocation requires the ancillary protein PapI, which binds to Lrp [226] and preferentially increases its affinity for sites 4-6. Binding of Lrp to sites 4-6 inhibits methylation of $GATC^{dist}$ and permits methylation of $GATC^{prox}$, contributing to propagate the ON state. One of the products of the *pap* operon, PapB, activates *papI* transcription [227,228], further propagating the ON state by a positive feedback loop.

agn43

The *agn43* gene of *Escherichia coli* encodes the outer membrane protein Ag43, which belongs to the autotransporter family [229]. Expression of Ag43 promotes aggregation [230], biofilm formation [231,232] and virulence-related phenotypes such as persistence in the urinary tract [233,234] and increased uptake and survival in neutrophils [235]. Ag43 was initially denominated Flu (for fluffing) [230], although the original flu^{+} phenotype actually corresponds to non-expression of *agn43*.

Transcription of *agn43* is subject to phase variation under the control of Dam methylation and binding of OxyR [236,237] (**Figure I6**). The regulatory region of *agn43* contains a single OxyR binding site overlapping with three GATC sites and the -10 sequence of the promoter [238]. Binding of OxyR to the *agn43* regulatory region results in repression of transcription and nonmethylation of the GATC sites [239–241]. Conversely, methylation of the GATC sites results in abrogation of OxyR binding [239,242]. Thus, methylation of the GATC sites and binding of OxyR are mutually exclusive, and the expression state of *agn43* depends on the outcome of competition between OxyR binding and Dam methylation upon DNA replication [238,240]. The oxidation state of OxyR is not relevant for its role in regulation of *agn43* [96].

Phase variation rates of *agn43* are altered in a *seqA* mutant, and SeqA has been shown to bind hemimethylated DNA from the *agn43* regulatory region *in vitro* [154]. The biological relevance of this is however unclear, since SeqA bound to *agn43* DNA is easily displaced *in vitro* by both Dam and OxyR [243]. However, higher-order SeqA structures *in vivo* might behave in a different way. Indeed, introduction of additional SeqA-binding sites (GATC sites) in the proximity of *agn43* also altered phase variation rates [243].

The ON to OFF transition rate is affected by the availability of OxyR at the replication fork: addition of three OxyR-binding sites upstream of *agn43* acts like a sink that increases the local concentration of OxyR and biases the system toward the OFF state [243].

gtr

Glycoltransferase (*gtr*) operons encode proteins that mediate the addition of sugars onto the basic LPS O-antigen structure [244,245]. *Salmonella* serovars generally carry between one and four *gtr* operons, although they are absent in some serovars [246]. These operons have also been found the genomes of *Shigella* [247] and in bacteriophages, including P22 [248]. There is evidence of extensive phage-mediated transfer of *gtr* operons [246].

Salmonella enterica serovar Typhimurium harbors two *gtr* operons [93]. One of them, *gtrABC1,* has been shown to be crucial for faecal shedding and intestinal persistence in *Salmonella,* although constitutive high levels of expression lead to a defect in association with epithelial cells and reduced invasion of both epithelial cells and macrophages [244]. As already mentioned, phase variation of the same *gtr* operon confers transient resistance to the bacteriophage SPC35 [219]. Phase variation of *gtr* could also play a role in virulence [93].

Expression of most *gtr* operons is phase-variable [93], and all phase-varying *gtr* operons share a similar upstream regulatory element that contains three OxyR binding half-sites known as Oxy(A), OxyR(B), and OxyR(C); and four overlapping GATC sites: $GATC^1$ and $GATC^2$ in OxyR(A), and $GATC^3$ and $GATC^4$ in OxyR(C). The OxyR binding half-sites are placed in a way that the OxyR tetramer can bind either OxyR(AB) or OxyR(BC) [93,246].

OxyR acts as a repressor or an activator depending on which of its two possible complete binding sites is occupying. In the OFF state, $GATC^1$ and $GATC^2$ are methylated and OxyR binds to the OxyR(BC) binding site, acting as a repressor by blocking the access of the RNA polymerase to the promoter. In the ON state, the inverse methylation pattern is observed ($GATC^3$ and $GATC^4$ are methylated) and OxyR binds to the OxyR(AB) binding site, promoting transcription of *gtr* (**Figure I6**). DNA methylation confers heritability to the system by affecting which of the OxyR binding

sites is occupied, given that OxyR binding is decreased by methylation of GATC sites in each binding site. In turn, OxyR binding prevents Dam methylation of the overlapping GATC sites.

As in *agn43*, the spacing of the OxyR binding sites is consistent with binding of the reduced form of OxyR, and *gtr* phase variation is not altered as a result of oxidative stress [93].

Bacteriophages

There are eight different major phyla of bacteriophages, with very different molecular lifestyles and extremely distant relatedness, if any [249]. Tailed bacteriophages include 95% of all the phages reported in the scientific literature, and probably make up the majority of phages in nature [250]. It is estimated that there are at least 10^{31} tailed virions in the biosphere, and that phages are 10 to 25-fold more abundant than their bacterial hosts [251–253], which makes phage the predominant biological entity on our planet [251,254]. Their abundance and ability to kill their bacterial hosts means that they play a critical role in virtually all natural processes. Phages are known to alter competition between bacterial strains and species [255,256], maintain bacterial diversity [257,258], and mediate horizontal gene transfer between bacteria [259,260].

Phages and bacteria are in a constant arms race that results in continuous cycles of mutually influenced co-evolution [261,262]. As an example, the adsorption machinery is the most rapidly evolving part of the tailed phage genome [263]. In turn, bacterial defense systems also show high variability (including phase variation) [222], rapid evolution, and a tendency for horizontal gene transfer [264].

The specificity in the interaction between a bacteriophage and a bacterial cell is mostly determined by specificity of adsorption, which in turn is dependent on the nature and structural peculiarities of the receptors on the surface of the bacterial envelope [265]. Known receptors of *Salmonella* phages are the LPS O-antigen [266–269], flagellar proteins [270–272], the outer membrane protein for vitamin B_{12} uptake BtuB [271,273,274], the outer membrane protein OmpC [275,276], the outer membrane protein for drug efflux pump TolC [277], the outer membrane transport protein FhuA [278], and the Vi capsular antigen [279].

A common feature of bacteriophages using the O-antigen as receptor is that their tail spike proteins not only recognize but also hydrolize the O-antigen, allowing the phage to penetrate through the O-antigen layer during infection [280].

Tailed phages have been traditionally assigned to the order Caudovirales and share a common structure consisting of a polyhedral, often icosahedral, head that contains a double-stranded DNA genome and is attached to a flexible tail. They also share a similar DNA packaging system relying on an ATP cleavage-powered DNA translocase [281].

Tailed phages can go through a lytic or lysogenic life cycle. Lytic infection results in production of phage progeny and destruction of the host. Lysogenic infection results in the integration of the phage genome in the host chromosome (creating a prophage) or in the persistence of the phage genome as an extrachromosomal element. The genes that are expressed from the prophage typically alter certain traits of the bacterial host. Prophages can be induced and result in a new lytic cycle [282].

The bacteriophages used in this work belong the traditional three families in the order Caudovirales: P22 belongs to Podoviridae (which includes 14% of tailed phages), 9NA to Siphoviridae (62%), and Det7 to Myoviridae (24%) [249]. These families are defined by morphology: the Podoviridae have short non-contractile tails, the Siphoviridae have long non-contractile tails, and the Myoviridae have long contractile tails (**Figure I7**).

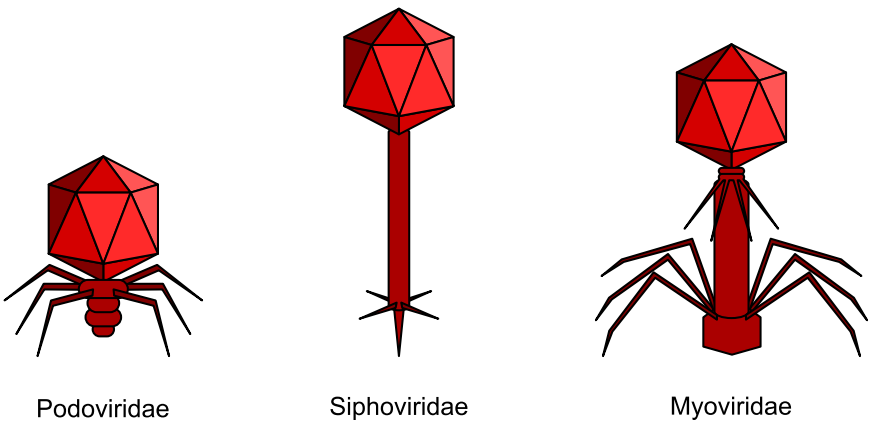

Figure I7. Idealized structures of bacteriophages belonging to the three families in the order Caudovirales. Podoviridae have short non contractile tails. Siphoviridae have long non-contractile tails. Myoviridae have long contractile tails. Modified from [283].

A recent classification based on sequence similarity of 337 fully sequenced tailed phages infecting 18 bacterial genera belonging to the family Enterobacteriaceae [284] identified 56 different clusters and confirmed that, although tail morphology has been shown not to be the best indicator of relatedness [285,286], these three phages are indeed in very different groups.

P22 belongs to the lambda supercluster of temperate phages which includes 81 different phages. A virulent version of P22 called P22 H5 carrying a mutation in the *c2* gene [287] was used in some of our experiments.

9NA constitutes the prototype phage of an isolated cluster which no close relatives. It forms clear plates with no indication of a lysogenic lifestyle [288].

Det7 is also lytic [289] and belongs to the Vi01-like cluster which is distantly related to T4 [284,290].

Clustering of the bacteriophages also showed a correlation with genome size and lifestyle. Again, the three phages were placed in three different groups: small temperate phages (P22, 44 Kb), small lytic phages (9NA, 53 Kb) and large phages (Det7, 158 Kb).

Resistance to bacteriophages can be attained by a variety of mechanisms [291], including inhibition of DNA penetration, production of modified restriction endonucleases and blockage of the receptor by increased production of the extracellular matrix, but the most frequent cause of phage resistance are mutations affecting phage receptors [47,291,292]. Resistance to phages comes at a fitness cost, including an increased cost of deleterious mutations [293], decreased ability to metabolize carbon [294], reduced competitive ability [295], increased susceptibility to other phages [296] and reduction in virulence [297,298]. This may explain the adaptive value of phase variation in bacterial defense mechanisms [219,220,299].

OBJECTIVES

A previous study from our laboratory showed that *STM2209-STM2208* (later renamed *opvAB*), a small locus of unknown function in the genome of *Salmonella enterica*, was derepressed in a Dam$^-$ mutant background [300]. Inspection of the region immediately upstream of *opvAB* revealed the existence of an element composed of four GATC sites arranged in perfect symmetry. This suggested that Dam might repress these genes directly through methylation of these GATC sites. Results obtained in this work pointed to a more complex regulation of *opvAB*: Dam methylation does not simply repress *opvAB* but controls a phase variation mechanism that results in the formation of OpvAB^{OFF} and OpvAB^{ON} populations.

On these grounds, we addressed the study of this locus with the following objectives:

Objective 1. Characterization of the mechanism of regulation of *opvAB* by Dam methylation.

Objective 2. Identification of the function of OpvA and OpvB.

Objective 3. Analysis of the formation of OpvAB^{OFF} and OpvAB^{ON} epigenetic lineages.

MATERIALS AND METHODS

Bacterial strains and strain construction

The strains of *Salmonella enterica* used in this study (**Table M1**) belong to serovar Typhimurium, and derive from ATCC 14028. For simplicity, *S. enterica* serovar Typhimurium ATCC 14028 is often abbreviated as *S. enterica*.

Escherichia coli BTH101 (F^- *cya-99 araD139 galE15 galK16 rpsL1*(Str^r) *hsdR2 mcrA1 mcrB1*) was used for bacterial two-hybrid assays. *Escherichia coli* CC118 λ *pir* [*phoA20 thi-1 rspE rpoB argE* (*Am*) *recA1* (λ *pir*)] and *E. coli* S17-1 λ *pir* [*recA pro hsdR* RP4-2-Tc::Mu-Km::Tn*7* (λ *pir*)] were used for directed construction of point mutations. *Escherichia coli* M15 [pREP4] (Qiagen, Valencia, CA) was used for 6xHis-$OxyR^{C199S}$ production.

Bertani's lysogeny broth (LB) was used as standard liquid medium. Solid LB contained agar at 1.5% final concentration. Green plates [301] contained methyl blue (Sigma-Aldrich, St. Louis, MO) instead of aniline blue. The indicator for monitoring β-galactosidase activity in plate tests was 5-bromo-4-chloro-3-indolyl-β-D-galactopyranoside (X-gal; Sigma-Aldrich, 40 µg/ml). Antibiotics were used at the concentrations described previously [302]. To grow *oxyR* strains on LB agar, 75 µl of a 10 mg/ml catalase solution (Sigma-Aldrich, St. Louis, MO) were spread on the surface of the plates.

Table M1. Basic strains of Salmonella enterica used in this study. Additional strains were constructed by introducing point mutations in some of these backgrounds.

Strain name	Genotype
ATCC 14028	wild type
SV4536	Δ*dam*-230
SV5573	*opvB*::3xFLAG
SV5574	Δdam-230 *opvB*::3xFLAG
SV5675	Δ*opvB*
SV5676	*opvA*::*lac* (transcriptional)
SV5677	*opvB*::*lac* (transcriptional)
SV5679	*opvB*::*lac* (translational)
SV5680	Δ*dam*-230 *opvA*::*lac* (transcriptional)
SV5681	Δ*dam*-230 *opvB*::*lac* (transcriptional)
SV5683	Δ*dam*-230 *opvB*::*lac* (translational)
SV5734	*opvA*::*lac* (translational)

SV5735	Δ*dam*-230 *opvA*::lac (translational)
SV5812	*opvA*::3xFLAG
SV5813	Δ*dam*-230 *opvA*::3xFLAG
SV5925	Δ*oxyR*::Cm^r
SV5989	Δ*oxyR*::Cm^r *opvB*::*lac* (translational)
SV5990	Δdam-230 Δ*oxyR*::Cm^r *opvB*::*lac* (translational)
SV6001	Δ*oxyR*::Cm^r *opvB*::3xFLAG
SV6002	Δ*dam*-230 Δ*oxyR*::Cm^r *opvB*::3xFLAG
SV6004	Δ*oxyR*::Cm^r *opvA*::3xFLAG
SV6005	Δ*dam*-230 Δ*oxyR*::Cm^r *opvA*::3xFLAG
SV6013	Δ*opvAB*
SV6397	*oxyR*^{C199S}
SV6401	OpvAB^{ON} (mut. GATC)
SV6727	*opvAB*::*gfp*
SV6728	Δ*dam*-230 *opvAB*::*gfp*
SV6786	Δ*wzz*$_{ST}$
SV6791	Δ*wzz*$_{fepE}$
SV6796	Δ*wzz*$_{ST}$ Δ*wzz*$_{fepE}$
SV6815	*seqA*::Tn10 *opvB*::*lac* (translational)
SV7031	mut. GATC *opvB*::*lac* (translational)
SV7032	Δ*dam*-230 mut. GATC *opvB*::lac (translational)
SV7232	Δ*oxyR*::Cm^r mut. GATC *opvB*::lac (translational)
SV7233	Δ*dam*-230 Δ*oxyR*::Cm^r mut. GATC *opvB*::lac (translational)
SV7406	Δ*oxyR*
SV7643	*opvB*::*mCherry*
SV7645	*opvB*::*mCherry*^{ON}
SV7874	*seqA*::Tn10 *opvAB*::*gfp*
SV8020	Δ*opvA*
SV8117	OpvB^{ON} (Δ*opvA*)
SV8118	OpvA^{ON} (Δ*opvB*)
SV8153	OpvB^{ON} Δ*wzz*$_{ST}$ (Δ*opvA*)
SV8154	OpvB^{ON} Δ*wzz*$_{fepE}$ (Δ*opvA*)
SV8155	OpvB^{ON} Δ*wzz*$_{ST}$ Δ*wzz*$_{fepE}$ (Δ*opvA*)
SV8488	Δ*hupA opvAB::gfp*
SV8489	Δ*hupB*::Km^r *opvAB*::*gfp*
SV8490	Δ*hupA* Δ*hupB*::Km^r *opvAB*::*gfp*
SV8491	Δ*hupA opvB::lac* (translational)
SV8492	Δ*hupB*::Cm^r *opvB::lac* (translational)
SV8493	Δ*hupA* Δ*hupB*::Cm^R *opvB::lac* (translational)

The oligonucleotides used in this study are listed in **Table M2**. Targeted gene disruption was achieved using plasmids pKD3, pKD4 and pKD13 [303] and oligonucleotides *PS1*, *PS2* or *PS4*. Verification of the constructs was achieved using oligonucleotides *E1* and *E2*. Antibiotic resistance cassettes introduced during strain

construction were excised by recombination with plasmid pCP20 [303]. For the construction of transcriptional and translational *lac* fusions in the *Salmonella* chromosome, FRT sites generated by excision of Km^r cassettes were used to integrate plasmids pCE36, pCE37 or pCE40 [304]. Addition of 3xFLAG tag to protein-coding DNA sequences was carried out using plasmid pSUB11 as a template [305] and oligonucleotides *F2209-5* + *F2209-3* (for *opvA*), and *F2208-5* + *F2208-3* (for *opvB*).

Table M2. List of oligonucleotides used in this work.

Oligonucleotide name	Sequence (5'→3')
2208mut1DIRnuevo	gaaccgtcacataaaacaaaaaccatcaattttatttatatgatag
2208mut1INVnuevo	ctatcatataaataaaattgatggtttttgttttatgtgacggttc
2208mut23DIRnuevo	gaggaattttcatcgattttaattatttataaccatcgatatcatg
2208mut23INVnuevo	catgatatcgatggttataaataattaaaatcgatgaaaattcctc
2208mut2DIRnuevo	gaggaattttcatcgattttaattatttataacgatcgatatcatg
2208mut2INVnuevo	catgatatcgatcgttataaataattaaaatcgatgaaaattcctc
2208mut3DIRnuevo	gaggaattttgatcgattttaattatttataaccatcgatatcatg
2208mut3INVnuevo	catgatatcgatggttataaataattaaaatcgatcaaaattcctc
2208mut4DIRnuevo	ctatcattgatgtatttacccatcgatataaccagtgtgaatgtattg
2208mut4INVnuevo	caatacattcacactggttatatcgatgggtaaatacatcaatgatag
Clo2208-3	agtcgagctcccatcatcgatataccatgc
Clo2208-5	cgactctagactgatcatgatgacgtccac
ClooxyR-3	tttttctagataacgccttgtcgaaatggc
ClooxyR-5	ttttgagctcgaatatctggtggcgttagc
delGATC-PS1	ccccgttggtgcctgaacgtgtaccgaatgaaccgtcacagtgtaggctggagctgcttc
delGATC-PS2	agaattcgagtattttaaaggaaaataacaatacattcaccatatgaatatcctccttag
deloxyR199-PS1	ccgatctggcgggcgagaaattgctgatgctggaagatgggtgtaggctggagctgcttc
deloxyR199-PS2	tccgctcccgcttcaaaacagaaccccatcgcctgatcgccatatgaatatcctccttag
envR-For-Dnase	atcattcaacgtcgtgttgg
envR-Rev-Dnase	ttattttgggatggggttca
F2208-3	ttcgacacatttcagcgcagagtttatctctgcgcaatgtcatatgaatatcctccttag
F2208-5	agaatatcgtattgagaaaaagacaatgaatgaccgcgcagactacaaagaccatgacgg
F2209-3	aacgtcgactaaatcaatttcactattttctccccgcattcatatgaatatcctccttag
F2209-5	ttcagtattcgggttgactattagcgttttaaaagggatggactacaaagaccatgacgg
FAMGATClargo-3	ttctccccgcatttcacatc
FAMGATClargo-5	FAM-accttaccatgagctatgcc
FAMGATClargoconFAM-3	FAM-ttctccccgcatttcacatc
fepE3-PS1	atcgccagcgcgttttccattttacgcgagaccatcgcgtgtgtaggctggagctgcttc
fepE5-PS4	acaagaaaaaaatcagtcatttgcaggttattcactgccgattccggggatccgtcgacc
fepE-E1	aaactatcgggcccatcatc
fepE-E2	tcctgcatgacctgaatcag
HindIII-opvB-mCherry-5	gctaagcttagaatatcgtattgagaaaaagacaatgaatgaccgcgcaatggtgagcaagggcgagga
His-oxyR-BamHI-5	aaaaggatccatgaatattcgtgatcttgaatatctggtg
His-oxyR-SalI-3	aaaagtcgacttaaaccgcctgttttaacgc

hupA-E1	ttgtcgtgccataaggcttc
hupA-E2	ttatgactgcaggcagtcag
hupA-PS1-5	cgatgcttagcaagcgataaacacattgtaaggataacttgtgtaggctggagctgcttc
hupA-PS2-3	tgatgagccccttcgataaaactgttcacagttatgcgtccatatgaatatcctccttag
hupB-E1	gcattgaggaagttctgacg
hupB-E2	atagagacttcacgcgcatc
hupB-PS1-5	ggattcaggtgcgatataaattataaagaggaagagaagagtgtaggctggagctgcttc
hupB-PS2-3	gcgcccttgtactttgtcacatccccgaggggataacgccatatgaatatcctccttag
KpnI-opvA-plasmidoGFP-3	ttttggtacccatccctttaaaacgctaa
KpnI-opvA-plasmidoGFP-5	ttttggtaccctgatcatgatgacgtccac
mCherry	tgatggccatgttatcctcc
NdeI-opvB-mCherry-3	cgacatatgtttgacacatttcagtgcagagtttatctctgcgcaatgtagtcacgacgttgtaaaacg
ompA-RT-Dir	tgtaagcgtcagaaccgatacg
ompA-RT-Rev	gagcaacctggatccgaaag
oxyR3-PS1	gtacgacgcggctccggcttaatgcatggcagataaaccagtgtaggctggagctgcttc
oxyR3-PS2	gtacgacgcggctccggcttaatgcatggcagataaaccacatatgaatatcctccttag
oxyR5-PS1	actgcgtgaggtcaaggtgctcaaggagatggcaagccaagtgtaggctggagctgcttc
oxyR5-PS4	actgcgtgaggtcaaggtgctcaaggagatggcaagccaaattccggggatccgtcgacc
OxyRBDIR	gaggaattttgatcgattttaactatttataacgatcgatatc
OxyRBINV	gatatcgatcgttataaatagttaaaatcgatcaaaattcctc
oxyRC199SDIR	ggaagatggccactctctgcgcgatcagg
oxyRC199SINV	cctgatcgcgcagagagtggccatcttcc
OxyRDDIR	gtatttaccgatcgatataacctatgtgaatgtattgttattttc
OxyRDINV	gaaaataacaatacattcacataggttatatcgatcggtaaatac
oxyR-E1	ggttaaacgagaaaccgctc
oxyR-E2	caccttaactacccaacc
PE2208	cgacggatccaaggaaacgtcgactaaatc
PE2209	cgacggatccctgcgaacgtatatttcttc
PE5	attaggatccagccttgtcttcggaatgtc
pKT25-seq3	ctgcaaggcgattaagttgg
pKT25-seq5	ttatgccgcatctgtccaac
pKT25-STM2208-PstI-5	aactgcagggatgcggggagaaaatagtg
pKT25-STM2209-BamHI-3	cgggatcctcacatccctttaaaacg
pKT25-STM2209-PstI-5	aactgcagggatgaagaaatatacgttcg
pUT18C-STM2208-BamHI-3	cgggatcctcatgcgcggtcattcattg
pUT18C-STM2208-PstI-5	aactgcaggatgcggggagaaaatagtg
pUT18C-STM2209-PstI-5	aactgcaggatgaagaaatatacgttcg
RT2208-3	agctttgcatatgtttccgtttg
RT2208-5	aatggcggcatggtatatcg
RT2209-3	gctaatagtcaacccgaatac
RT2209-5	gaagaaatatacgttcgcagc
seqGATC-5	ccttaccatgagctatgcc
STM2208-E1	aatatacgttcgcagccagg
STM2208-E2	ttcgacacatttcagcgcag
STM2208-PS1	gcgcggtcattcattgtctttttctcaatacgatattctggtgtaggctggagctgcttc
STM2208-PS4	gggagaaaatagtgaaattgatttagtcgacgtttccttaattccggggatccgtcgacc
STM2208stop-GFP-3	acttttactcttcgacacatttcagcgcagagtttatctctgcgcaatgtttatcacttattcaggcgta
STM2208stop-GFP-5	cgctaacagaatatcgtattgagaaaaagacaatgaatgaccgcgcatgataagaaggagatatacatatgag
STM2209-E1	ttaccgatcgatataaccag

STM2209-E2	ttgtatcatgctgcacgctc
STM2209-PS1	tttcactattttctccccgcatttcacatccctttaaaagtgtaggctggagctgcttc
STM2209-PS4bis	gttgctttttgttatttcagtattcgggttgactattagcattccggggatccgtcgacc
STM2209-PS4tris	aattcttatgtgtgggttttatcttatgaagaaatatacgattccggggatccgtcgacc
wzzB3-PS1	tagctacgtagcgcattgcgtcccagcacaatcccggcacgtgtaggctggagctgcttc
wzzB5-PS4	gtcttccgggcgtgggaacgatccggaacagattgatttgattccggggatccgtcgacc
wzzB-E1	agagtggctccgataacttc
wzzB-E2	atcaactggagcagctactg

For the construction of strain SV7643 (*opvB*::mCherry), a fragment containing the promoterless *mCherry* gene and the kanamycin resistance cassette was PCR-amplified from pDOC-R, an mCherry-containing derivative of plasmid pDOC [306] using primers *HindIII-opvB-mCherry-5* and *NdeI-opvB-mCherry-3*. The construct was integrated into the chromosome of *S. enterica* using the Lambda Red recombination system [303]. For the construction of strain SV6727 (*opvAB*::*gfp*), a fragment containing the promoterless green fluorescent protein (*gfp*) gene and the chloramphenicol resistance cassette was PCR-amplified from pZEP07 [307] using primers *STM2208stop-GFP-5* and *STM2208stop-GFP-3*. The fragment was integrated into the chromosome of *S. enterica* using the Lambda Red recombination system [303]. An *opvB*::*gfp* transcriptional fusion was formed downstream of the *opvB* stop codon, and the strain remained OpvAB$^+$. For the construction of strains SV7645, SV8117, and SV8118, plasmid pKD46 was introduced in SV6401, and the PCR products used for construction of strains SV7643, SV8020 and SV5675 were integrated into the chromosome of SV6401 using the Lambda Red recombination system [303].

Transductional crosses using phage P22 HT 105/1 *int201* ([308] and G. Roberts, unpublished data) were used for construction of strains with altered chromosomal markers. The transduction protocol has been described elsewhere [309]. To obtain phage-free isolates, transductants were purified by streaking on green plates. Phage sensitivity was tested by cross-streaking with the clear-plaque mutant P22 H5.

Plasmids

Plasmids constructed for this study are listed in **Table M3**.

DNA fragments were amplified using oligonucleotides pairs PE5 + PE2209 and PE5 + PE2208. The resulting PCR fragments were cloned onto the pGEM-T plasmid (Promega, Madison, WI) to obtain plasmids pIZ1758 and pIZ1759, respectively.

For construction of pIZ1885, a DNA fragment containing *oxyR*^{C199S} was amplified using oligonucleotides *His-oxyR-BamHI-5* and *His-oxyR-SalI-3*, and cloned into pQE30 (Qiagen, Valencia, CA) using the BamHI and SalI sites.

The *opvA* and *opvB* genes were PCR amplified using oligonucleotides *pKT25-STM2209-PstI-5 + pKT25-STM2209-BamHI-3* (pIZ1812), *pUT18C-STM2208-PstI-5 + pUT18C-STM2208-BamHI-3* (pIZ1905), *pUT18C-STM2209-PstI-5 + pKT25-STM2209-BamHI-3* (pIZ1906), *pKT25-STM2208-PstI-5 + pUT18C-STM2208-BamHI-3* (pIZ1907), and cloned onto plasmids pUT18C and pKT25 using the PstI and BamHI sites. Recombinant plasmids carrying *opvA* and *opvB* were sequenced using oligonucleotides *pKT25-seq5* and *pKT25-seq3*.

For construction of the plasmid pIZ2011, a DNA fragment containing *opvA* and the native *opvAB* promoter was PCR-amplified using primers *KpnI-opvA-plasmidoGFP-5 + KpnI-opvA-plasmidoGFP-3*). The amplification product was cloned into pDOC-R [306]. The resulting plasmid produces an OpvA-mCherry fusion protein.

Plasmid pTP166 [310] was kindly provided by Martin G. Marinus, University of Massachusetts, Worcester, MA.

Table M3. List of plasmids constructed for this study.

Plasmid name	Description
pIZ1758	pGEM-T::[PE5-PE2209]
pIZ1759	pGEM-T::[PE5-PE2208]
pIZ1812	pKT25::*opvA*
pIZ1885	pQE30::*oxyR*^{C199S}
pIZ1905	pUT18C::*opvB*
pIZ1906	pUTC18C::*opvA*
pIZ1907	pKT25::*opvB*
pIZ2011	pDOC-R::*opvA*

Bacteriophages

Bacteriophages 9NA [288,311] and Det7 [31,289] were kindly provided by Sherwood Casjens, University of Utah, Salt Lake City. Bacteriophage P22 H5 is a virulent derivative of bacteriophage P22 that carries a mutation in the *c2* gene [287], and was kindly provided by John R. Roth, University of California, Davis. For simplicity, P22 H5 is abbreviated as P22 throughout the text.

RNA extraction

RNA was extracted from *S. enterica* stationary phase cultures ($O.D._{600}$ ~3), using the SV total RNA isolation system (Promega, Madison, WI) as described at http://www.ifr.ac.uk/safety/microarrays/protocols.html. The quantity and quality of the extracted RNA were determined using an ND-1000 spectrophotometer (NanoDrop Technologies, Thermo Scientific, Waltham, MA). To diminish genomic DNA contamination, the preparation was treated with DNase I (Turbo DNA free; Applied Biosystems, Foster City, CA).

Quantitative reverse transcriptase PCR and calculation of relative expression levels

An aliquot of 0.6 µg of DNase I-treated RNA was used for complementary DNA (cDNA) synthesis using the High-Capacity cDNA Archive kit (Applied Biosystems, Foster City, CA). Quantitative reverse transcriptase (RT)-PCR reactions were performed in an Applied Biosystems 7500 Fast Real-Time PCR System. Each reaction was carried out in a total volume of 25 µl on a 96-well optical reaction plate (Applied Biosystems, Foster City, CA) containing 12.5 µl Power SYBR Green PCR Master Mix (Applied Biosystems, Foster City, CA), 11.5 µl cDNA (1/10 dilution), and two gene-specific primers (*RT2209-5* + *RT2209-3* for *opvA*, *RT2208-5* + *RT2208-3* for *opvB*) at a final concentration of 0.2 µM each. Real-time cycling conditions were as follows: (i) 95ºC for 10 min and (ii) 40 cycles at 95ºC for 15 sec, and 60ºC for 1 min. A no-template control was included for each primer set. Melting curve analysis verified that each reaction contained a single PCR product. Gene expression levels were normalized to

transcripts of *ompA*, a housekeeping gene that served as an internal control, using oligonucleotides *ompA-RT-Dir* and *opmA-RT-Rev*.

β-galactosidase assays

Levels of β-galactosidase activity were assayed as described previously [312], using the $CHCl_3$-sodium dodecyl sulfate permeabilization procedure.

Protein extracts and Western blotting analysis

Total protein extracts were prepared from bacterial cultures grown at 37ºC in LB medium until stationary phase ($O.D._{600}$ ~3). A volume containing ~2.5 x 10^8 cells were collected by centrifugation and suspended in 50 µl of Laemmli sample buffer [1.3% SDS, 10% (v/v) glycerol, 50 mM Tris-HCl, 1.8% β-mercaptoethanol, 0.02% bromophenol blue, pH 6.8]. Proteins were resolved by Tris-Glycine-PAGE using 12% gels (for OpvB) or Tris-Tricine-PAGE 15% gels (for OpvA). Conditions for protein transfer have been described elsewhere [155]. Primary antibodies were anti-Flag M2 monoclonal antibody (1:5,000, Sigma-Aldrich, St. Louis, MO) and anti-GroEL polyclonal antibody (1:20,000; Sigma-Aldrich, St. Louis, MO). Goat anti-mouse horseradish peroxidase-conjugated antibody (1:5,000; Bio-Rad, Hercules, CA) or goat anti-rabbit horseradish peroxidase-conjugated antibody (1:20,000; Santa Cruz Biotechnology, Santa Cruz, CA) was used as secondary antibody. Proteins recognized by the antibodies were visualized by chemoluminescence using the luciferin–luminol reagents of Supersignal West Pico Chemiluminiscent Substrate (Thermo Scientific, Waltham, MA) and developed in a LAS3000 mini system (Fujifilm, Tokyo, Japan).

Subcellular fractionation

Subcellular fractionation was performed as previously described [313], with some modifications. Briefly, bacteria were grown in LB medium at 37ºC and spun down by centrifugation at 15,000 x g for 5 min at 4ºC, then resuspended twice in cold phosphate-buffered saline (PBS, pH 7.4). The bacterial suspension was either mixed with Laemmli

buffer (total protein extract) or disrupted by sonication. Unbroken cells were further removed by low-speed centrifugation (5,000 x g, 5 min, 4ºC). The supernatant was centrifuged at high speed (100,000 x g, 30 min, 4ºC) and the new supernatant was recovered as the cytosol fraction. The pellet containing envelope material was suspended in PBS with 0.4% Triton X-100 and incubated for 2 h at 4ºC. The sample was centrifuged again (100,000 x g, 30 min, 4ºC) and divided into the supernatant containing mostly inner membrane proteins and the insoluble fraction corresponding to the outer membrane fraction. An appropiate volume of Laemmli buffer was added to each fraction. After heating (100ºC, 5 min) and clearing by centrifugation (15,000 x g, 5 min, room temperature), the samples were analyzed for protein content by SDS-PAGE.

Primer extension

The oligonucleotides *PE2209* and *PE2208*, complementary to internal regions of the genes *opvA* and *opvB* respectively, were end-labeled with [^{32}P]ATP and annealed to 10 µg of total RNA prepared from *S. enterica* strains bearing plasmids pIZ1758 and pIZ1759. The end-labeled primer was extended with avian myeloblastosis virus reverse transcriptase (Boehringer Mannheim, Mannheim, Germany) under conditions described previously [314]. The products of reverse transcription were analyzed in urea-polyacrylamide gels and visualized using a FLA-5100 Imaging system (Fujifilm, Tokyo, Japan).

Directed construction of point mutations

Mutation of GATC sites within the *opvAB* regulatory region was achieved using the QuikChange® Site-Directed Mutagenesis Kit (Stratagene, La Jolla, CA). Briefly, a ~1.3 Kb fragment of the *opvAB* region containing the 4 GATC sites was cloned into the pGEM-T plasmid using the oligonucleotides *Clo2208-5* and *Clo-2208-3*. Mutations in every GATC were then introduced using oligonucleotides harboring CATC changes (labeled as *DIRnuevo* and *INVnuevo*). The resulting plasmids containing the fragment with one or more CATC sites was then digested with XbaI and SacI, cloned onto the suicide plasmid pDMS197 [307] and propagated in *E. coli* CC118 λ *pir*. Plasmids

derived from pMDS197 were transformed into *E. coli* S17-1 λ *pir*. The resulting strains were used as donors in matings with *S. enterica* ATCC 14028 harboring a Cm^r cassette from pKD3 in place of the 4 GATC sites (constructed using oligonucleotides *delGATC-PS1* and *delGATC-PS2*) as recipients. Antibiotic resistance cassettes from pKD3 and pKD4 were also introduced in *opvB*::*lac* and *opvAB*::*gfp* backgrounds. The resulting strains were used as intermediates in the construction of point mutations. Tc^r transconjugants were selected on E plates supplemented with tetracycline. Several Tc^r transconjugants were grown in nutrient broth (beef extract, 5 g/l, peptone, 5 g/l) and plated in plates containing nutrient broth supplemented with 5% sucrose. Individual tetracycline-sensitive segregants were then screened for cloramphenicol or kanamycin sensitivity and examined for the incorporation of the mutant allelle by Sau3AI digestion and DNA sequencing using external oligonucleotides. Mutation of OxyR binding sites was achieved in the same way using primers labelled *OxyRB* and *OxyRD*.

Construction of the $oxyR^{C199S}$ mutation was achieved with the same protocol, using the oligonucleotides *ClooxyR-5* and *ClooxyR-3* for cloning onto pGEM-T, and the oligonucleotides *oxyRC199SDIR* and *oxyRC199SINV* for site-directed mutagenesis. A strain with an antibiotic resistance cassette in place of the *oxyR* gene (constructed using oligonucleotides *deloxyR199-PS1* and *deloxyR199-PS2*) was used as a recipient in this case.

Measurement of the efficiency of phage adsorption

The efficiency of phage adsorption was calculated as described by Gabig *et al.* [315]. Briefly, P22 bacteriophages were added to *S. enterica* cells from an LB liquid overnight culture at a multiplicity of infection of 0.1, and the mixture was incubated at 37ºC. Samples were taken every 2 min, centrifuged for 1 min at 15,000 x g, and the supernatant was titrated on the *S. enterica* wild type strain ATCC 14028. The sample obtained at time zero (a sample taken immediately after addition of bacteriophages to the cell suspension) was considered to correspond to 100% unadsorbed phages, and the remaining numbers were calculated relative to this.

Electrophoretic visualization of lipopolysaccharide profiles

To investigate LPS profiles, bacterial cultures were grown in LB overnight. Bacterial cells were harvested and washed with 0.9% NaCl. The $O.D._{600}$ of the washed bacterial suspension was measured to calculate cell concentration. A bacterial mass containing about 3 x 10^8 cells was pelleted by centrifugation. Treatments applied to the bacterial pellet, electrophoresis of crude bacterial extracts, and silver staining procedures were performed as described by Buendía-Clavería *et al.* [316].

Calculation of phase transition frequencies

Phase transition rates were estimated as described by Eisenstein [317]. Briefly, a strain harboring an *opvB*::*lac* fusion was plated on LB + X-gal. After 16 h growth at 37ºC, colonies displaying ON and OFF phenotypes were chosen, resuspended in PBS and respread on new plates. Phase transition frequencies were calculated using the formula (M/N)/*g* where M is the number of cells that underwent a phase transition, N the total number of cells scored, and *g* the total number of generations that gave rise to the colony.

Macrophage infection experiments

The rate of intramacrophage replication after 18 h infection was performed in J774 mouse macrophages as described previously [318]. Briefly, macrophages were seeded at a density of 5 x 10^5 in 24-well plates and grown in DMEM medium supplemented with 10% (v/v) fetal bovine serum at 37°C, 5% CO2. Bacteria were added to the wells at macrophage-to-bacteria ratio of 0.1. Phagocytosis was allowed to proceed for 30 min before washing three times with PBS and adding fresh DMEM media supplemented with 20 µg/ml gentamicin. Macrophages were lysed by using 1% Triton X-100, and the number of viable bacteria that survived the gentamicin treatment was determined by subsequent plating onto LB agar plates. The replication rate was determined as the ratio between the number of bacteria at time 18 h and the number of internalized bacteria after 30 min phagocytosis.

Measurement of survival in serum

Survival in guinea pig serum (Sigma-Aldrich, St. Louis, MO) was analyzed as described elsewhere [45] with some modifications. Briefly, exponential cultures of *S. enterica* were serially diluted in PBS + 2 mM $MgCl_2$ to 2 x 10^4 c.f.u./ml. Guinea pig serum was added to 30% final concentration and the mixtures were incubated at 37ºC without shaking. Samples were taken at 30 min intervals by plating on LB agar, and viable counts were expressed as a percentage of the initial concentration (% survival).

Bacterial two-hybrid analysis

The Bacterial Adenylate Cyclase Two-Hybrid (BACTH) system [319] was used to test interaction between two membrane proteins. Plasmid pairs pKT25::*opvA* + pUT18C::*opvB* and pKT25::*opvB* + pUT18C::*opvA* (as well as pertinent controls) were co-transformed into an *E. coli* $CyaA^-$ strain (BTH101). Transformants were plated on LB + ampicillin + kanamycin + X-gal medium at 30°C for 30 h. To quantify the interaction between hybrid proteins, bacteria were grown overnight at 30°C in LB + ampicillin + kanamycin liquid medium supplemented with 0.5 mM isopropyl-β-D-1-thiogalactopyranoside (IPTG). β-galactosidase assays were carried out as described above. A level of β-galactosidase activity at least five fold higher than that measured for vectors alone is considered a positive interaction.

Fluorescence microscopy

Bacterial cells from 1.5 ml of an exponential culture in LB at 37°C ($O.D._{600}$ ~0.15) were collected by centrifugation, washed and resuspended in PBS. Cells were fixed in 4% formaldehyde solution and incubated at room temperature for 30 minutes. Finally, cells were washed, resuspended in PBS, and stored at 4ºC. Images were obtained by using an Olympus IX-70 Delta Vision fluorescence microscope (Olympus, Tokyo, Japan) equipped with a 100X UPLS Apo objective. Pictures were taken using a CoolSNAP HQ/ICX285 camera (Roper Technologies, Sarasota, FL) and analyzed using ImageJ software (Wayne Rasband, Research Services Branch, National Institute of Mental

Health, MD). Z-stacks (optical sections separated by 0.2 µm) of mCherry fluorescence were taken with the same microscope. Maximal intensity projections are shown.

Flow cytometry

Bacterial cultures were grown at 37ºC in LB or LB + phage (P22 H5, 9NA, or Det7) until exponential ($O.D._{600}$ ~0.3) or stationary phase ($O.D._{600}$ ~4). Cells were then diluted in PBS to a final concentration of ~10^7/ml. Data acquisition and analysis were performed using a Cytomics FC500-MPL cytometer (Beckman Coulter, Brea, CA). Data were collected for 100,000 events per sample, and were analyzed with CXP and FlowJo8.7 software. Data are represented by a dot plot (forward scatter [cell size] *vs* fluorescence intensity [*opvAB::gfp* expression]).

Bacteriophage challenge

Overnight cultures were diluted 1:100 in 3 ml LB and grown in aeration by shaking at 37ºC until they reached an optical density $O.D._{600}$ ~0.3. One hundred µl of a bacteriophage lysate (P22 H5, 9NA, or Det7) were added (M.O.I. ≥10), and $O.D._{600}$ was subsequently measured at 1 h intervals.

Virulence assays

Eight-week-old female BALB/c mice (Charles River Laboratories, Santa Perpetua de Mogoda, Spain) were inoculated with pairwise combinations of the wild type, an $OpvAB^{ON}$ strain, and a Δ*opvAB* strain at a 1:1 ratio. Bacterial cultures were previously grown overnight at 37°C in LB without shaking. Oral inoculation was performed by feeding the mice with 25 µl of PBS containing 0.1% lactose and 10^8 bacterial colony-forming units (c.f.u.). Intraperitoneal inoculation was performed with 10^4 c.f.u. in 200 µl of PBS. Bacteria were recovered from the spleen and the liver of infected mice at 2 days post-infection (intraperitoneal challenge) or 5 days post-infection (oral challenge). A competitive index (CI) was calculated as described elsewhere [320]. To permit strain

discrimination, ATCC 14208 was tagged with *trg*::MudJ (Km^r), an allele that is neutral for virulence [321]. When necessary, cross-streaking on green plates with P22 H5 was used to discriminate phage-resistant isolates [301].

Purification of OxyR protein

For 6xHis-$OxyR^{C199S}$ purification, plasmid pIZ1885 was transformed into *E. coli* M15 [pREP4] (Qiagen, Valencia, CA). M15/pIZ1885 was grown in LB broth containing ampicillin, and expression of 6xHis-$OxyR^{C199S}$ was induced with 1 mM IPTG. After 3 h of induction, cells were centrifuged and resuspended in 10 ml of lysis buffer (20 mM Tris, 300 mM NaCl, 10 mM imidazole) per g of pelleted cells, and were lysed by sonication. The suspension was centrifuged at 10,000 x g for 30 min and the supernatant containing the soluble fraction of 6xHis-$OxyR^{C199S}$ was transferred to a HisTrap HP nickel affinity chromatography column (GE Healthcare, Wauwatosa, WI). The column was washed with 4 ml of lysis buffer, 4 ml of washing buffer (20 mM Tris, 300 mM NaCl, 30 mM imidazole) and 4 ml of the same buffer with 50 mM imidazole. Protein elution was performed with 3 ml of elution buffer (20 mM Tris, 300 mM NaCl, 300 mM imidazole). Elution fractions enriched in 6xHis-$OxyR^{C199S}$ were selected and combined. Imidazole was removed by transferring to an Amicon® ultra centrifugal filter (Merck Millipore, Darmstadt, Germany) and washing with storage buffer (20 mM Tris, 300 mM NaCl, 10% glycerol) or by dialyzing in cellulose membranes (Sigma-Aldrich, St. Louis, MO). 6xHis-$OxyR^{C199S}$ was either used immediately or frozen in liquid nitrogen and stored at -80ºC.

Gel mobility shift assay

A DNA fragment containing predicted OxyR binding sites in the *opvAB* regulatory region and labelled with 6-carboxyfluorescein (6-FAM) was prepared by PCR amplification using primers *FAMGATClargo-5* and *FAMGATClargo-3*. The PCR product was purified with the Wizard® SV Clean-Up System (Promega, Madison, WI). The *envR* control fragment was prepared using primers *envR-For-Dnase* and *envR-Rev-Dnase* [322], and was kindly provided by Elena Espinosa. Thirty five ng were used for

each reaction. The FAM-labelled probe was incubated at room temperature for 30 min with increasing concentrations of purified 6xHis-OxyR^{C199S} in a final volume of 20 µl with 1x OxyR binding buffer [25 mM Tris-HCl pH 7.5, 50 mM KCl, 5 mM $MgCl_2$, 5% glycerol, 50 µg/ml bovine serum albumin (BSA), 1 mM DTT, 1 µg/ml poly(dI-dC)]. Protein-DNA complexes were subjected to electrophoresis at 4ºC in a 5% non-denaturing polyacrylamide gel in Tris-glycine-EDTA buffer (25 mM Tris-HCl pH 7.5, 380 mM glycine, 1.5 mM EDTA). The gel was then analysed in a FLA-5100 Scanner (Fujifilm, Tokyo, Japan).

DNA methylation *in vitro*

PCR fragments were methylated in vitro using Dam methylase (New England Biolabs, Ipswich, MA) according to the manufacturer's instructions and subsequently digested with MboI (New England Biolabs). The undigested product was purified using the Wizard® SV Clean-Up system (Promega, Madison, WI).

DNase I footprinting

DNA probes containing the *opvAB* promoter and the upstream regulatory region, labelled with 6-carboxyfluorescein (6-FAM) at the opposite ends, were prepared by PCR amplification using the primer pairs *FAMGATClargo-5* + *FAMGATClargo-3* and *seqGATC-5* + *FAMGATClargoconFAM-3*. Dam-methylated versions of the probes were prepared as described above. DNase I footprinting was performed as described elsewhere [323] with minor modifications. DNase I footprinting reactions were performed in 15 µl reaction volumes containing 1x OxyR binding buffer and 2 µM 6xHis-OxyR^{C199S}. The binding reaction was allowed to equilibrate at room temperature for 30 min. One µl (0.05 units) of DNase I (Roche Farma, Barcelona, Spain) was then added, mixed gently and incubated at room temperature for 5 min. The reaction was stopped by addition of 2 µl EDTA 100 mM followed by vigorous vortexing and thermal denaturation at 95ºC for 10 min. Digestion products were desalted using MicroSpin G-25 columns (GE Healthcare, Wauwatosa, WI) and analysed on an ABI 3730 DNA

Analyzer along with GeneScan 500-LIZ size standards (Applied Biosystems, Foster City, CA).

SMRT sequencing

Cultures of *S. enterica* were enriched in OpvAB^{ON} cells if needed. SMRTbell™ template libraries were prepared according to the instructions from Pacific Biosciences (Menlo Park, CA), following the procedure and checklist for 1 kb template preparation and sequencing. Briefly, for preparation of 600 base pair libraries, 4 µg of genomic DNA were sheared in microTubes using adaptive focused acoustics (Covaris, Woburn, MA). Size range was monitored on an Agilent 2100 Bioanalyzer f (Agilent Technologies, Santa Clara, CA). DNAs were end-repaired and ligated to hairpin adapters applying components from the DNA/Polymerase Binding Kit 2.0 from Pacific Biosciences. Reactions were carried out according to the manufacturer´s instructions. SMRTbell™ templates were exonuclease-treated for removal of incomplete reaction products. A mixture of exonuclease III and exonuclease VII (Affymetrix, High Wycombe, UK) was utilized. Conditions for annealing of sequencing primers and binding of polymerase to purified SMRTbell™ templates were assessed with the Calculator in RS Remote, Pacific Biosciences. Six movies were taken for both states on the PacBio *RSII* (Pacific Biosciences, Menlo Park, CA) using P4-C2 chemistry at 2 h collection time. Secondly, stationary phase cultures were enriched for OpvAB^{ON} cells and libraries were prepared as given above. In this case five movies were taken using P4-C2 chemistry at 3 h collection time.

Resulting data were mapped to the complete genome sequence (GenBank accession number CP001363.1) of *Salmonella enterica* subsp. *enterica* serovar Typhimurium strain ATCC 14028, using the BLASR algorithm (PMID 22988817) as implemented in Pacific Biosciences' SMRT Portal 2.1.0 within the "RS_Modification_and_Motif_Analysis.1" protocol applying default parameter settings. According to the setup of the experiment the secondary analysis jobs were named "OpvAB^{OFF}" and "OpvAB^{ON}". Besides the global methylation pattern, the methylation status of four GATC sites upstream of the *opvAB* operon was inferred using SMRT View investigating the chromosomal positions 2,361,489 and 2,361,490

($GATC_1$), 2,361,439 and 2,361,440 ($GATC_2$), 2,361,416 and 2,361,417 ($GATC_3$) and 2,361,366 and 2,361,367 ($GATC_4$).

Southern blot

Genomic DNA was isolated by phenol extraction and ethanol precipitation from stationary cultures in LB ($O.D._{600}$ ~4). Sixteen µg of each DNA sample were digested with HaeIII and AccI (New England Biolabs, Ipswich, MA), purified and divided into four fractions, three of which were subsequently digested with DpnI, MboI or Sau3AI (New England Biolabs). After digestion the samples were run in a 2% TAE-agarose gel at 100 V for 2 hours. After electrophoresis, the DNA was denatured by treatment of the gel in acid conditions (0.25 M HCl, two washes 15 min each), followed by alkalinization (0.5 M NaOH, 1.5 M NaCl) and neutralization (0.5 M Tris, 1.5 M NaCl, pH 7.5; two washes, 30 min each). The gel was then washed in SSC 10x buffer (1.5 M NaCl, 150 mM trisodium citrate, pH 7) and the DNA was transferred by vacuum to an Amersham Hybond-N+ membrane (GE Healthcare, Wauwatosa, WI) using a model 785 Vacuum Blotter (Bio-Rad, Hercules, CA). The DNA in the membrane was then immobilized by UV crosslinking. A radioactive probe was prepared by PCR using dCTP [α-^{32}P] (Perkin Elmer, Waltham, MA) and oligonucleotides *2208mut1DIRnuevo* and *2208mut4INVnuevo*. After the PCR reaction, non-incorporated nucleotides were removed by treatment in a Sephadex G-25 column (illustra MicroSpin G-25 columns, GE Healthcare, Wauwatosa, WI) following manufacturer's instructions. Prior to hybridization the double-stranded DNA probe was denatured by heating at 95ºC for 3 min, followed by incubation on ice. Hybridization with the probe was performed overnight at 42ºC in hybridization buffer (0.5 M sodium phosphate pH 7.2, 10 mM EDTA, 7% SDS). Excess probe was removed with washing buffer (40 mM sodium phosphate pH 7.2, 1% SDS) at 38ºC (three washes, 30 min each). The membrane was developed using a FLA-5100 Scanner (Fujifilm, Tokyo, Japan).

Statistical analysis

The Student's *t* test was used to determine if the differences in our experiments were statistically significant.

RESULTS

CHAPTER I

STM2209-STM2208 (*opvAB*): a phase variation locus of *Salmonella enterica* involved in control of O-antigen chain length

STM2209-STM2208 (*opvAB*) is a *S. enterica*-specific locus

S*TM2209* and *STM2208* are contiguous loci annotated as putative protein-coding genes in the chromosome of *Salmonella enterica*. The *STM2209* and *STM2208* ORFs are conserved in *Salmonella enterica* serovar Typhimurium strains ATCC 14028, SL1344, and LT2 (GenBank accession numbers CP001363.1, FQ312003.1 and AE006468.1, respectively), in the vicinity of the sugar transport gene *setB* [324]. The *STM2209* and *STM2208* ORFs are also conserved in other *Salmonella enterica* serovars but not in *Salmonella bongori* nor in the genera *Escherichia* and *Shigella*. Alignment of the predicted amino acid sequences of STM2209 and STM2208 using BLASTP [325] detected no obvious homologs of *STM2209-STM2208* outside *Salmonella enterica*. A diagram of the chromosome region in *Salmonella enterica* and related Enterobacteriaceae is shown in **Figure C1.1**.

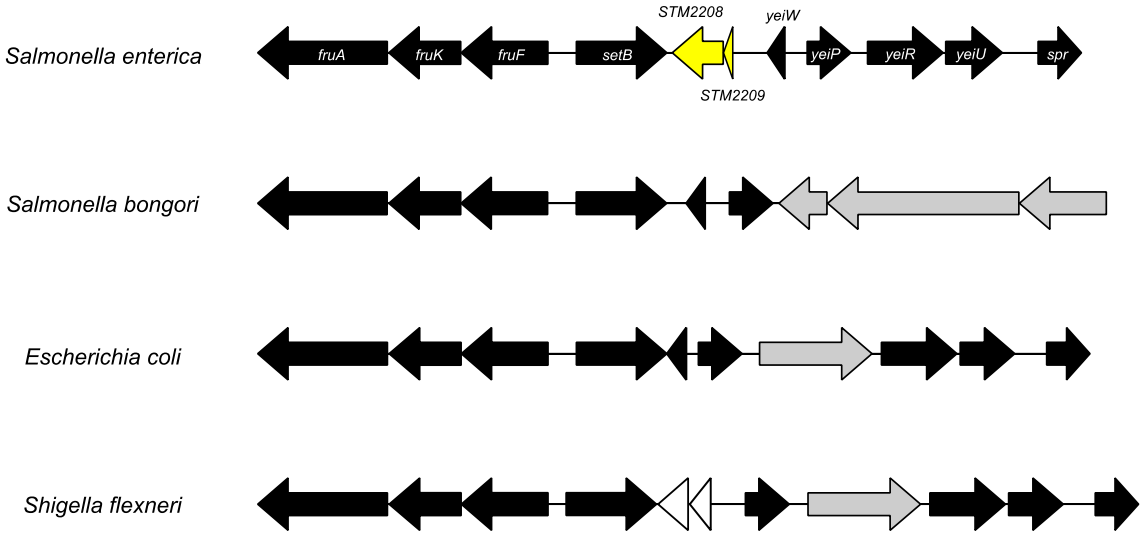

Figure C1.1. Diagram of the region containing *STM2209-STM2208* on the *Salmonella enterica* chromosome. The homologous regions of *Salmonella bongori*, *E.coli*, and *Shigella flexneri* are also shown. The *STM2209-STM2208* operon is shown in yellow. Black arrows represent conserved genes. White arrows represent non conserved genes. Grey arrows represent genes found at a different chromosome location on the *S. enterica* chromosome.

Both *STM2209* and *STM2208* have low G+C content (37% for *STM2209* and 38% for *STM2208*) compared to both the average of the region (53%) and that of the *Salmonella enterica* genome (52%) [326]. Because horizontally acquired genes often have distinctive base composition, specifically low G+C content [327,328], these observations suggest that *STM2209-STM2208* may have been acquired by horizontal gene transfer. The organization of the *STM2209* and *STM2208* ORFs suggests that they may be part of a single transcriptional unit: both coding sequences are on the same DNA strand, and are separated by only one nucleotide. Genome sequence analysis *in silico* predicts that STM2209 may encode a small peptide of 40 amino acids, while STM2208 may be a larger protein product of 221 amino acids. *In silico* analysis of protein structure using the TMHMM transmembrane prediction software [329] predicts the existence of one transmembrane domain in STM2209, and two transmembrane domains in STM2208 (**Figure C1.2**). *In silico* analysis also indicates that STM2208 shares a domain with proteins belonging to the Wzz superfamily of O-antigen chain length regulators. This family includes proteins involved in lipopolysaccharide biosynthesis that confer a modal distribution of chain length on the O-antigen component of lipopolysaccharide [58]. This domain is also found in bacterial tyrosine kinases [330]. Because *STM2209-STM2208* was later confirmed to be involved in O-antigen chain length control and it is subject to phase variation (see below), in the course of this work we renamed the *STM2209-STM2208* locus as *opv* (for O-antigen phase variation) so that the *STM2209* gene is henceforth known as *opvA*, and the *STM2208* gene as *opvB*.

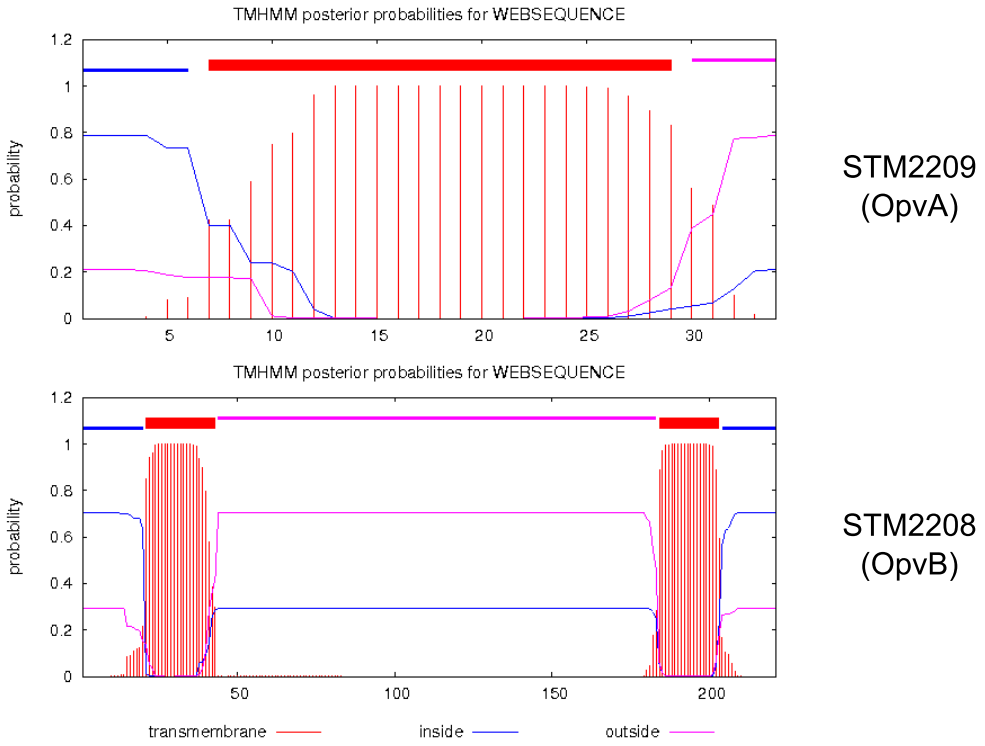

Figure C1.2. Prediction of STM2209 (OpvA) and STM2208 (OpvB) transmembrane domains using the the TMHMM transmembrane prediction software. Red bars indicate one transmembrane domain in STM2209 and two transmembrane domains in STM2208. The x axis indicates amino acid residues.

Expression of the *opvAB* locus is regulated by Dam methylation

A previous study showed that *opvA* and *opvB* are expressed at higher levels (13 fold for *opvA* and 8 fold for *opvB*) in a *S. enterica* Dam$^-$ mutant [300]. These observations suggested that expression of the putative *opvAB* transcriptional unit might be repressed by Dam methylation. To confirm Dam-dependent regulation, transcriptional and translational *lac* fusions were constructed in both genes. Protein variants tagged with the 3xFLAG epitope were also constructed. The effect of Dam methylation on *opvAB* expression was monitored by β-galactosidase assays, qRT-PCR, and Western blotting in isogenic Dam$^+$ and Dam$^-$ strains. Higher level of β-galactosidase activity, higher amount of retrotranscribed *opvAB* mRNA, and increased level of the OpvB-3xFLAG product were detected in the Dam$^-$ background (**Figure C1.3**). The OpvA-3xFLAG product was easily detected in a Dam$^-$ background but was hardly visible in the Dam$^+$ background, presumably due the combined effects of its low level of expression and its small size. Although the extent of derepression differed slightly depending on the

method, expression of *opvAB* was significantly higher in a Dam$^-$ background in all experiments. These results confirm that Dam methylation represses *opvAB*. Furthermore, our ability to detect Dam-dependent regulation with both transcriptional *lac* fusions and qRT-PCR suggests that Dam-dependent regulation of *opvAB* may be transcriptional.

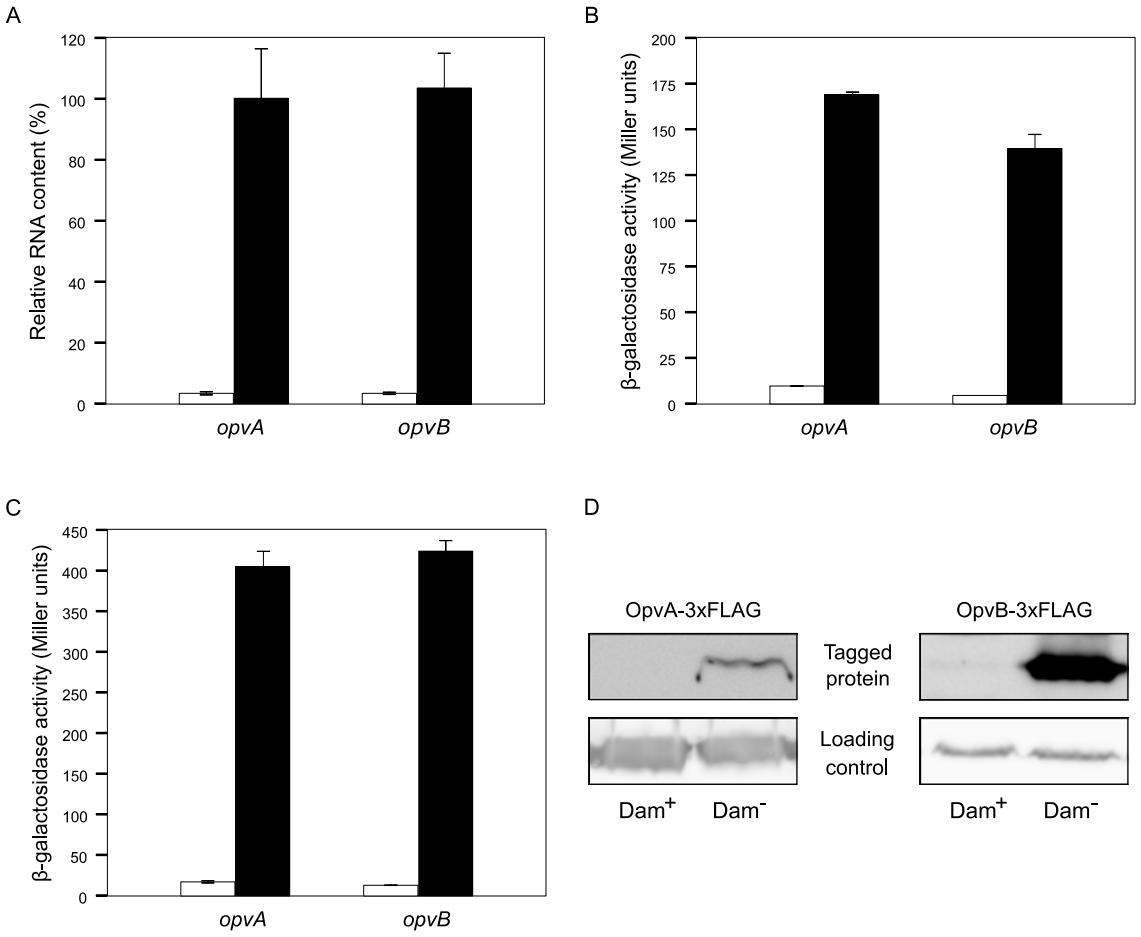

Figure C1.3. Regulation of *opvAB* by Dam methylation. A. Levels of *opvA* and *opvB* mRNAs, measured by qRT-PCR (Dam$^+$: white histograms; Dam$^-$: black histograms). Level of *opvA* mRNA in Dam$^-$ background is considered 100%. Values are averages and standard deviations from 7 independent experiments. **B.** β-galactosidase activity of transcriptional *opvA*::*lac* and *opvB*::*lac* fusions in Dam$^+$ and Dam$^-$ backgrounds (white and black histograms, respectively). Values are averages and standard deviations from 3 independent experiments. **C.** β-galactosidase activities of translational *opvA*::*lac* and *opvB*::*lac* fusions in Dam$^+$ and Dam$^-$ backgrounds (white and black histograms, respectively). Values are averages and standard deviations from 3 independent experiments. **D.** Western blot analysis of OpvA-3xFLAG and OpvB-3xFLAG proteins in Dam$^+$ and Dam$^-$ backgrounds.

Characterization of the *opvAB* transcriptional unit

To characterize the *opvAB* transcriptional unit, we mapped the 5' terminus of the putative *opvAB* transcript using primer extension (**Figure C1.4**). Because *opvA* and *opvB* are expressed at low levels in Dam$^+$ *S. enterica* [300], a DNA fragment containing the region upstream of *opvAB* and part of the coding sequence of *opvAB* was cloned on the pGEM-T multicopy vector to obtain higher amounts of transcript(s). The resulting plasmids (pIZ1758 and pIZ1759) were introduced in the wild type strain, and two primer extension reactions were performed. One reaction was primed by an oligonucleotide complementary to *opvA* (*PE2209*), and the second reaction by an oligonucleotide complementary to *opvB* (*PE2208*). Both reactions yielded extension products with identical 3' ends (**Figure C1.4**), indicating the existence of a single transcription initiation site, six nucleotides upstream of the start codon of *opvA* proposed in the XBASE (http://www.xbase.ac.uk/) and NCBI (http://www.ncbi.nlm.nih.gov/) databases. A DNA sequence reminiscent of a canonical ribosome-binding site is however missing in this putative mRNA organization. For this reason, we propose that translation of *opvA* may be actually initiated at position +25, 10 nucleotides downstream a putative ribosome binding site (5' TGTGG 3'). This hypothesis is supported by additional evidence: a translational *lac* fusion constructed upstream +25 proved to be non functional: β-galactosidase activity was not detected in a Dam$^-$ background. Altogether, these observations may indicate that OpvA consists of 34 amino acids and not 40 amino acids as described in the *Salmonella enterica* ATCC 14028 genome annotation.

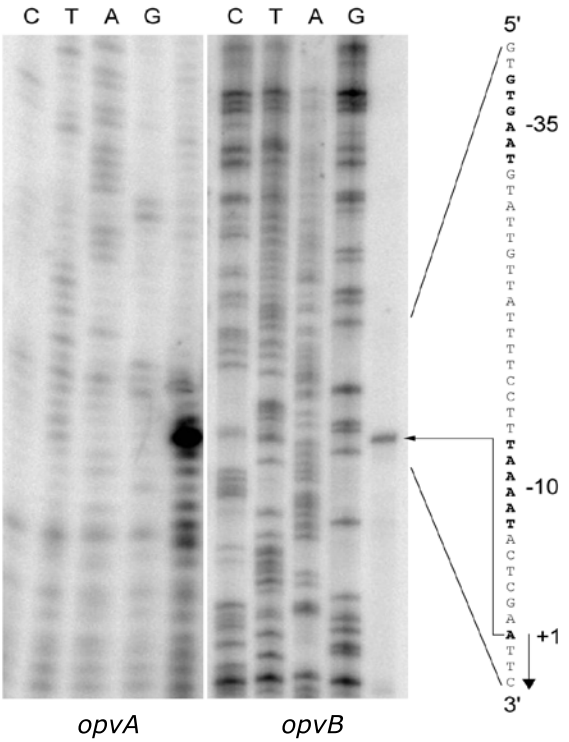

Figure C1.4. Identification of the transcription initiation site of *opvAB* by primer extension. Putative -35 and -10 promoter modules and the +1 site are shown in boldface. The transcription initiation site is indicated by an arrow.

In silico analysis of the DNA sequence upstream of the +1 site identified DNA sequences with features similar to those of canonical, sigma^{70}-dependent promoters [331]: (i) a putative -10 module including the motif 5' TAAAAT 3', which shows 5/6 matches with the consensus sequence [331]; (ii) a putative spacer, 17 nucleotides long; and (iii) a 5' GTGAAT 3' sequence defining a putative -35 module, with 3/6 matches with the consensus sequence [331]. We propose that *opvA* and *opvB* are co-transcribed from this promoter, an hypothesis consistent with the observation that the OpvA and OpvB products are co-expressed (**Figure C1.3**).

Identification of OxyR as a regulator of *opvAB*

A genetic screen based on the T-POP3 transposon [332] was used to search for positive regulators of *opvAB*. For this purpose, a Dam$^-$ strain carrying a *lac* translational fusion in *opvB* (SV5683) was used. This strain forms deep blue colonies on LB supplemented with X-gal. Isolates carrying T-POP3 insertions were selected on LB + tetracycline +

kanamycin + X-gal, and white colonies were sought. Only a small white colony was obtained in the screen. Cloning and sequencing of T-POP3 boundaries indicated that T-POP3 had inserted in the *oxyR* gene. OxyR$^-$ mutants are severely impaired to form colonies on LB plates [333], thus explaining the small colony size of the isolate. However, the isolate formed large colonies on LB + catalase, a standard procedure that permits colony formation by OxyR$^-$ mutants [333]. To confirm that *oxyR* loss-of-function abolished *opvAB* expression in a Dam$^-$ background, the *oxyR* gene was disrupted using lambda Red recombineering. The resulting strain (SV5925), which carries a null *oxyR* allele, was used in further experiments.

Analyses of β-galactosidase activity and Western blotting showed that expression of *opvAB* is virtually abolished in an OxyR$^-$ background (**Figure C1.5**). As above (**Figure C1.4**), high levels of β-galactosidase and of the OpvA-3xFLAG and OpvB-3xFLAG products were detected in the Dam$^-$ background only. These experiments indicate that OxyR is essential for the expression of *opvAB*. Interestingly, putative OxyR binding sites are found in the promoter region of *opvAB* (see below).

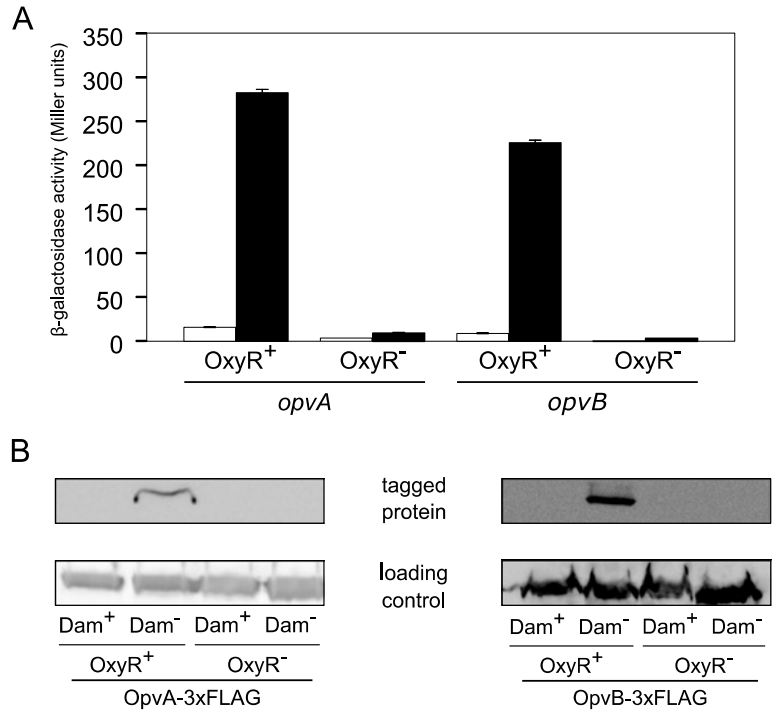

Figure C1.5. Regulation of *opvAB* expression by Dam methylation and OxyR. A. Effect of an *oxyR* null mutation on the β-galactosidase activity of translational *opvA*::*lac* and *opvB*::*lac* fusions in Dam$^+$ and Dam$^-$backgrounds (white and black histograms, respectively). Values are averages and standard deviations from 3 independent experiments. **B.** Western blot analysis of the effect of an *oxyR* null mutation on the levels of OpvA-3xFLAG and OpvB-3xFLAG proteins in Dam$^+$ and Dam$^-$ backgrounds.

OxyR is a global transcription factor that can sense oxidative stress by direct oxidation. In the oxidized state, OxyR activates the expression of oxidative stress-responding genes [84]. However, OxyR also acts as a transcriptional regulator irrespective of its oxidation state. In the absence of oxidative stress, OxyR remains mostly in the reduced form due to the reducing environment of the cell [91]. Several observations suggested that the oxidative state of OxyR is not relevant for *opvAB* regulation. One was that an H_2O_2 concentration sufficient to promote the expression of genes belonging to the classical OxyR regulon (genes activated by oxidative damage) showed no effect on the expression of *opvAB*. Furthermore, the spacing between the half sites in the putative OxyR binding sites described below is consistent with specific binding of the reduced form of OxyR [90]. To determine the effect of oxidation of OxyR upon *opvAB* expression, we constructed a point mutant version of the *oxyR* gene (strain SV6397). The resulting $OxyR^{C199S}$ protein is locked in the reduced form as it cannot form the disulfide bond required for oxidation [90,91]. Dam^+ and Dam^- strains harboring this mutation showed levels of *opvAB* expression similar to those described above for strains carrying the wild type *oxyR* allele. These observations suggest that oxidation of OxyR is not necessary for *opvAB* expression.

opvAB expression undergoes phase variation under the control of Dam methylation and OxyR

In the course of our experiments with strains carrying *opvA::lac* or *opvB::lac* fusions in a wild type background, we detected phenotypic heterogeneity when culture aliquots were spread on plates containing X-gal. These strains formed white colonies that later turned pale blue, indicating low expression of *opvA* and *opvB*. However, deep blue colonies were also seen, especially on plates that contained high numbers of colonies (e. g., ≥ 1,000 colonies). Whenever a blue colony was isolated and streaked out for single colonies, a mixture of white and blue colonies was obtained. This observation suggested that *opvAB* expression might undergo phase variation, and that switching from OFF to ON might occur at lower frequencies than switching from ON to OFF.

Phase variation frequencies in the *opvAB* locus were calculated using the formula *(M/N)/g* where *M* is the number of cells that underwent a phase transition, *N* the total number of cells, and *g* the total number of generations that gave rise to the colony [317]. An *opvB::lac* translational fusion was used for these experiments. The frequency of OFF→ON transition was estimated to be (6.1 ± 1.7) x 10^{-5} per cell and generation. The ON→OFF switching rate was around 1,000-fold higher: (3.7 ± 0.1) x 10^{-2} per cell and generation. Phase variation of *opvAB* expression was also unaffected by the oxidation state of OxyR. The OFF→ON transition rate calculated in LB + catalase in an *oxyR*^{C199S} background was (1.4 ± 0.3) x 10^{-4} compared to (1.2 ± 0.1) x 10^{-4} in the wild type. The ON→OFF transition rate was also virtually identical: (3.2 ± 0.1) x 10^{-2} compared to (3.0 ± 0.1) x 10^{-2} in the wild type

Phase variation was abolished in both Dam$^-$ and OxyR$^-$ mutants (**Figure C1.6**). Lack of Dam methylation locks *opvAB* expression in the ON state, and lack of OxyR locks *opvAB* expression in the OFF state. An *oxyR* mutation is epistatic over a *dam* mutation, an observation that may indicate that activation of *opvAB* transcription by OxyR is Dam-methylation sensitive. However, both Dam methylation and OxyR are needed to establish phase-variable expression of *opvAB*.

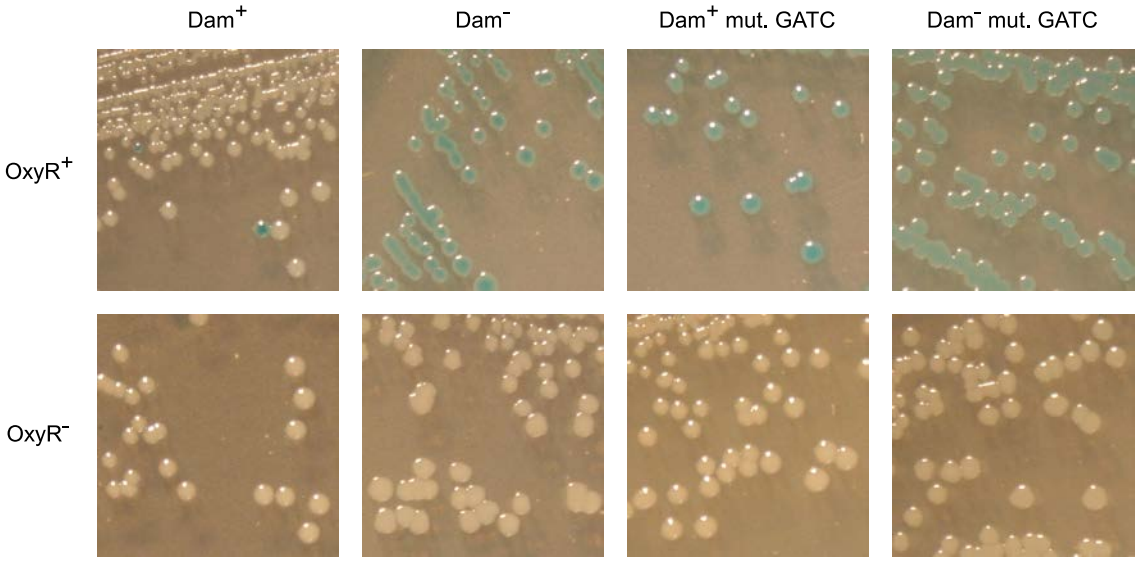

Figure C1.6. Visual observation of phase variation on LB + X-gal plates in strains carrying an *opvB*::*lac* fusion in different backgrounds. Strains in the upper row are SV5679 (Dam$^+$ OxyR$^+$), SV5683 (Dam$^-$ OxyR$^+$), SV7031 (Dam$^+$ OxyR$^+$ mut. GATC) and SV7032 (Dam$^-$ OxyR$^+$ mut. GATC). OxyR$^-$derivatives (SV5989, SV5990, SV7232 and SV7233) are shown in the lower row.

Site-directed mutagenesis of GATC sites upstream of the *opvAB* promoter abolishes phase variation

In silico analysis of the DNA sequence upstream of the *opvAB* promoter revealed the existence of 4 GATC sites arranged in a symmetrical pattern (**Figure C1.7A**). In addition, the region contains two putative OxyR binding sites very similar to the consensus sequence [91]. These sites overlap with GATC sites number 2 and 4 respectively (**Figure C1.7A**).

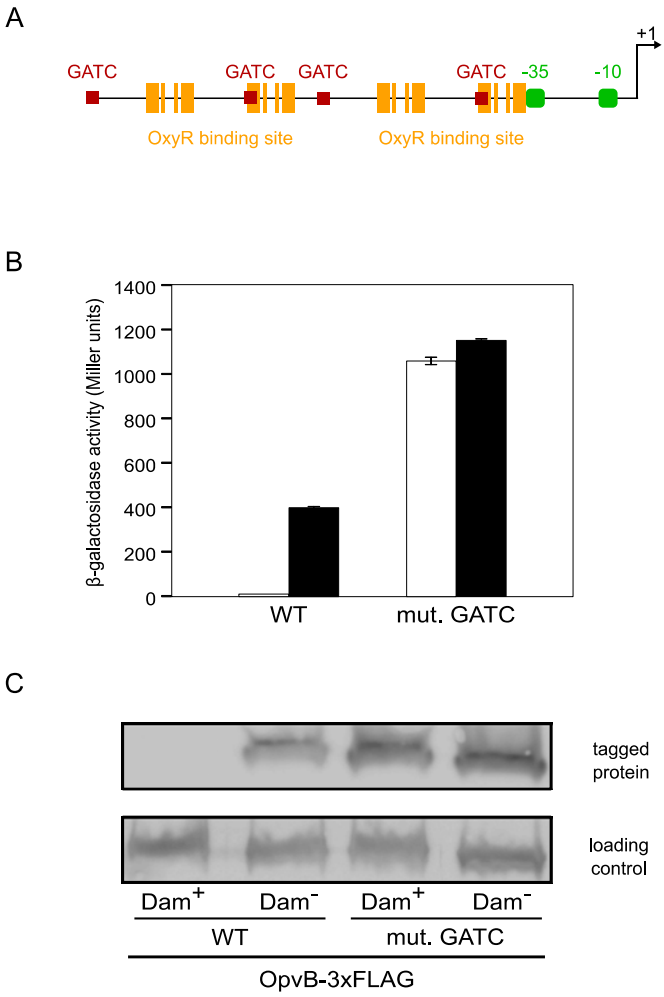

Figure C1.7. Effect of GATC mutations on *opvAB* expression. A. Diagram of the regulatory region of *opvAB*, showing GATC sites (red squares), putative OxyR-binding-sites (orange bars), putative -35 and -10 modules (green boxes) and the transcription initation site (black arrow). **B.** Effect of eliminating the 4 GATC sites upstream of the *opvAB* promoter on *opvAB* expression, monitored by comparing the β-galactosidase activity of a translational *opvB*::lac fusion in Dam^+ and Dam^- backgrounds (white and black histograms, respectively). Values are averages and standard deviations from 6 independent experiments. **C.** Effect of eliminating the 4 GATC sites upstream of the *opvAB* promoter on *opvAB* expression, monitored by Western blot analysis of OpvB-3xFLAG levels in different backgrounds.

Because of the pleiotropy of *dam* mutations, alteration of gene expression in Dam$^-$ mutants does not necessarily indicate direct Dam-dependent control [122]. To confirm that Dam methylation directly controls *opvAB* expression, the GATC sites present in the promoter region of *opvAB* were eliminated by site-directed mutagenesis. If *opvAB* repression by Dam methylation depends directly on methylation of the GATC sites within the *opvAB* regulatory region, we reasoned, elimination of the GATC sites should lock *opvAB* expression in the ON state. To test this prediction, point mutations were engineered to transform the *opvAB* 5'GATC3' sequences to 5'CATC3' sequences, which are not a substrate for Dam methylase activity (strain SV6401). Furthermore, the four base pair substitutions introduced in the *opvAB* regulatory region do not destroy known critical regions of the OxyR binding sequence [90].

β-galactosidase activity assays and Western blotting analysis proved that regulation by Dam methylation was abolished when the GATC sites were eliminated (**Figure C1.7, A and B**). Expression of *opvAB* was ~2 fold higher in the GATC-less mutant (SV7031) than the Dam$^-$ mutant (SV5683) (**Figure C1.7, A and B**), but *opvAB* expression was locked in the ON state in both strains (**Figure C1.6**). Construction of strain SV6401 thus permitted to analyze the consequences of *opvAB* constitutive expression avoiding the pleiotropic effects of *dam* mutations (see below). From now on this strain will be referred to as *opvAB*-constitutive or OpvAB^{ON}.

The OpvA and OpvB gene products are proteins located in the inner (cytoplasmic) membrane of *Salmonella enterica*

The subcellular location of OpvA and OpvB was investigated using 3xFLAG-tagged variants. Electrophoretic separation of cell fractions (cytosol, cytoplasmic membrane and outer membrane) was performed, and Western analysis of the separated protein preparations was carried out with a commercial anti-FLAG antibody. The results unambiguously showed that OpvA and OpvB are located in the *S. enterica* inner (cytoplasmic) membrane (**Figure C1.8**).

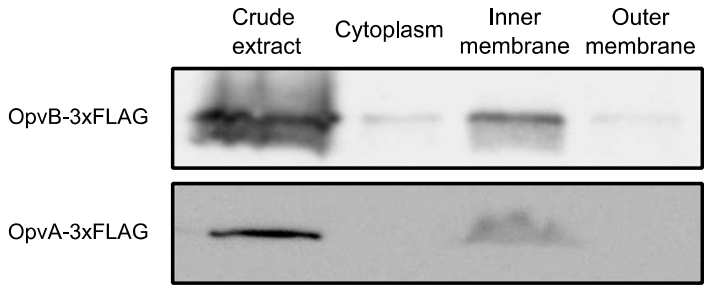

Figure C1.8. Distribution of OpvA and OpvB proteins tagged with a 3xFLAG epitope in subcellular fractions of *S. enterica*. Anti-FLAG Western hybridization is shown for three fractions: cytoplasm, inner membrane, and outer membrane.

Localization of the OpvA and OpvB proteins in the envelope

To further determine the location and distribution of OpvA and OpvB, a chromosomal *opvB*::mCherry fusion was constructed downstream of the *opvB* gene (so that the strain remains $OpvAB^{+}$). In a wild type background, expression of *opvB*::mCherry was low in most cells (**Figure C1.9A**). However, rare cells with high levels of expression of *opvB*::mCherry were detected (**Figure C1.9A**), an observation consistent with the occurrence of phase variation skewed towards the OFF state. Expression of *opvB*::mCherry was also monitored in an *opvAB*-constitutive ($OpvAB^{ON}$) strain engineered by elimination of GATC sites upstream of the *opvAB* promoter. In an $OpvAB^{ON}$ background, all cells displayed high levels of fluorescence, similar to those of the rare fluorescent cells visualized in a wild type background (**Figure C1.9B**). In fluorescent cells, OpvB was seen forming helical intertwining ribbons in the inner membrane (**Figure C1.9, A and B**).

The subcellular distribution of OpvA was examined using a plasmid-borne *opvA*::mCherry fusion. This experimental choice was based on the consideration that construction of an mCherry fusion in the upstream gene *opvA* would likely prevent *opvB* expression because of a polarity effect. In the strain carrying plasmid-borne *opvA*::mCherry, intense fluorescence was observed in all cells (**Figure C1.9C**), presumably because *opvA*::mCherry overexpression from the multicopy plasmid abolished phase variation. This construction was useful, however, to permit clear-cut observation of helical intertwining ribbons formed by OpvA (**Figure C1.9D**).

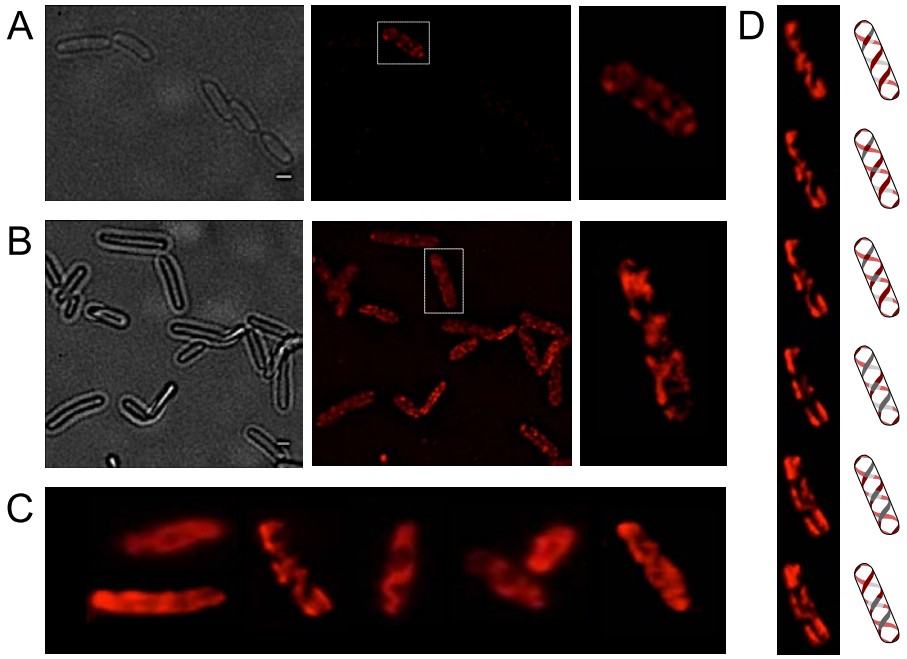

Figure C1.9. Analysis of OpvA and OpvB localization by fluorescence microscopy. A. Localization of OpvB-mCherry in a wild type background. **B.** Localization of OpvB-mCherry in an OpvAB^{ON} strain. In both panels, cells enclosed in boxes are shown with higher magnification on the right. **C.** Localization of plasmid-borne OpvA-mCherry. **D.** Z-stacks of a single cell from panel C accompanied by an idealized representation of the ribbon-like protein distribution. Scale bar: 1 µm.

Evidence for interaction between OpvA and OpvB in the cytoplasmic membrane

OpvA may represent a novel example of a membrane peptide, an emerging class of functional molecules [334,335]. Because certain membrane peptides have been shown to interact with membrane protein partners, we investigated whether OpvA interacts with the inner membrane protein OpvB. To test interaction between OpvA and OpvB *in vivo*, we used the Bacterial Adenylate Cyclase Two-Hybrid (BACTH) assay, a procedure that permits the detection of specific interactions between inner membrane proteins [336]. *opvA* and *opvB* were independently cloned on plasmids pUT18C and pKT25. Four plasmid constructs were obtained (pUT18C-*opvA*, pKT25-*opvA*, pUT18C-*opvB*, and pKT25-*opvB*), and their interaction was tested in an *E. coli* CyaA^{-} mutant (BTH101). Functional complementation was determined by measuring β-galactosidase activity. High levels of β-galactosidase activity were obtained with both plasmid pairs,

compared with the basal activities of the plasmid vectors or with the activity of one fusion protein only (**Figure C1.10**). These results suggest that OpvA and OpvB may interact indeed, an observation consistent with the similar distribution pattern described for OpvA and OpvB.

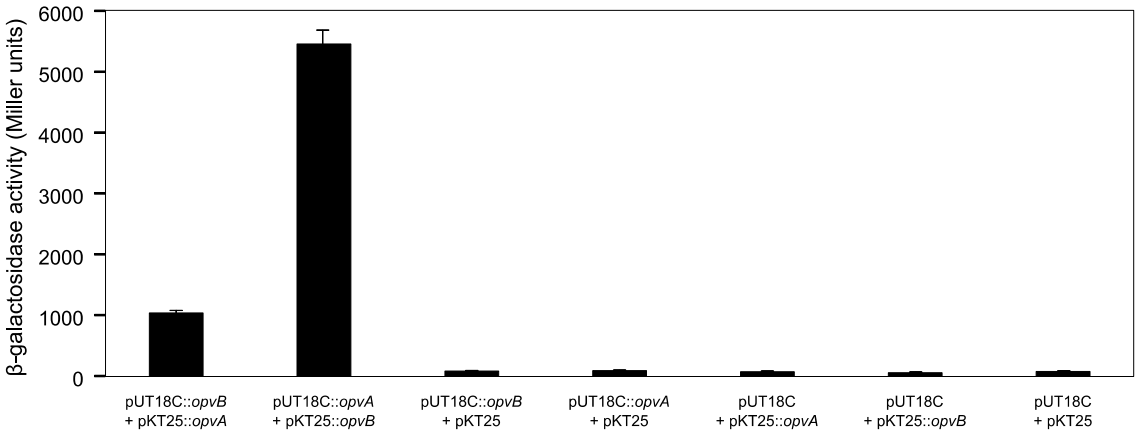

Figure C1.10. Analysis of the *in vivo* interaction between OpvA and OpvB using the BACTH system. The *E. coli* BTH101 strain was co-transformed with plasmids encoding fusion proteins or empty. The basal level of β-galactosidase activity measured with empty vectors was approximately 90 Miller units. Values are averages and standard deviations from 3 independent experiments.

Constitutive expression of *opvAB* reduces P22 adsorption to *S. enterica*

During strain construction experiments by P22 HT transduction, we obtained reduced numbers of transductants whenever the OpvAB^{ON} strain (SV6401) was used as a recipient. This observation, combined with the fact that OpvA and OpvB are components of the cell envelope, raised the possibility that constitutive synthesis of OpvA and OpvB might impair adsorption of bacteriophage P22. To test this hypothesis, we compared the kinetics of P22 adsorption to the wild type strain, to an OpvAB^{ON} strain (SV6401), and to a strain that harbors a deletion of *opvAB* (SV6013). Suspensions of P22 bacteriophage and *S. enterica* were mixed, and samples were taken every two minutes, and centrifuged. The supernatant was subsequently titrated to monitor the presence of unattached phages (**Figure C1.11**). Adsorption of P22 to *S. enterica* cells was found to be severely impaired in the OpvAB^{ON} strain (SV6401), which proved to be largely refractory to phage P22 attachment. In contrast, P22 adsorption remained

unaltered in a strain carrying a *opvAB* deletion (SV6013). These experiments suggest that phase variation of *opvAB* may split clonal populations of *S. enterica* into two subpopulations, one of which is P22-sensitive while the other is P22-resistant.

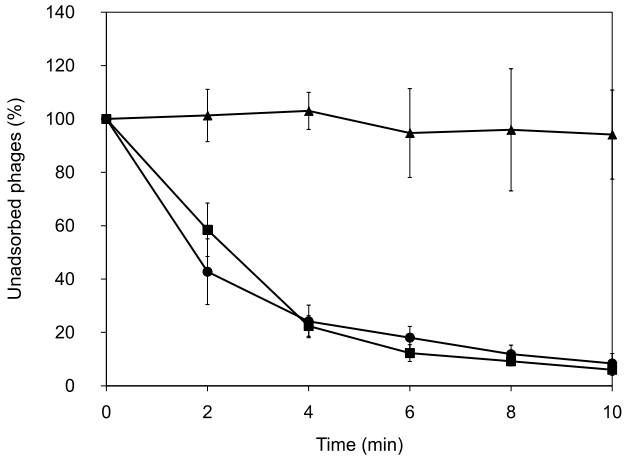

Figure C1.11. Effect of constitutive expression of *opvAB* on adsorption of bacteriophage P22 to *S. enterica*. The efficiency of P22 attachment to *S. enterica* is shown as the percentage of non adsorbed phages relative to the initial number. Strains are represented by squares (wild type), triangles (SV6013, Δ*opvAB*), and circles (SV6401, OpvAB^{ON}). Values are averages and standard deviations from 6 independent experiments.

Constitutive expression of *opvAB* alters chain length distribution in the lipopolysaccharide O-antigen of *S. enterica*

Because phage P22 is known to attatch to the LPS of *Salmonella enterica* to initiate infection [337], we examined whether the OpvAB^{ON} strain (SV6401) showed LPS alterations. Migration of the LPS in polyacrylamide gel is known to be affected by the number and size of repeating oligosaccharide units in long-chain LPS, such that bands in the profile represent progressively larger concatemers of the repeating oligosaccharide units [338]. Comparison of the LPS profiles in strain SV6401 and the wild type revealed drastic alterations in the length of O-antigen chains (**Figure C1.12**). Wild type *Salmonella* LPS shows a bimodal distribution typical of many Enterobacteriaceae, with higher amounts of bands with 16-35 and >100 repeats [49,52,58,339]. Strain SV6401 showed a unimodal distribution, with bands concentrated in the 3-8 repeat range. This short and homogeneous LPS might well

explain reduced phage P22 attachment. No alteration of the LPS profile was detected in a strain carrying a *opvAB* deletion (SV6013), in agreement with its ability to permit a normal level of P22 adsorption (**Figure C1.11**). The main conclusion from these experiments was that expression of *opvAB* alters O-antigen chain length.

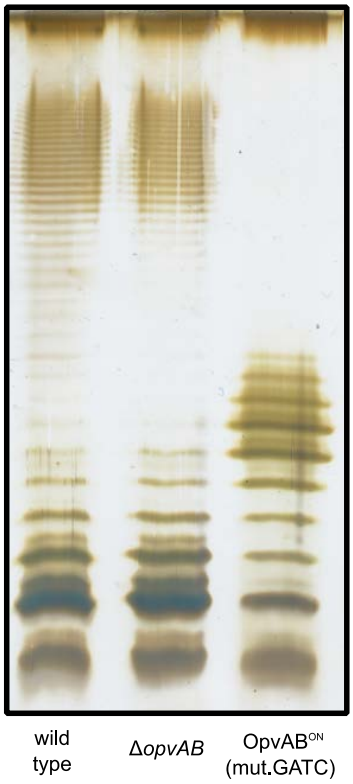

Figure C1.12. Lipopolysaccharide profiles of the wild type strain (lane 1), SV6013 (Δ*opvAB*) (lane 2), SV6401 (OpvAB^{ON}) (lane 3), as observed by electrophoresis and silver staining.

Roles of OpvA and OpvB in control of O-antigen chain length

Constitutive expression of *opvAB* leads to the production of a particular form of O-antigen in the *S. enterica* LPS with a modal length of 3-8 repeat units. To investigate the role of individual OpvA and OpvB proteins in control of O-antigen chain length, non-polar mutations in *opvA* and *opvB* were constructed in the wild type and in an OpvAB^{ON} background. In the wild type, lack of either OpvA or OpvB did not alter the electrophoretic profile of LPS (**Figure C1.13**), an observation consistent with two known facts: the subpopulation of cells that express *opvAB* in wild type *Salmonella* is very small, and an OpvAB^{-} mutant displays an LPS profile identical to that of the wild

type. In contrast, OpvA^{-} OpvB^{ON} and OpvA^{ON} OpvB^{-} mutants showed differences with the parental OpvAB^{ON} strain and also with the wild type:

(i) Absence of OpvB (OpvA^{ON}) yielded a seemingly disorganized LPS with no clear modal length (**Figure C1.13**), reminiscent of the LPS produced in the absence of the modal length regulators Wzz$_{ST}$ and Wzz$_{fepE}$ [52,57,340].

(ii) Absence of OpvA (OpvB^{ON}) yielded an LPS with the modal lengths typically conferred by Wzz$_{ST}$ and Wzz$_{fepE}$ [52] but also showed a preferred OpvAB^{ON} -like modal length in the lower weight band region (**Figure C1.13**).

These observations suggested that the function of OpvA might be to prevent the formation of normal O-antigen so that OpvB could then impose its preferred modal length. To test this hypothesis, LPS structure was analyzed in an OpvA^{-} OpvB^{ON} background in the absence of either Wzz$_{ST}$ or Wzz$_{fepE}$. The results support the view that OpvB needs OpvA to prevent O-antigen formation by customary modal length regulators. In the absence of Wzz$_{ST}$, OpvB alone was able to produce an O-antigen similar to that found in the OpvAB^{ON} strain (**Figure C1.13**). In contrast, lack of Wzz$_{fepE}$ did not seem to facilitate OpvB function, suggesting that OpvB may mainly compete with Wzz$_{ST}$. This preference may be related to the fact that both Wzz$_{ST}$ and OpvB convey relatively short preferred modal lengths: 3-8 for OpvB and 16-35 for Wzz$_{ST}$ [53,57,341] compared with >100 for Wzz$_{fepE}$ [52].

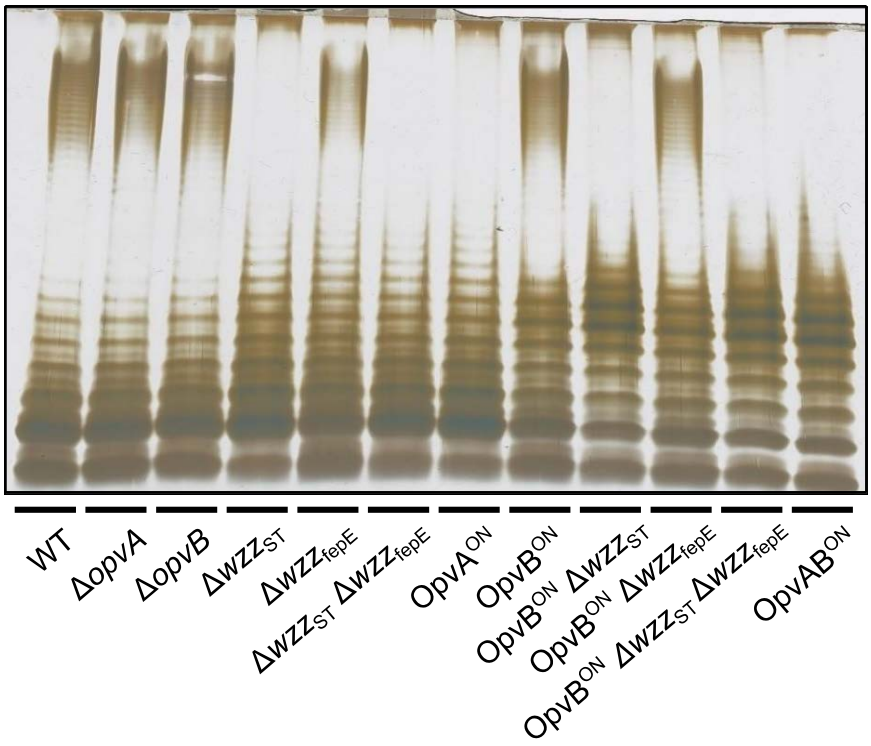

Figure C1.13. Analysis of the roles of OpvA and OpvB in the control of O-antigen chain length. LPS profiles of *S. enterica* strains carrying mutations in *opvAB* and O-antigen length regulator genes wzz_{ST} and wzz_{fepE}, as observed by electrophoresis and silver staining.

CHAPTER II

Epigenetic control of *Salmonella enterica* O-antigen chain-length: a tradeoff between bacteriophage resistance and virulence

Selection of OpvAB^{ON} *S. enterica* cells upon bacteriophage challenge

Because the LPS O-antigen is a typical receptor for bacteriophages [47], we considered the possibility that *opvAB* phase variation might cause resistance to bacteriophages that use the O-antigen as receptor. On these grounds, we tested whether *opvAB* expression resulted in increased *Salmonella* resistance to the virulent phages 9NA [288,311] and Det7 [31,289]. We also tested the historic phage P22, using a virulent mutant to avoid lysogeny [287]. Three strains (wild type, Δ*opvAB* and OpvAB^{ON}) were challenged with 9NA, Det7, and P22. The experiments were carried out by inoculating an exponential culture of *S. enterica* with an aliquot of a phage suspension at a multiplicity of infection ≥10, and monitoring bacterial growth afterwards. The results are shown in **Figure C2.1**, and can be summarized as follows:

(i) Growth of the OpvAB^{ON} strain was not affected by the presence of 9NA, Det7, or P22, suggesting that the strain was resistant to these bacteriophages.

(ii) A culture of the wild type strain became clear 1-2 hours after P22 infection, suggesting that cell lysis had occurred. However, bacterial growth was observed around 4 hours after infection, and was interpreted as occurrence of P22 resistance. Infection with either 9NA or Det7 did not cause clearing but growth retardation. As in P22 infection, growth resumed 4 hours after infection.

(iii) Cultures of the Δ*opvAB* strain infected with 9NA, Det7, or P22 became clear or almost clear. Growth was detected later, albeit with significant delay compared with the wild type. The explanation of this phenomenon is that growth of the Δ*opvAB* strain in the presence of 9NA, Det7, or P22 selects phage-resistant mutants (see below).

A tentative interpretation of these observations was that the wild type strain contained a subpopulation of OpvAB^{ON} cells that survived phage challenge. Because *opvAB* phase variation is skewed towards the OFF state, the small size of the OpvAB^{ON} subpopulation caused growth retardation (albeit to different degrees depending on the phage). In contrast, the OpvAB^{ON} strain grew normally, an observation consistent with the occurrence of phage resistance in the entire bacterial population. This interpretation was supported by analysis of the LPS profiles of wild type and OpvAB^{ON} strains grown in the presence of P22, 9NA, and Det7 until stationary phase ($O.D._{600}$ ~4) (**Figure C2.1**). After phage challenge, the wild type contained an LPS different from the LPS

found in LB (**Figure C2.1D**), and similar or identical to the LPS found in the OpvAB^{ON} strain (**Figure C1.12**). In contrast, the LPS from the OpvAB^{ON} strain did not change upon phage challenge (**Figure C2.1D**).

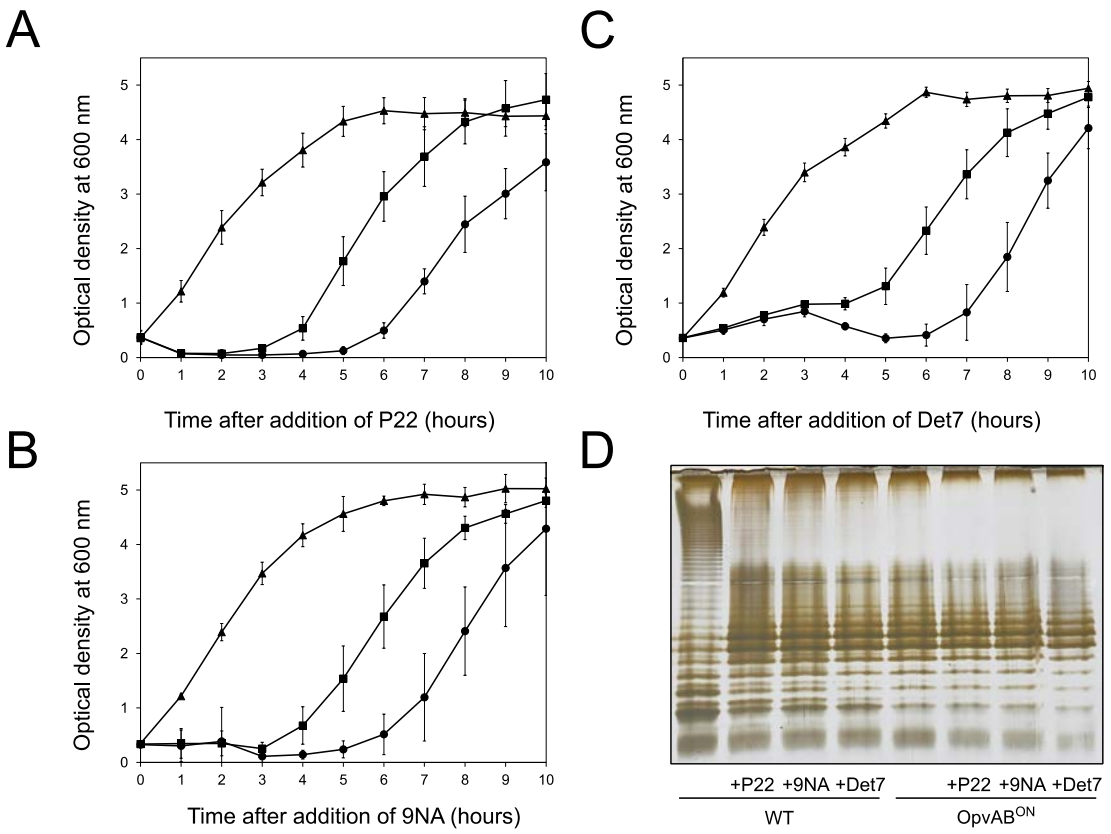

Figure C2.1. Effect of phage challenge on *S. enterica* growth and LPS structure. Growth of the wild type strain (squares), a Δ*opvAB* strain (circles), and an OpvAB^{ON} strain (triangles) in LB + P22 (**A**), LB + 9NA **(B),** and LB + Det7 **(C)**. Values are averages and standard deviations from ≥ 6 independent experiments. **D.** LPS structure of the wild type and OpvAB^{ON} strains after growth in LB, LB + P22, LB + 9NA, and LB + Det7.

Confirmation that challenge of the wild type with P22, 9NA, and Det7 selected OpvAB^{ON} *S. enterica* cells was obtained by flow cytometry analysis (**Figure C2.2**). Expression of *opvAB* was monitored using a green fluorescent protein (*gfp*) fusion constructed downstream *opvB* (so that the strain remains OpvAB^{+}). In the absence of phage, most *S. enterica* cells expressed *opvAB* at low levels; however, a small subpopulation (approximately 0.18%) that expressed *opvAB* at high levels was also detected. Phage challenge yielded mostly *S. enterica* cells with high levels of *opvAB*

expression. These observations provide additional evidence that phages P22, 9NA, and Det7 kill the OpvAB^{OFF} subpopulation, and that OpvAB^{ON} cells overtake the culture.

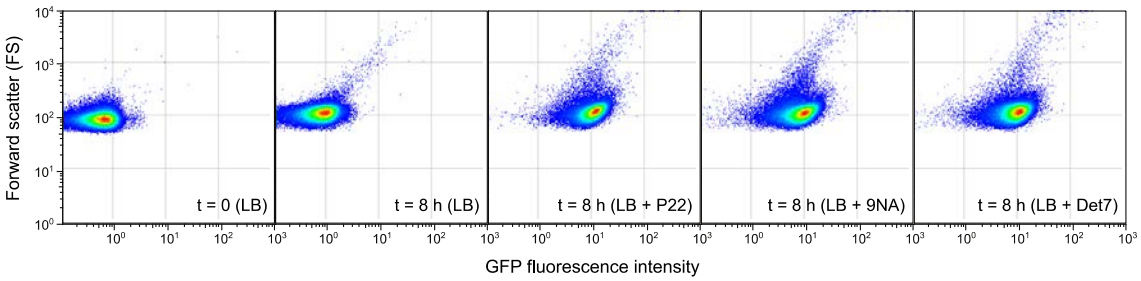

Figure C2.2. Flow cytometry analysis of OpvAB^{OFF} and OpvAB^{ON} subpopulations. GFP fluorescence distribution in an ATCC 14028 derivative carrying an *opvB::gfp* fusion before (t = 0) and after growth in LB, LB + P22, LB + 9NA, and LB + Det7 (t= 8 h).

Reversibility of OpvAB-mediated bacteriophage resistance

If the above model was correct, we reasoned, cessation of phage challenge should permit resuscitation of a phage-sensitive subpopulation as a consequence of *opvAB* phase variation. This prediction was tested by isolating single colonies from cultures in LB + phage. After removal of phage by streaking on green plates, individual isolates were cultured in LB and re-challenged with P22, 9NA, and Det7 (≥ 20 isolates for each phage). All were phage-sensitive and their LPS profile was identical to that obtained before phage challenge. Representative examples are shown in **Figure C2.3**. Unlike the wild type, individual isolates of the Δ*opvAB* strain remained phage-resistant after single colony isolation and were considered mutants (see below).

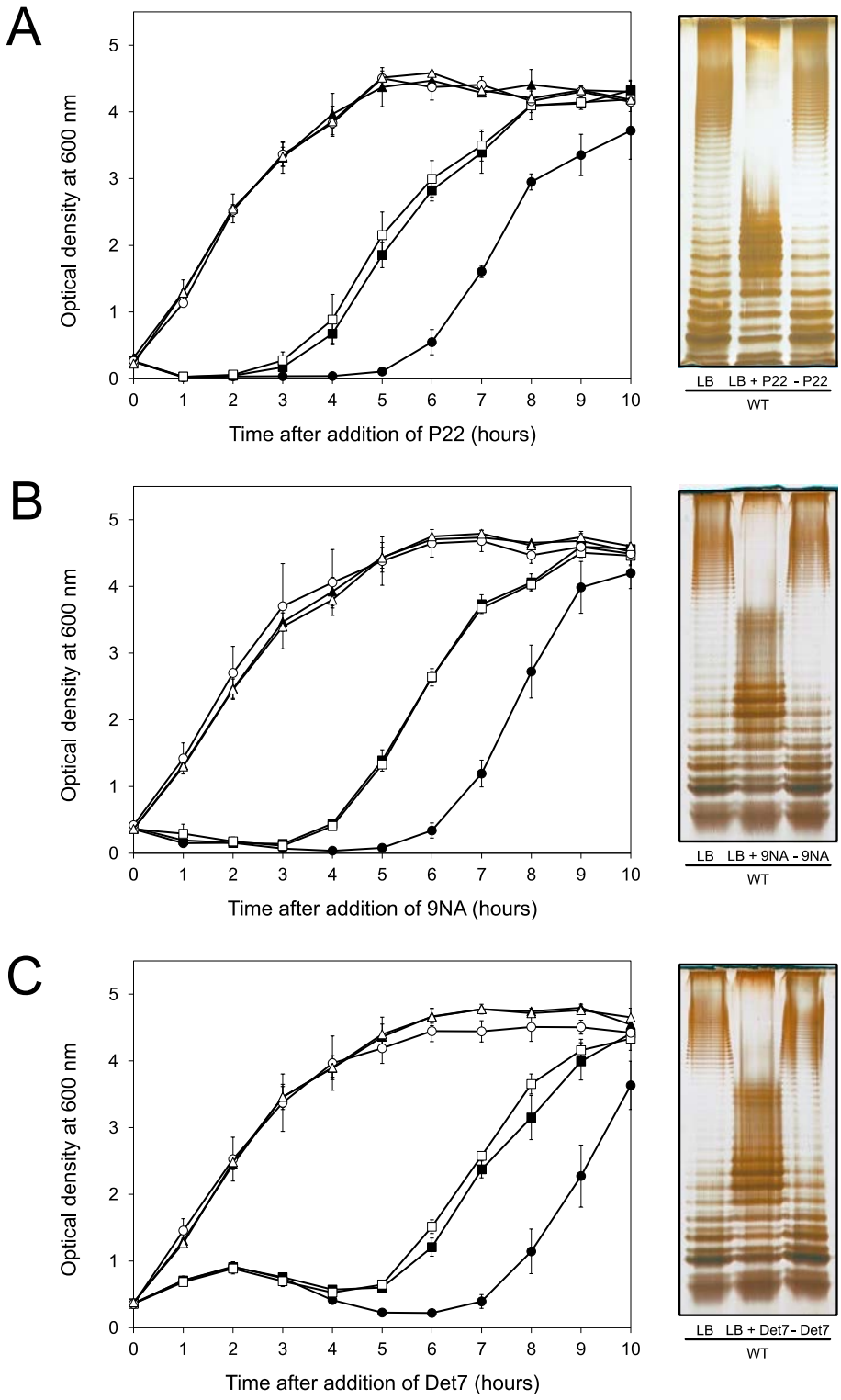

Figure C2.3. Reversibility of the phage-resistant phenotype in the wild type strain. Left: Growth of the wild type strain (black squares), a Δ*opvAB* strain (black circles), and an OpvAB^{ON} strain (black triangles) in LB + P22 (**A**), LB + 9NA (**B**), and LB + Det7 (**C**). The same symbols in white indicate phage-resistant isolates which were re-challenged. Values are averages and standard deviations from ≥ 3 independent experiments. **Right:** LPS profiles of the wild type strain in LB (left), LB + phage (center) and of an isolate that had survived phage challenge, subsequently grown in LB (right).

Mutational bacteriophage resistance in the absence of OpvAB

Challenge of a Δ*opvAB* strain with phages P22, 9NA, and Det7 prevented growth for 4-6 h, and growth resumed afterwards (**Figures C2.1 and C2.3**). To investigate the cause(s) of phage resistance in the absence of OpvAB, individual colonies were isolated from stationary cultures of a Δ*opvAB* strain in LB + P22, LB + 9NA, and LB + Det7. Phage was removed by streaking on green plates. Independent isolates (each from a different culture) were then tested for phage resistance. Sixty seven out of 72 independent isolates turned out to be phage-resistant, thus confirming that they were mutants. Analysis of LPS in independent phage-resistant mutants revealed that a large fraction of such mutants displayed visible LPS anomalies (**Figure C2.4**). The few mutant isolates (5/67) that did not show LPS alterations may have LPS alterations that cannot be detected in gels or carry mutations that confer phage resistance by mechanisms unrelated to the LPS. Whatever the case, these experiments support the conclusion that resistance of *S. enterica* to phages P22, 9NA, and Det7 in the absence of OpvAB is mutational.

To determine whether isolates resistant to one phage were also resistant to other phages that target the O-antigen, cross-resistance was tested by growth in LB upon phage inoculation. Sixty seven mutants (24 P22-resistant, 24 9NA-resistant, and 19 Det7-resistant) were tested (**Table C2.1**). The main conclusions from these experiments were as follows:

(i) Major alteration of LPS conferred resistance to all three phages.

(ii) More subtle LPS alteration (as observed in 16/24 P22-resistant mutants) conferred incomplete resistance to 9NA but did not confer resistance to Det7. Five P22-resistant mutants that did not show clear LPS alterations also conferred incomplete resistance to 9NA.

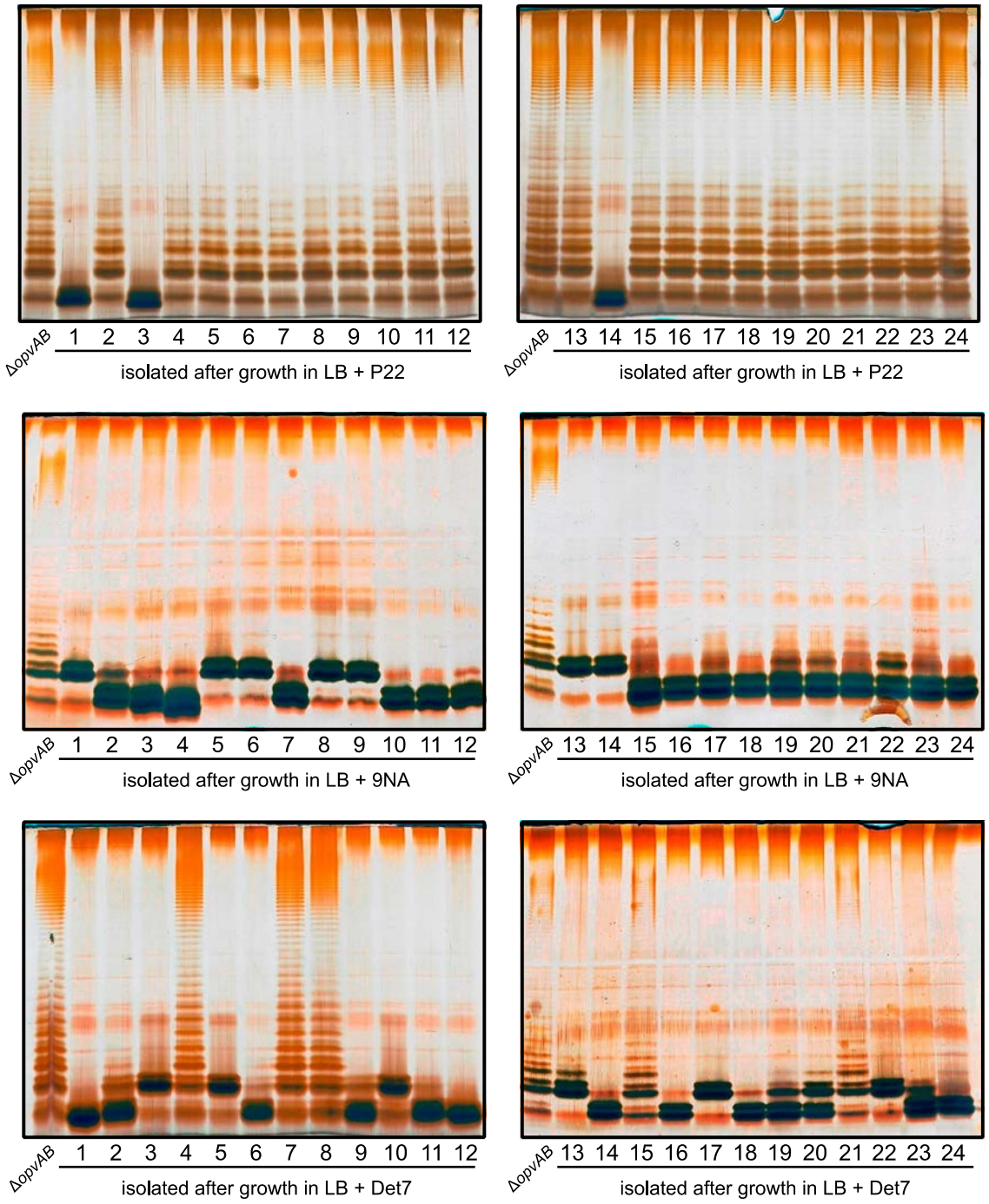

Figure C2.4. Mutational resistance to bacteriophage in a Δ*opvAB* strain. Top. LPS profiles of a *ΔopvAB* strain (first lane from the left on each gel) and 24 independent P22-resistant derivatives, as observed by electrophoresis and silver staining. **Middle.** LPS profiles of a *ΔopvAB* strain and 24 independent 9NA-resistant derivatives. **Bottom**. LPS profiles of a *ΔopvAB* strain and 24 independent Det7-resistant derivatives.

	P22	9NA	Det7			P22	9NA	Det7
Δ*opvAB*	-	-	-		**9NA-10**	+	+	+
P22-1	+	+	+		**9NA-11**	+	+	+
P22-2	+	+/-	-		**9NA-12**	+	+	+
P22-3	+	+	+		**9NA-13**	+	+	+
P22-4	+	+/-	-		**9NA-14**	+	+	+
P22-5	+	+/-	-		**9NA-15**	+	+	+
P22-6	+	+/-	-		**9NA-16**	+	+	+
P22-7	+	+/-	-		**9NA-17**	+	+	+
P22-8	+	+/-	-		**9NA-18**	+	+	+
P22-9	+	+/-	-		**9NA-19**	+	+	+
P22-10	+	+/-	-		**9NA-20**	+	+	+
P22-11	+	+/-	-		**9NA-21**	+	+	+
P22-12	+	+/-	-		**9NA-22**	+	+	+
P22-13	+	+/-	-		**9NA-23**	+	+	+
P22-14	+	+	+		**9NA-24**	+	+	+
P22-15	+	+/-	-		**Det7-1**	+	+	+
P22-16	+	+/-	-		**Det7-2**	+	+	+
P22-17	+	+/-	-		**Det7-3**	+	+	+
P22-18	+	+/-	-		**Det7-5**	+	+	+
P22-19	+	+/-	-		**Det7-6**	+	+	+
P22-20	+	+/-	-		**Det7-9**	+	+	+
P22-21	+	+/-	-		**Det7-10**	+	+	+
P22-22	+	+/-	-		**Det7-11**	+	+	+
P22-23	+	+/-	-		**Det7-12**	+	+	+
P22-24	+	+/-	-		**Det7-13**	+	+	+
9NA-1	+	+	+		**Det7-14**	+	+	+
9NA-2	+	+	+		**Det7-16**	+	+	+
9NA-3	+	+	+		**Det7-17**	+	+	+
9NA-4	+	+	+		**Det7-18**	+	+	+
9NA-5	+	+	+		**Det7-19**	+	+	+
9NA-6	+	+	+		**Det7-20**	+	+	+
9NA-7	+	+	+		**Det7-22**	+	+	+
9NA-8	+	+	+		**Det7-23**	+	+	+
9NA-9	+	+	+		**Det7-24**	+	+	+

Table C2.1. Cross-resistance in phage-resistant mutants. Resistance to P22, 9NA and Det7 was measured by growth in LB upon phage inoculation, indicated by symbols + (complete resistance), +/- (partial resistance) and – (no resistance).

Constitutive expression of *opvAB* reduces *S. enterica* resistance to guinea pig serum

O-antigen chain length has been described to be crucial for serum resistance in *Salmonella* [52,342–345]. Survival in serum was analyzed by treating exponentially growing cells with 30% non-immune guinea pig serum. Constitutive expression of *opvAB* caused increased killing by serum (**Figure C2.5**).

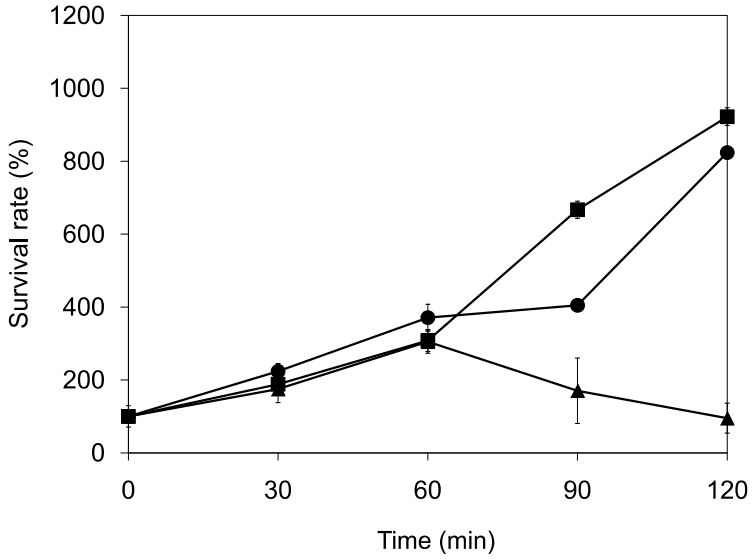

Figure C2.5. Survival in presence of 30% guinea pig serum. Strains are represented by squares (wild type), circles (Δ*opvAB*), and triangles (OpvAB^{ON}). Values are averages and standard deviations from 5 independent experiments.

Constitutive expression of *opvAB* reduces *S. enterica* proliferation in macrophages

Additional screens and phenotypic assays were performed in search for functions of *ovpAB* phase variation besides the formation of a P22-resistant subpopulation with reduced resistance to serum. The trials included: (i) growth in various media at different temperatures and different osmolarities; (ii) resistance to acidic pH, cationic peptides, bile, and hydrogen peroxide; (iii) motility; (iv) biofilm formation; (v) and invasion of and proliferation in epithelial and macrophage cell lines. Most trials did not show differences associated either to loss or constitutive expression of *opvAB*. A remarkable exception was that constitutive expression of *opvAB* impaired intracellular proliferation within macrophages (**Figure C2.6**). On the other hand, a strain carrying an *opvAB* deletion showed intramacrophage proliferation at a level similar to that of the wild type strain.

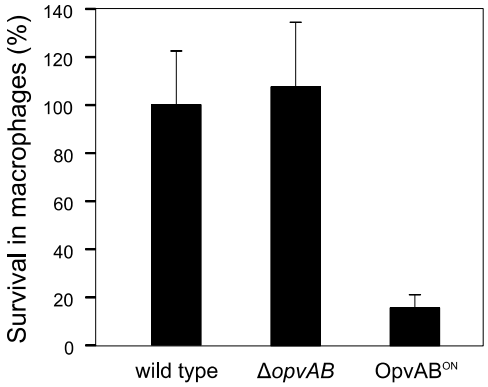

Figure C2.6. Rate of intramacrophage proliferation for the wild type strain, a Δ*opvAB* strain, and an OpvAB^{ON} strain. Values are averages and standard deviations from 3 independent experiments. Proliferation of the wild type strain is considered 100%.

Constitutive expression of *opvAB* reduces *S. enterica* virulence

Because the LPS plays roles in the interaction between *S. enterica* and the animal host [49,52,344], and virulence-related phenotypes had been found for the OpvABON strain (**Figures C2.5 and C2.6**) we tested whether OpvAB-mediated alteration of O-antigen chain length affected *Salmonella* virulence. For this purpose, competitive indexes (CI's) [320] were calculated upon oral and intraperitoneal challenge of BALB/c mice. The CI's of the OpvAB^{ON} strain were found to be lower than those of the wild type and the *ΔopvAB* strain (**Table C2.2**). Because the wild type, the OpvAB^{ON} strain and the *ΔopvAB* strain show similar or identical growth rates in LB (**Figure C2.7**), the conclusion from these experiments was that expression of *opvAB* reduces *Salmonella* virulence.

Pair of strains	Mouse, oral infection	Mouse, intraperitoneal infection
OpvAB^{ON} *vs* wild type	0.15 ± 0.07	0.32 ± 0.10
Δ*opvAB vs* wild type	1.11 ± 0.18	1.15 ± 0.16
OpvAB^{ON} *vs* Δ*opvAB*	0.25 ± 0.10	0.38 ± 0.15

Table C2.2. Competitive indexes of *opvAB*^{ON} and *ΔopvAB* strains of *S. enterica.* Values are averages ± standard deviations of 4 experiments.

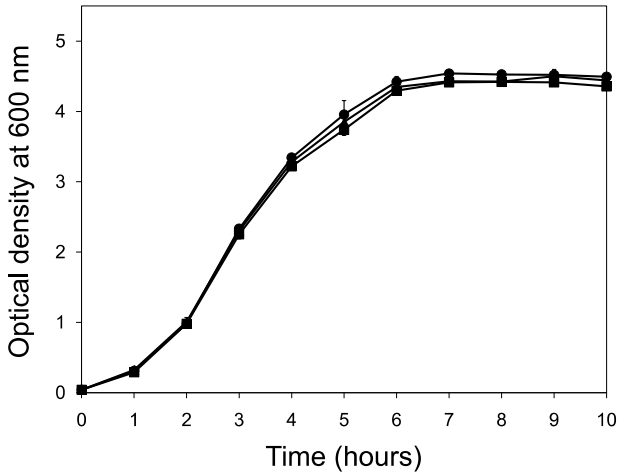

Figure C2.7. Effect of *opvAB* expression on growth in LB. Growth in LB of a wild type strain (squares), a Δ*opvAB* strain (circles), and an OpvAB^{ON} strain (triangles). Values are averages and standard deviations of 3 independent experiments.

CHAPTER III

OxyR-dependent formation of DNA methylation patterns in $OpvAB^{OFF}$ and $OpvAB^{ON}$ cell lineages of *Salmonella enterica*

Both the absence and the overexpression of Dam methylase increase *opvAB* expression and abolish phase variation

Genes under Dam methylation control fall into two categories. One includes genes in which methylation and nonmethylation provide opposite signals [200]. An example is the *traJ* gene of the *Salmonella* virulence plasmid, which is repressed by GATC methylation [346]. In this class of genes, expression of the *dam* gene from a multicopy plasmid does not alter the wild type phenotype [346]. In other genes, however, a plasmid-borne *dam* gene does alter the gene expression pattern. This phenomenon is usually an indication that Dam dependent transcriptional control involves the formation of Dam methylation patterns (combinations of methylated and nonmethylated GATC sites) [200]. To ascertain whether *opvAB* belonged to the "simple" or the "complex" class of Dam methylation-dependent genes, the effect of introducing a *dam* gene carried on plasmid pTP166 was assayed. The results were as follows:

(i) In a wild type background, an *opvB*::*lac* translational fusion showed phase variation, and formed white (OpvAB^{OFF}) and blue (OpvAB^{ON}) colonies in the presence of X-gal. In a *dam* background, phase variation was abolished, and all colonies were Lac^{+} (OpvAB^{ON}). Plasmid pTP166 yielded an intermediate phenotype (**Figure C3.1A**), suggesting that formation of the OpvAB^{OFF} and OpvAB^{ON} subpopulations might involve the establishment of a DNA methylation pattern in the GATC sites of the *opvAB* control region, rather than methylation or nonmethylation of the full set of GATC sites. A similar phenomenon occurs in the *gtr* operon [93] which is repressed in a *dam* background while introduction of a cloned *dam* gene results in an intermediate phenotype.

(ii) Expression of *opvB::lac* was also monitored by β-galactosidase assays (**Figure C3.1B**). Lack of Dam methylation increased expression of the *opvAB* operon as previously described. Introduction of the *dam* gene carried on the pTP166 plasmid yielded an intermediate *opvAB* expression level, as in the colonies described above.

(ii) Expression of an *opvAB*::*gfp* transcriptional fusion was monitored by fluorescence analysis (**Figure C3.1C**). A major OpvAB^{OFF} subpopulation and a minor OpvAB^{ON} subpopulation were detected in the wild type. In a *dam* background, a single population in the ON state was observed, in accordance with the results obtained with a *opvB::lac* fusion. In the presence of a cloned *dam* gene (pTP166), a single population with

intermediate levels of expression was detected and a shift towards the ON state remained visible (**Figure C3.1C**).

Altogether, the above observations suggested that DNA methylation patterns might be formed at the *opvAB* control region. This region, located upstream of the *opvAB* promoter, contains four GATC sites separated by 46, 19, and 46 nucleotides and centered at the -172.5, -122.5, -99.5, and -49.5 positions upstream of the transcription start site (**Figure C3.2A**). From now on, these GATC sites will be referred to as $GATC_1$ to $GATC_4$, the latter being closest to the -35 module of the *opvAB* promoter.

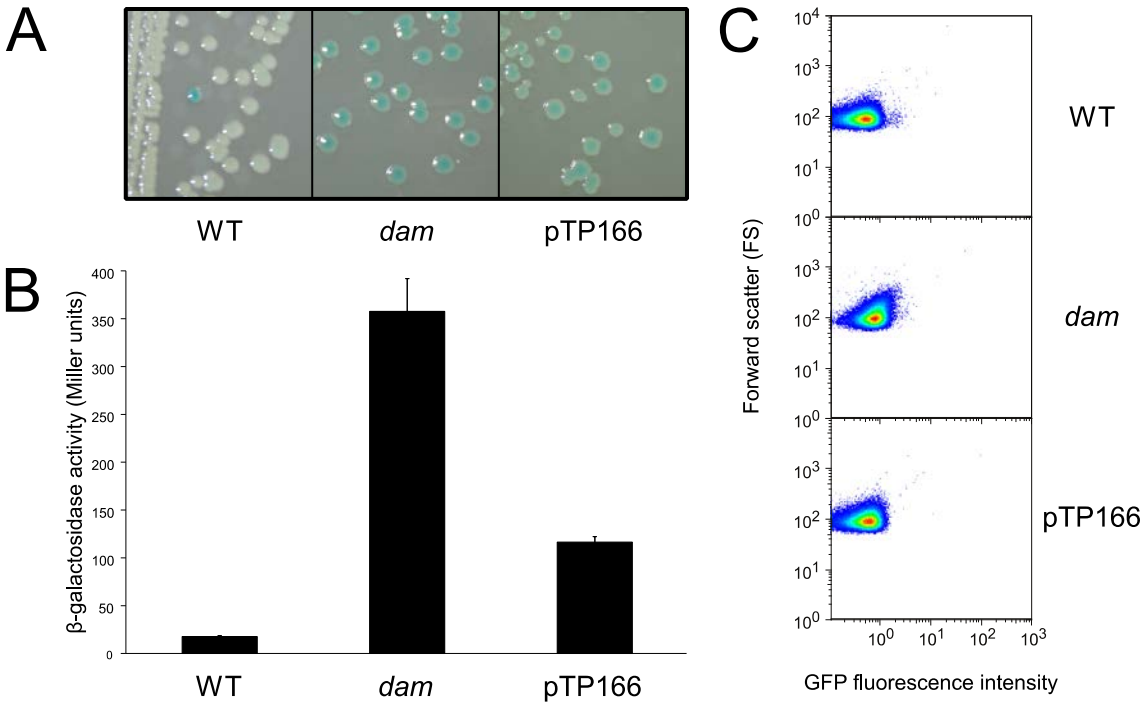

Figure C3.1. Regulation of *opvAB* expression and formation of OpvAB subpopulations by Dam methylation. A. Visual observation of phase variation on LB + X-gal plates in *S. enterica* strains carrying an *opvB::lac* fusion in the wild type, a *dam* mutant, and a strain that overproduced Dam methylase (ATCC 14028/pTP166). **B.** β-galactosidase activity of the same strains. **C.** GFP fluorescence distribution in a strain carrying an *opvAB::gfp* fusion in the same backgrounds.

Roles of individual *opvAB* GATC sites in the formation of OpvAB^{OFF} and OpvAB^{ON} cell lineages

To study the contribution of each GATC site to *opvAB* regulation, mutations were introduced by site-directed mutagenesis. The mutations were designed to change GATC sites so that they would no longer be a substrate for Dam methylation. Because OxyR is essential for *opvAB* expression (**Figures C1.5 and C1.6**), alteration of consensus sequences was avoided inside putative OxyR binding sites. CATC sites were thus introduced in place of GATC sites, and every combination of mutated and nonmutated GATC sites was produced.

The effect of GATC mutations on *opvAB* expression was first analyzed by comparing the β-galactosidase activity of an *opvB::lac* translational fusion in *dam*$^+$ and *dam* backgrounds (**Figure C3.2B**). Relevant observations were as follows:

(i) Mutation of $GATC_1$ and $GATC_3$ had a small effect on regulation by Dam methylation, although the absolute values of β-galactosidase activity were higher. Mutation of $GATC_2$ resulted in diminished regulation by Dam methylation. When $GATC_4$ was mutated, control by Dam methylation showed an inverted pattern (expression was higher in a *dam*$^+$ background).

(ii) As a general rule, combinations of two or more mutations seemed to have an additive effect. A remarkable case was the combination of mutated $GATC_2$ and $GATC_4$ which exacerbated the inversion of regulation by Dam methylation caused by mutation of $GATC_4$ alone. It is noteworthy that mutations in $GATC_1$, $GATC_2$ and $GATC_3$ together did not abolish Dam-dependent regulation, whereas a single mutation in $GATC_4$ inverted the pattern of Dam-dependent regulation.

The overall conclusion from these experiments was that all four GATC sites are necessary for Dam-dependent control of *opvAB* expression, and that the $GATC_4$ site may have an especially prominent role.

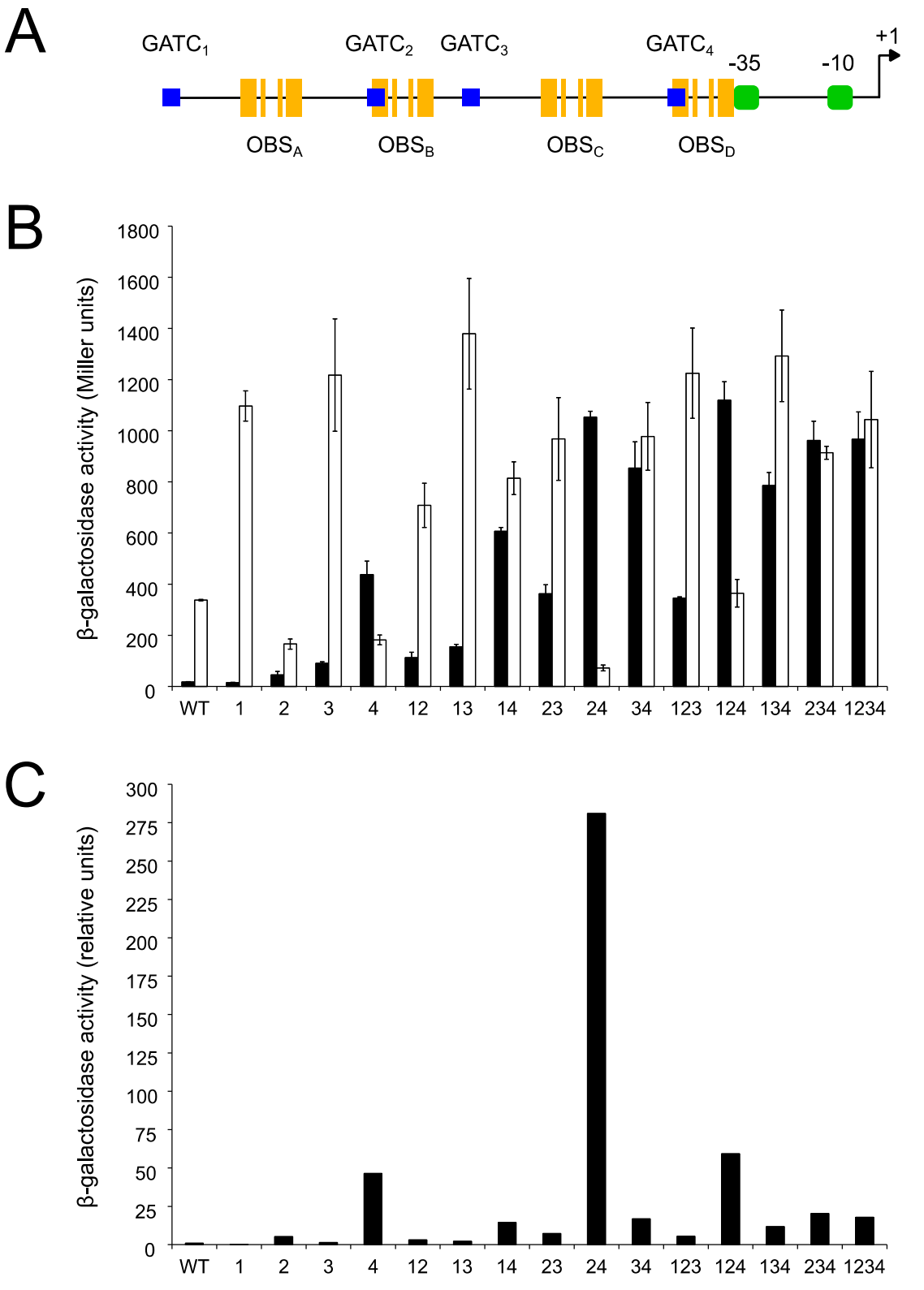

Figure C3.2. Effect of mutations in the *opvAB* GATC sites on the expression of *opvAB*. A. Diagram of the *opvAB* regulatory region, with the GATC sites and the OxyR binding sites outlined. **B**. β-galactosidase activity of strains carrying an *opvB::lac* fusion in a wild type background (black bars) and in a *dam* background (white bars). Mutated GATC sites are indicated by numbers 1 to 4. **C**. Relative β-galactosidase activity of the *opvB::lac* fusion in the same strains (activity in the wild type divided by activity in a *dam* background).

Even though disruption of OxyR binding sites had been avoided, GATC mutations affected *opvAB* expression irrespective of the presence or absence of DNA methylation, as observed in a *dam* background (**Figure C3.2B**). In the absence of Dam methylation, mutations in $GATC_1$ and $GATC_3$ increased *opvAB* expression whereas mutations in $GATC_2$ and $GATC_4$ resulted in lower *opvAB* expression. To separate such effects from those of Dam methylation itself, the β-galactosidase activity of *opvB::lac* in a wild type background was relativized to the β-galactosidase activity in a *dam* background (**Figure C3.2C**). This representation leads to the interesting conclusion that mutations in $GATC_1$ and $GATC_3$ repress *opvAB* expression, whereas mutations in $GATC_2$ and $GATC_4$ activate *opvAB* expression. Again, methylation of $GATC_4$ was found to be crucial for *opvAB* regulation. Mutations in $GATC_1$ and $GATC_3$ show little effect on their own because *opvAB* expression is low in the wild type, but they repress *opvAB* expression when combined with activating mutations in $GATC_2$ and/or $GATC_4$. Hence, the GATC sites in the *opvAB* regulatory region can be tentatively divided in two pairs: methylation of pair $GATC_1$ + $GATC_3$ seems to be associated with the $OpvAB^{ON}$ state while methylation of pair $GATC_2$ + $GATC_4$ seems to be associated with the $OpvAB^{OFF}$ state.

Analysis of fluorescence using an *opvAB*::*gfp* transcriptional fusion (**Figure C3.3**) allowed us to distinguish whether the differences in *opvAB* expression in GATC mutant backgrounds reflected differences in gene expression or differences in the sizes of the $OpvAB^{ON}$ and $OpvAB^{OFF}$ subpopulations. The main observations were as follows:

(i) In the wild type, the $OpvAB^{ON}$ subpopulation comprised approximately 0.18% cells.

(ii) Mutation of $GATC_4$ caused a drastic increase in the size of the $OpvAB^{ON}$ subpopulation. Mutations in $GATC_1$, $GATC_2$, and $GATC_3$ had a smaller effect, which was more clearly seen when they were combined with each other and/or a mutation in $GATC_4$.

(iii) Two subpopulations were still distinguished when three GATC sites were mutated, provided that either $GATC_3$ or $GATC_4$ remained unaltered. The relative size of the $OpvAB^{OFF}$ and $OpvAB^{ON}$ subpopulations was however different in each case, with a predominant $OpvAB^{OFF}$ subpopulation when $GATC_4$ remained unaltered, and a predominant $OpvAB^{ON}$ subpopulation when $GATC_3$ remained unaltered.

(iv) Mutation of both $GATC_3$ and $GATC_4$ eliminated subpopulation formation regardless of the presence of mutations in $GATC_1$ and $GATC_2$, and yielded an $OpvAB^{ON}$ population.

These observations are consistent with the gene expression analyses reported above, and permit to interpret the gene expression results in terms of subpopulation formation. Mutation of $GATC_4$ caused the most drastic increase in the proportion of $OpvAB^{ON}$ cells, thereby confirming that methylation of the $GATC_4$ site may have a relevant role in the formation of the $OpvAB^{OFF}$ subpopulation. Increase of $OpvAB^{ON}$ subpopulation was likewise observed when a mutated $GATC_4$ was combined with other mutated GATC sites (**FigureC3.3**).

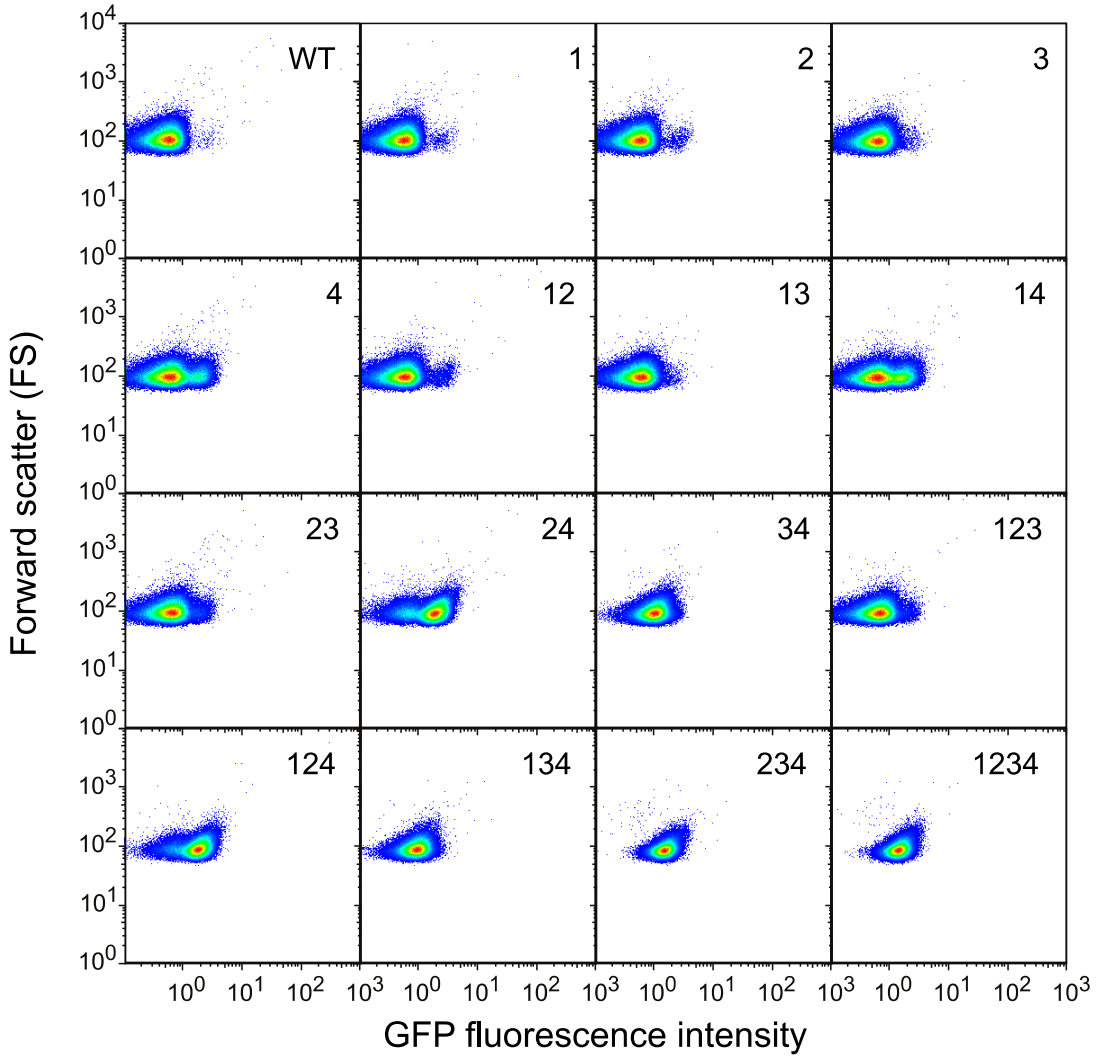

Figure C3.3. GFP fluorescence distribution in *S. enterica* strains carrying an *opvAB::gfp* fusion and mutations in the *opvAB* GATC sites. Mutated GATC sites are indicated by numbers 1 to 4.

OxyR binds the *opvAB* regulatory region

Four putative OxyR binding half-sites are found in the regulatory region of *opvAB* centered in the -148, -116, -75, and -43 positions, and sharing 10, 8, 10, and 7 nucleotides respectively with the 10-nucleotide consensus sequence. The OxyR binding half-sites upstream of the *opvAB* promoter will be from now on referred to as OBS_A to OBS_D, the latter being immediately upstream of the *opvAB* -35 promoter module (**Figure C3.2A**). Assuming a helical periodicity of 10.5 base pairs [347] the OBS are predicted to be spaced by one, two and one helical turns, which means that all the OxyR binding sites may be on the same face of the DNA helix. The distance between OBS_A and OBS_B, and between OBS_C and OBS_D as well, is canonical for binding of the reduced form of OxyR [90]. $GATC_2$ and $GATC_4$ overlap with OBS_B and OBS_D, respectively (**Figure C3.2A**).

To test whether OxyR binds the *opvAB* regulatory region, an electrophoretic mobility shift assay (EMSA) was carried out using purified OxyR protein (**Figure C3.4A**). To avoid uncontrolled oxidation of OxyR, and because it was previously shown that the oxidation state of OxyR is not relevant for *opvAB* regulation we used a mutant version of the OxyR protein, $OxyR^{C199S}$, which cannot be oxidized but retains the properties of the reduced form of OxyR [90,91]. Purified 6xHis-$OxyR^{C199S}$ protein (henceforth named OxyR for simplicity) was used. A DNA fragment containing the four regulatory GATC sites and the four OxyR binding half-sites was produced using a 6-FAM-labelled oligonucleotide and was incubated with increasing concentrations of OxyR. Binding was unambiguously detected. A DNA fragment from the regulatory region of an unrelated gene (*envR*) was used as a negative control, and binding was not detected (**Figure C3.4A**).

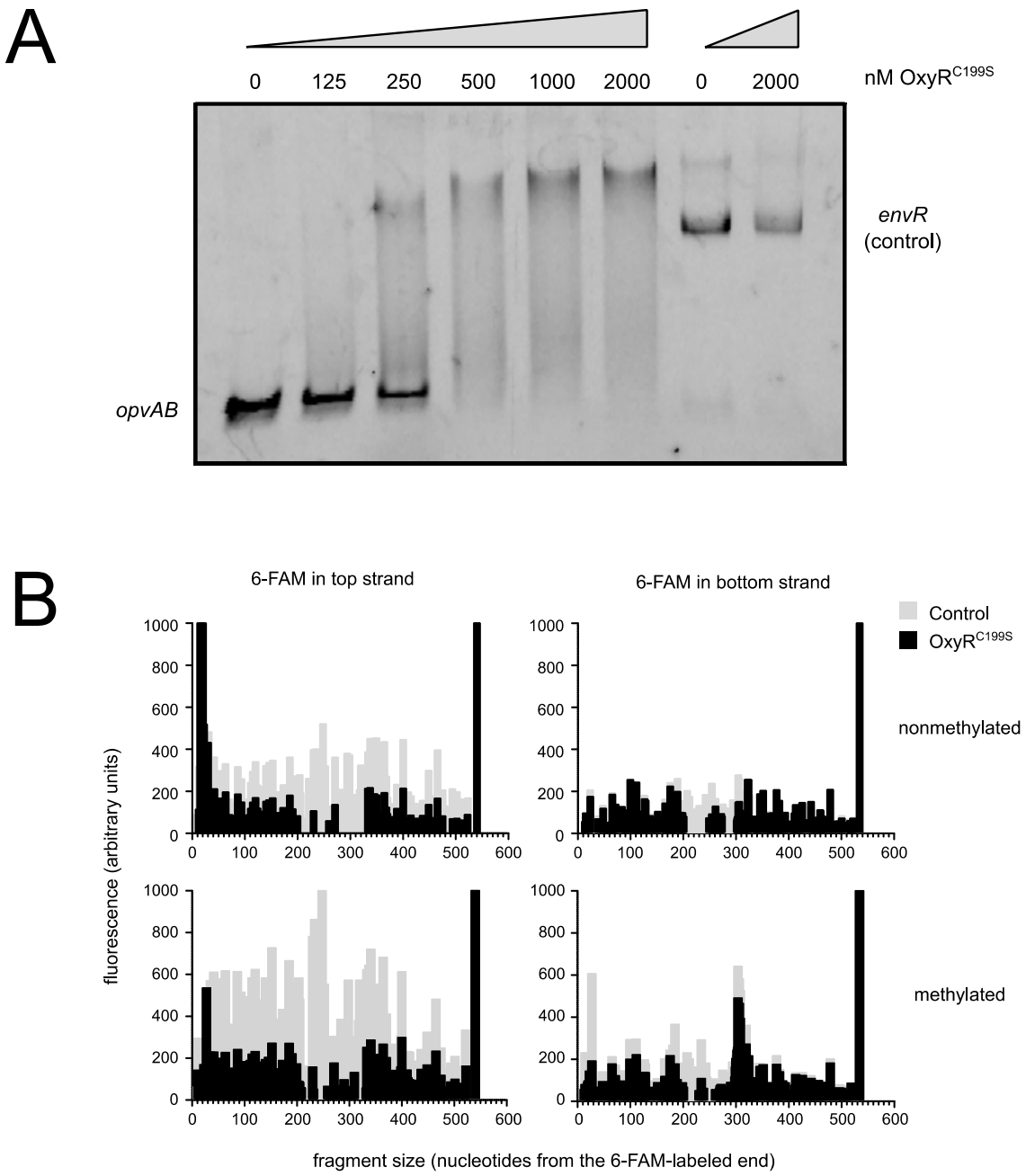

Figure C3.4. Binding of 6xHis-OxyR^{C199S} to the *opvAB* promoter region. A. Electrophoretic mobility shift assay of 6xHis-OxyR^{C199S} binding to a DNA fragment containing the *opvAB* promoter and the upstream regulatory region. The regulatory region of *envR* was used as a negative control. **B.** DNase I footprinting of 6xHis-OxyR^{C199S} binding to DNA fragments containing the *opvAB* promoter and regulatory region with a 6-FAM label in either the top or the bottom strand. Methylated and nonmethylated versions of the fragment were used.

OxyR protects the *opvAB* regulatory region

To confirm binding of OxyR to the *opvAB* regulatory region, purified OxyR was used in a footprinting assay performed using 6-FAM-labelled DNA fragments and DNase I (**Figure C3.4B**). The same DNA fragment used in the EMSA assays, containing both the GATC sites and predicted OxyR binding sites, was labelled at alternate ends and used in parallel experiments. Methylated and nonmethylated DNA probes were used, and the analysis confirmed the ability of OxyR to bind the *opvAB* regulatory region *in vitro*. Relevant observations were as follows:

(i) Protection from DNase I digestion was detected in a 133 base pair DNA span, albeit with regional differences. $GATC_1$, $GATC_2$, $GATC_3$ are located in the protected region. Overall protection was less efficient when the DNA probe was methylated.

(ii) The OBS_A and OBS_C sites were fully protected, while OBS_B was partially protected.

(iii) OBS_D, which contains the $GATC_4$ site, was not protected.

The relevance of these observations may be limited as methylated and nonmethylated DNA probes were used, and evidence presented above had suggested that *opvAB* regulation involved both methylated and nonmethylated GATC sites (**Figure C3.1**). With this caveat, footprinting experiments confirmed the ability of OxyR to bind the *opvAB* regulatory region. An additional, interesting observation was that OxyR protection extended outside the OxyR binding sites, as previously described for other LysR-type factors [348–351] (see below).

$OpvAB^{OFF}$ and $OpvAB^{ON}$ subpopulations are characterized by inverse patterns of Dam methylation

SMRT sequencing results showed that >97 percent of the total of 38,458 GATC sites present in the genome of *S. enterica* serovar Typhimurium are methylated, and that nonmethylated sites are the exception in the *S. enterica* genome. Within this set, several nonmethylated GATC sites were detected upstream of the *opvAB* operon. In order to analyze them in more detail, position-specific base modification analyses were performed. Addition of the virulent P22 H5 phage to a culture of *S. enterica* results in

selection of the OpvAB^{ON} subpopulation (**Figure C2.2**). Using this procedure, a culture was enriched in OpvAB^{ON} cells, and the methylation state of the *opvAB* GATC sites was analyzed using single-molecule real-time (SMRT) sequencing [352]. An ordinary culture (mostly made of OpvAB^{OFF} cells) was also subjected to SMRT sequencing. The results The results from position-specific basemodification analysis were as follows were as follows:

(i) In an ordinary culture (>99% OpvAB^{OFF}), $GATC_1$ and $GATC_3$ were nonmethylated, whereas $GATC_2$ and $GATC_4$ were methylated (**Table C3.1**).

(ii) In the OpvAB^{ON} culture, an inverse DNA methylation pattern was found: nonmethylation of $GATC_2$ and $GATC_4$, and methylation of $GATC_1$ and $GATC_3$ (**Table C3.1**).

These observations confirm that establishment of the OFF and ON states of the *opvAB* locus involves the formation of DNA methylation patterns, as in other phase variation loci under Dam methylation control [353][216][93].

Site	Genome position	OpvAB^{OFF}	OpvAB^{ON}
$GATC_1$	2,361,489 +	unmodified (1.35, 31)	m6A (2.76, 59)
	2,361,490 -	unmodified (1.22, 31)	m6A (3.99, 46)
$GATC_2$	2,361,439 +	m6A (4.55, 55)	unmodified (0.93, 49)
	2,361,440 -	m6A (2.85, 54)	unmodified (0.85, 37)
$GATC_3$	2,361,416 +	unmodified (0.78, 55)	m6A (2.29, 45)
	2,361,417 -	unmodified (0.43, 55)	m6A (2.15, 36)
$GATC_4$	2,361,366 +	m6A (2.79, 45)	unmodified (1.02, 52)
	2,361,367 -	m6A (3.14, 37)	unmodified (0.59, 47)

Table C3.1. DNA modification status according to SMRT View for position specific base-modification analysis upstream of the *opvAB* operon. Inter pulse duration ratios as well as strand-specific coverage values are given in parentheses.

OxyR protects GATC sites from Dam methylation *in vivo*

OxyR has been previously described as a DNA methylation-blocking factor, able to induce the formation of nonmethylated GATC sites [93,239]. To test whether OxyR has a similar DNA methylation-blocking ability in the *opvAB* operon, the methylation state of the GATC sites in the *opvAB* regulatory region was tested *in vivo*. For this purpose, a Southern blot was performed using genomic DNA extracted from the wild type strain and from an *oxyR* mutant. The methylation state of individual GATC sites was inferred from restriction analysis using enzymes that cut GATC sequences depending on their methylation state (MboI, DpnI, and Sau3AI). $GATC_1$ and $GATC_3$ were found to be nonmethylated while $GATC_2$ and $GATC_4$ were found to be methylated (**Figure C3.5**). In contrast, in an *oxyR* background, all four GATC sites were found to be methylated (**Figure C3.5**). These observations confirmed that OxyR has DNA methylation-blocking ability *in vivo* at the *opvAB* regulatory region.

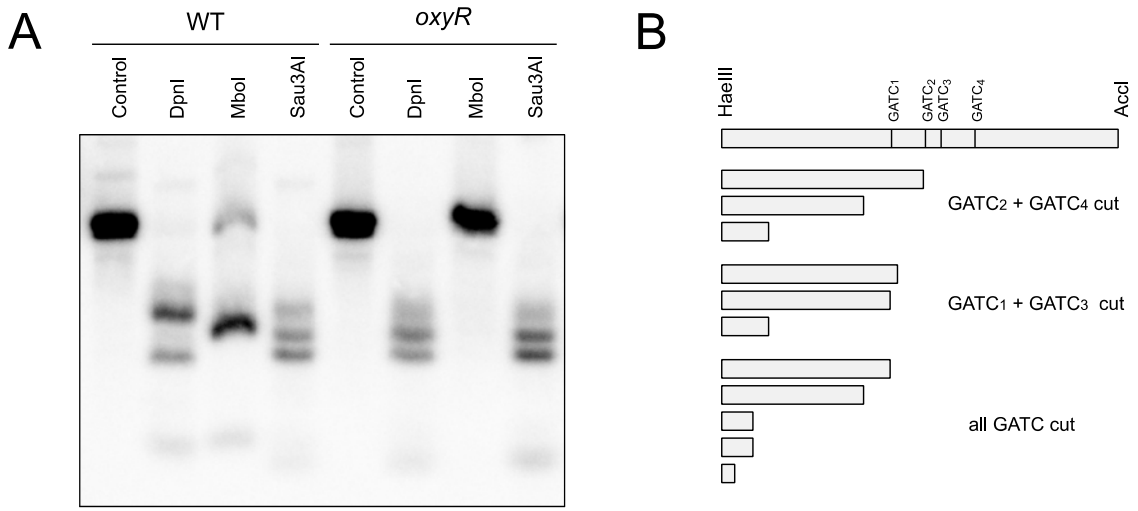

Figure C3.5. Methylation state of GATC sites in the *opvAB* regulatory region in wild type and *oxyR* backgrounds. A. Southern blot of genomic DNA obtained from wild type and *oxyR* cultures and digested with HaeIII and with AccI (control) and DpnI, MboI or Sau3AI. **B.** Diagram of the HaeIII-AccI fragment and patterns of fragments obtained.

Mutations in the OBS_B and OBS_D OxyR binding sites abolish phase variation

Of the four OxyR binding half-sites in the *opvAB* regulatory region, OBS_A and OBS_C are an absolute match (10 out of 10 nucleotides) to the consensus sequences defined for OxyR binding [90]. In contrast, OBS_B and OBS_D share only 8 and 7 out of 10 nucleotides with the consensus sequence, respectively. The fact that *opvAB* phase variation is skewed towards the OFF state led us to hypothesize that the degree of OxyR binding site perfection played a role in such bias. To test our hypothesis, one nucleotide change was introduced in OBS_B and two nucleotide changes in OBS_D so that their mutated versions would share 9 out of 10 nucleotides with the consensus sequence. Construction of a perfect consensus sequence was avoided since it would inevitably destroy $GATC_2$ and $GATC_4$.

The consequences of OBS_B and OBS_D DNA sequence amelioration were analyzed using *opvAB*::*gfp* (**Figure C3.6A**) and *opvB::lac* fusions (**Figure C3.6B**). Mutations in OBS_B and OBS_D both abolished *opvAB* phase variation, yielding a uniform $OpvAB^{ON}$ population. In the case of the mutation in OBS_B, a single nucleotide change led also to full expression of the operon. The mutation in OBS_D caused a smaller increase in expression and was epistatic to the mutation in OBS_B.

An interpretation of these observations is that OBS_B and OBS_D DNA sequence amelioration may "trap" OxyR in the $OpvAB^{ON}$ configuration. In support of this view, amelioration of the OBS_B and/or OBS_D sites had no effect on *opvAB* expression in a *dam* background (**Figure C3.6**). Hence, the preference of OxyR for certain OxyR-binding sites may be a key factor in regulation of *opvAB* phase variation, and alternative binding of OxyR upstream of the *opvAB* promoter may generate the $OpvAB^{OFF}$ and $OpvAB^{ON}$ subpopulations.

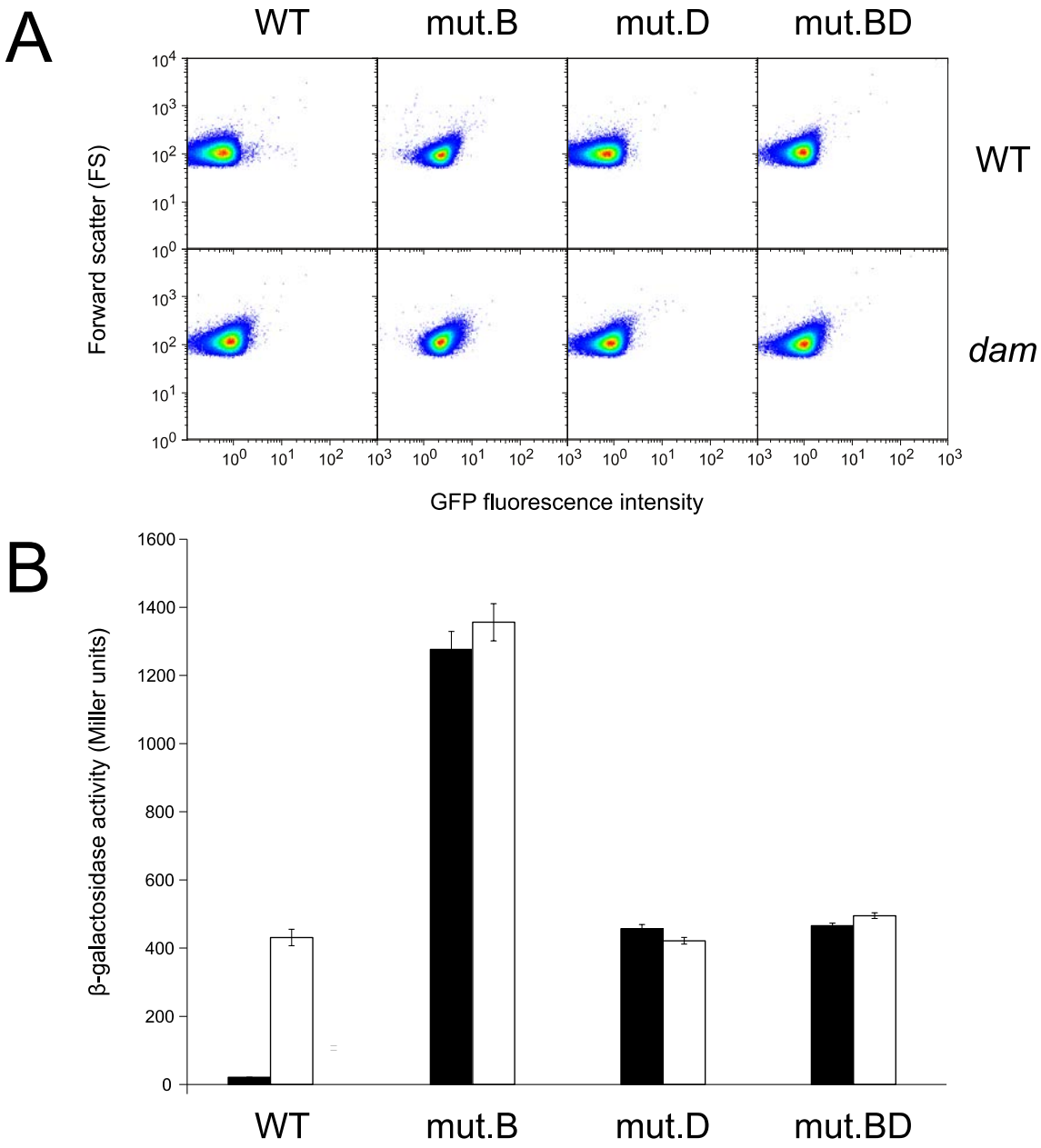

Figure C3.6. Effect of mutations in OBS_B and OBS_D on the expression of *opvAB*. A. GFP fluorescence distribution in *S. enterica* strains carrying an *opvAB::gfp* fusion and mutations in OBS_B (mut.B) and/or OBS_D (mut.D) in wild type and *dam* backgrounds. **B.** β-galactosidase activity of *S. enterica* strains carrying an *opvB::lac* fusion with mutations in OBS_B (mut.B) and/or OBS_D (mut.D) in wild type (black bars) and *dam* (white bars) backgrounds.

SeqA contributes to the small size of the $OpvAB^{ON}$ subpopulation

SeqA was considered a potential ancillary candidate for regulation of *opvAB* since it binds GATC sites [354] and is involved in regulation of other phase variation loci

[154,155]. Thus we analyzed the effect of a *seqA* mutation on *opvAB* expression and its influence on the formation of OpvAB subpopulations. A strain carrying a *seqA* null allele and an *opvB::lac* fusion formed darker (Lac^+) colonies on LB + X-gal than the wild type, and displayed frequent sectoring. Nonetheless, two groups of differently colored colonies (light blue and dark blue) were still distinguishable (**Figure C3.7A**), which allowed calculation of phase transition frequencies. The OFF→ON transition rate was found to be 50-fold higher in a *seqA* background: $(3.0 \pm 1.0) \times 10^{-3}$ compared with 6.1×10^{-5} in the wild type), whereas the ON→OFF transition rates were similar: $(3.1 \pm 0.1) \times 10^{-2}$ compared to 3.7×10^{-2} in the wild type). Not surprisingly, the β-galactosidase activity of an *opvB::lac* fusion was ~10 fold higher in a *seqA* background (**Figure C3.7B**).

Fluorescence assays showed that mutation of *seqA* caused an increase in the size of the $OpvAB^{ON}$ subpopulation (**Figure C3.8**). The effect was stronger in the presence of mutations in $GATC_1$ and/or $GATC_2$, and to a lesser extent in $GATC_3$ (**Figure C3.8**). Interestingly, when $GATC_4$ was mutated, a mutation in *seqA* had an effect opposite to that observed in the wild type: the $OpvAB^{ON}$ subpopulation was reduced (**Figure C3.8**). When both $GATC_3$ and $GATC_4$ were mutated, the *seqA* mutation did not have a significant effect (**Figure C3.8**). These results seem to indicate that the main role of SeqA in the regulation of *opvAB* is the maintenance of a low OFF→ON transition rate (in other words, repression of $OpvAB^{ON}$ subpopulation formation).

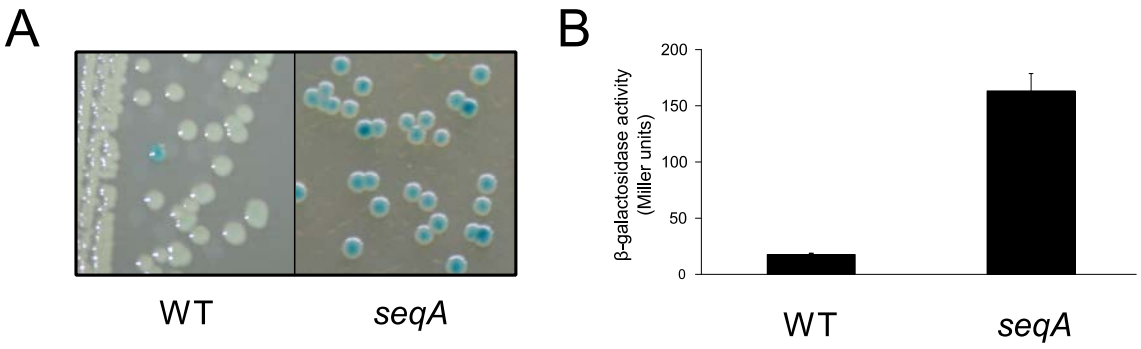

Figure C3.7. Role of SeqA on *opvAB* expression and on the formation of the $OpvAB^{OFF}$ and $OpvAB^{ON}$ subpopulations. A. Colonies formed by *S. enterica* strains carrying an *opvAB::lac* fusion in a wild type background and in a *seqA* background. **B**. β-galactosidase activity of *S. enterica* strains carrying an *opvAB::lac* fusion in a wild type background and in a *seqA* background.

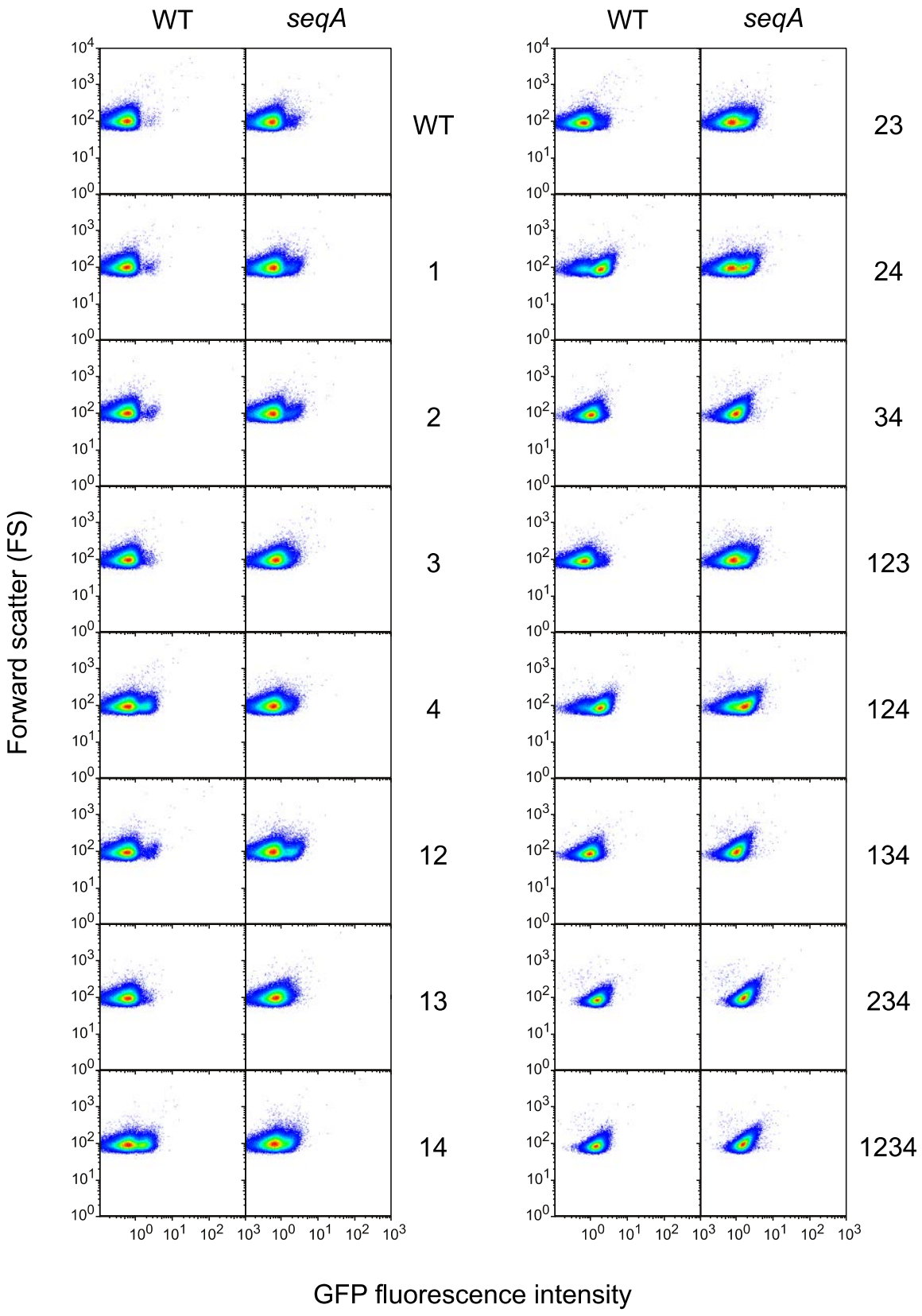

Figure C3.8. GFP fluorescence distribution in *S. enterica* strains carrying an *opvAB::gfp* fusion and mutations in the *opvAB* GATC sites in *seqA*$^+$ and *seqA* backgrounds. Mutated GATC sites are indicated by numbers 1 to 4.

HU is essential for the formation of the OpvAB^{ON} subpopulation

HU is a nucleoid-associated protein known to regulate a large number of genes in *E. coli* and *Salmonella* [163,184,355]. The HU protein can exist in three forms: the HU αβ heterodimer and the corresponding homodimers. The heterodimer is the predominant form *in vivo* [160]. We deleted *hupA* and/or *hupB*, the genes encoding the two proteins forming the HU heterodimer, and tested the effect of the mutations on the expression of an *opvAB*::*gfp* fusion (**Figure C3.9A**). The OpvAB^{ON} subpopulation was found to be reduced from approximately 0.18% in the wild type to 0.09% in single *hupA* and *hupB* mutants. Reduction of the OpvAB^{ON} subpopulation size was exacerbated in the double *hupA hupB* mutant: the OpvAB^{ON} subpopulation was virtually absent (**Figure C3.9A**).

When *hupA* and *hupB* mutations were introduced into an *opvB::lac* background, a decrease in the β-galactosidase activity of the *opvB::lac* fusion was likewise found (**Figure C3.9B**). In turn, when formation of Lac^{+} (OpvAB^{ON}) colonies was scored on LB + X-gal plates, blue (Lac^{+}) colonies were still visible in the *hupA* and *hupB* single mutants but not in the double mutant *hupA hupB* background (**Figure C3.9C**).

When the effect of the *hupA* and *hupB* mutations was tested in OpvAB^{ON}-locked backgrounds, lack of HU did not impair the OpvAB^{ON} state (**Figure C3.9D**), although *opvB::lac* expression was slightly lower (**Figure C3.9E**). Hence, HU seems to be necessary for maintenance of the OpvAB^{ON} state in the wild type but not in mutants locked in OpvAB^{ON} state.

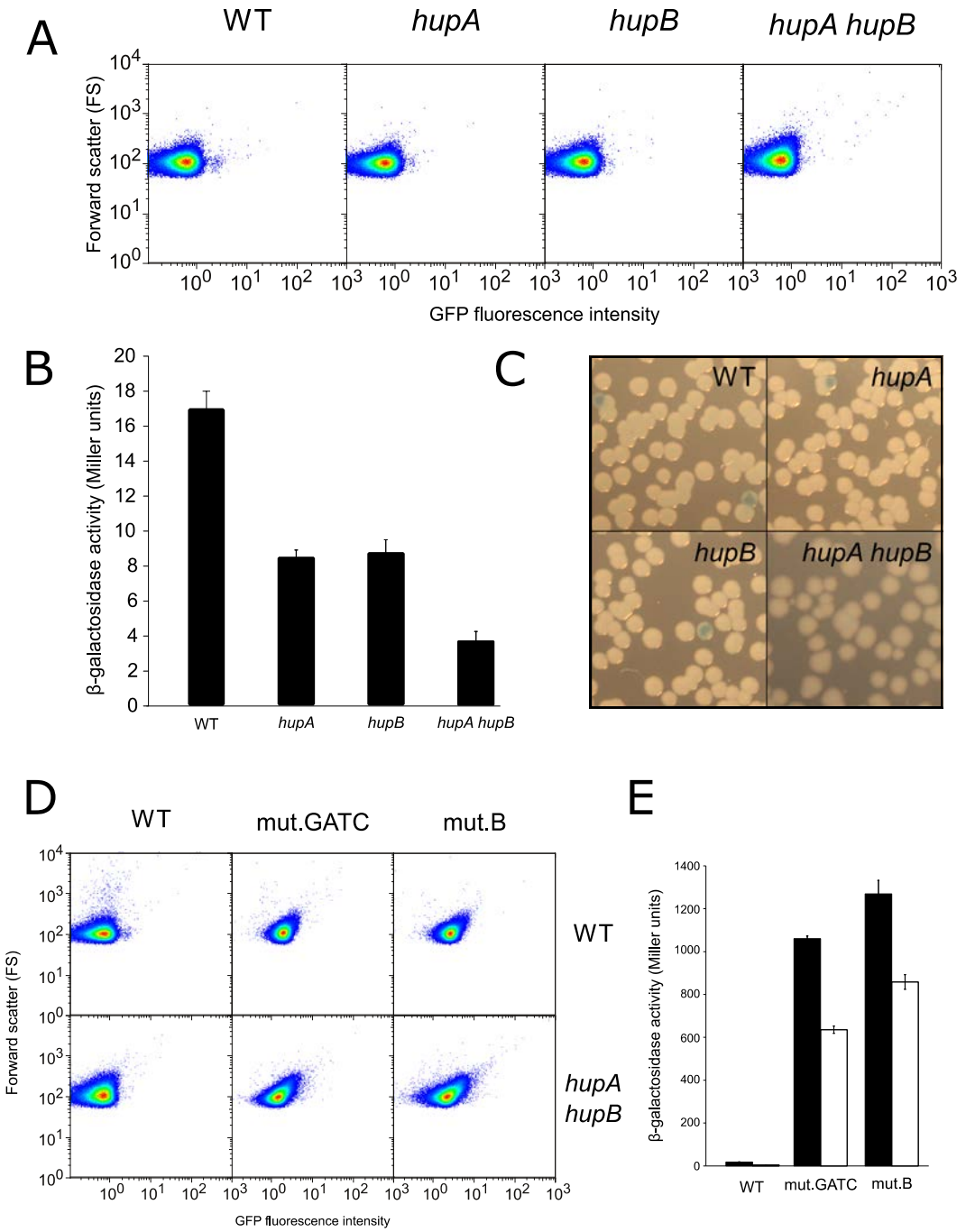

Figure C3.9. Role of HU on *opvAB* expression and on the formation of the OpvAB^{OFF} and OpvAB^{ON} subpopulations. A. GFP fluorescence distribution in *S. enterica* strains carrying an *opvAB::gfp* fusion in a wild type background and in the absence of genes *hupA* and/or *hupB*. **B.** β-galactosidase activity of *S. enterica* strains carrying an *opvB::lac* fusion in a wild type background and in the absence of genes *hupA* and/or *hupB*. **C.** Visual observation of phase variation on LB + X-gal plates in strains carrying an *opvB::lac* fusion a wild type background and in the absence of genes *hupA* and/or *hupB*. **D.** GFP fluorescence distribution in *S. enterica* strains carrying an *opvAB::gfp* fusion and a *hupA hupB* mutation in OpvAB^{ON}-locked backgrounds. **E.** β-galactosidase activity of *S. enterica* strains carrying an *opvB::lac* fusion in the wild type (black bars) and in a *hupA hupB* background (white bars).

DISCUSSION

STM2209 (*opvA*) and *STM2208* (*opvB*), hitherto annotated as putative genes of unknown function in the genome of *Salmonella enterica* serovar Typhimurium, are absent in *Salmonella bongori* and in other species of enteric bacteria (**Figure C1.1**). This assortment, combined with G+C content lower than the core *Salmonella* genome (38% *vs* 52%, approximately), suggests acquisition by horizontal transfer.

opvA and *opvB* are part of a single transcriptional unit, and are transcribed from a promoter upstream *opvA* (**Figure C1.4**). The *opvA* gene product is a small hydrophobic peptide (putatively, 34 amino acids) while *opvB* encodes a larger protein (putatively, 221 amino acids). Both OpvA and OpvB have predicted transmembrane domains (**Figure C1.2**). They are indeed inner membrane proteins (**Figure C1.8**) that form intertwining ribbons (**Figure C1.9**) reminiscent of those formed in the outer membrane by the LPS [356]. Synthesis of OpvA and OpvB alters the synthesis of the LPS O-antigen and confers a main modal length of 3-8 O-antigen repeat units (**Figure 1.12**). Genetic evidence presented in **Figure 1.13** suggests that OpvA may prevent the formation of normal O-antigen, allowing OpvB to compete with the Wzz_{ST} modal length regulator. A similar phenomenon occurs in *Pseudomonas aeruginosa*, where the Iap transmembrane peptide encoded by bacteriophage D3 disrupts endogenous O-antigen biosynthesis allowing a phage-encoded O-antigen polymerase to produce a different O-antigen [357].

Certain structural features of OpvA and OpvB are reminiscent of those found in interacting peptide-protein pairs located in the bacterial cytoplasmic membrane [334]. For instance, the putative transmembrane domain of OpvA and the putative N-terminus-proximal transmembrane domain of OpvB are rich in phenylalanine and share additional amino acid sequence features. OpvA and OpvB, however, lack common packing motifs described elsewhere for transmembrane-helix interactions, such as GxxxG, Ala-coil or motifs of serine and threonine [358–360]. Small regulatory peptides often interact with larger proteins encoded in the same transcriptional unit, modulating their activity or stability [334]. This study presents evidence that OpvA and OpvB interact indeed (**Figure C1.10**). The functional significance of OpvA-OpvB interaction remains unknown.

OpvB displays features typical of Gram-negative O-antigen chain length regulators such as Wzz_{ST} and Wzz_{fepE}: a common protein structure consisting of two transmembrane

domains and a hydrophilic periplasmic domain, relative richness in proline residues in the second transmembrane segment [54], and a particular set of conserved amino acid residues near the N-terminal end [55]. OpvB lacks, however, a predicted coiled-coil periplasmic domain typical of many O-antigen chain length regulators [54]. However, other O-antigen chain length regulators show little or no potential for coiled-coil formation. Furthermore, there is a correlation between coiled-coil potential of the periplasmic domain and the modal length conferred on the LPS O-antigen chains [54]. Because constitutive expression of *opvAB* leads to short modal length of the O-antigen (**Figure C1.12**), lack of coiled-coil potential is not surprising.

Expression of the *opvAB* locus is subject to phase variation (**Figure C1.6**), and the OFF→ON switching frequency in LB medium is 3 orders of magnitude lower than ON→OFF switching (6.1×10^{-5} *vs* 3.7×10^{-2} per cell and generation). Skewed frequencies of switching are also found in other phase variation loci: for instance, in the *E. coli pap* operon, the OFF→ON switching frequency is 5.5×10^{-4} per cell and generation, while the ON→OFF switching frequency is 2.3×10^{-2} per cell and generation [361]. Hence, like in *pap*, the subpopulation of cells that express *opvAB* in LB is smaller than the population of cells that do not express *opvAB*. However, the switching frequencies detected under laboratory conditions can be different from those occurring in natural environments [130,362]. In the *pap* operon, for instance, the switching frequencies are skewed by environmental inputs involving global regulators like Crp and H-NS and the stress-responsive system CpxRA [363–365].

Lack of Dam methylation locks *opvAB* in the ON state (**Figures C1.3 and C1.6**), thus explaining why *opvAB* was initially considered a locus repressed by Dam methylation [300]. Dam methylation has been previously shown to control phase variation systems along with a variety of transcriptional regulators [130]. However, Dam methylation can also regulate gene expression indirectly, either as a consequence of lack of DNA mismatch repair or by controlling expression of postranscriptional regulators [122,124]. In the case of *opvAB*, the observation that site-directed mutagenesis of GATC sites located upstream the *opvAB* promoter locks expression in the ON state (**Figure C1.7**) provides preliminary evidence that Dam methylation may regulate *opvAB* transcription. Evidence that *opvAB* is a new locus under the control of a Dam-sensitive transcriptional regulator is further supported by the identification of the LysR-like factor OxyR as a

positive regulator of *opvAB* expression (**Figure C1.5**). OxyR is a well known LysR-type transcriptional regulator [84], and has been previously shown to control phase variation of other Dam methylation-sensitive loci: the *E. coli agn43* gene [238,240] and the P22 *gtr* operon [93]. Unlike *agn43*, which is repressed by OxyR [238], and *gtr*, which is both activated and repressed by OxyR [93], *opvAB* is under positive control by OxyR (**Figure C1.5**). Like in *agn43* and in *gtr*, however, the oxidation state of OxyR is irrelevant for control of *opvAB* expression.

When *opvAB* expression is locked in the ON state, *Salmonella* cells become resistant to adsorption of phage P22 (**Figure C1.11**), presumably by alteration of O-antigen chain length in the lipopolysaccharide (**Figures C1.12 and D1**). Hence, phase variation of *opvAB* expression in wild type populations of *Salmonella* is expected to generate a subpopulation of P22-resistant cells. Phase variation in mechanisms of defense against bacteriophage infection has been previously described [222]. The *gtr* operon that controls *Salmonella* lipopolysaccharide modification is also subject to phase variation [93]. However, to our knowledge, *opvAB* may be the first example of a phase variation system that confers phage resistance through alteration of O-antigen chain length.

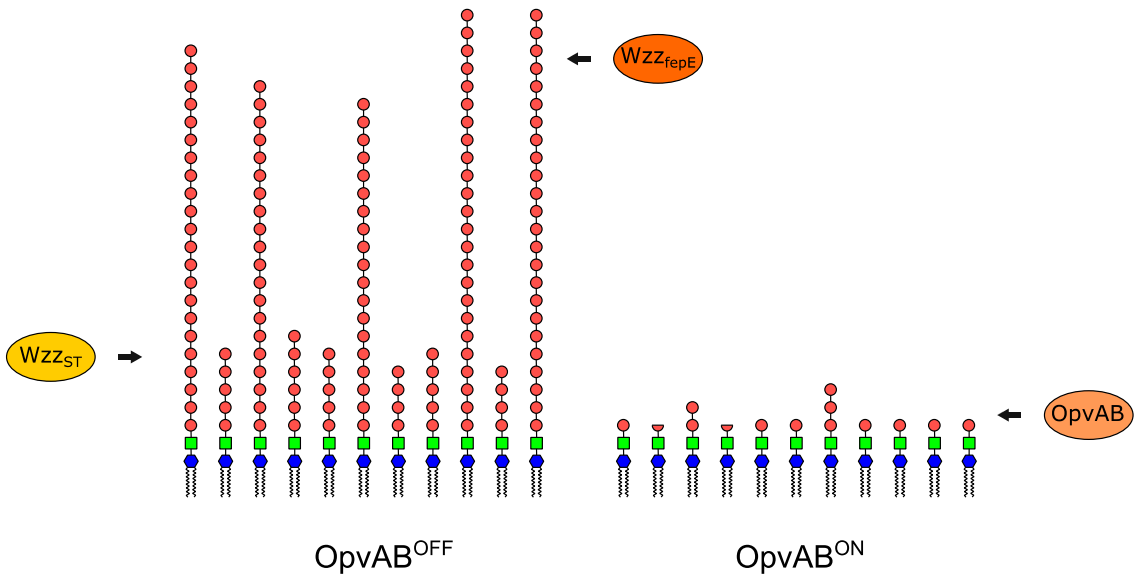

Figure D1. Diagrams of lipopolysaccharide structure in the OpvAB^{OFF} and OpvAB^{ON} subpopulations. Lipid A is represented in blue and core oligosaccharide in green. Every red circle represents five O-antigen repeat units. Modal lengths conferred by Wzz$_{ST}$, Wzz$_{fepE}$ and OpvAB are indicated.

The dramatic change in LPS structure caused by *opvAB* expression (**Figures C1.12 and D1**), renders *S. enterica* resistant to bacteriophages 9NA, Det7, and P22 (**Figures C2.1 and C2.2**), an observation consistent with the fact that the O-antigen is the bacterial surface receptor used by these bacteriophages [31,47,288,366].

As already stated, expression of *opvAB* undergoes phase variation under the control of DNA adenine methylation and the transcriptional regulator OxyR (**Figure C1.6**). Because *opvAB* phase variation is skewed towards the OFF state, *S. enterica* populations contain a major subpopulation of $OpvAB^{OFF}$ (phage-sensitive) cells and a minor subpopulation of $OpvAB^{ON}$ (phage-resistant) cells. In the presence of a bacteriophage, the $OpvAB^{OFF}$ subpopulation is killed and the $OpvAB^{ON}$ subpopulation is selected (**Figures C2.1, C2.2, and D2**). Hence, the existence of a small subpopulation of phage-resistant cells preadapts *S. enterica* to survive phage challenge. In $OpvAB^{-}$ *S. enterica*, acquisition of phage resistance is mutational only, and a frequent mechanism is alteration of LPS structure (**Figure C2.4**). Because the LPS plays major roles in bacterial physiology including resistance to environmental injuries and host-pathogen interaction [367], *opvAB* phase variation may have selective value by providing *S. enterica* with a non-mutational, reversible mechanism of phage resistance. This mechanism offers the additional advantage of protecting *Salmonella* from multiple phages, perhaps from all phages that bind the O-antigen (note that the phages used in this study belong to three different families: Podoviridae, Siphoviridae, and Myoviridae).

However, acquisition of phage resistance in $OpvAB^{ON}$ cells requires a payoff: reduced virulence in the mouse model (**Table C2.2**). In a phage-free environment, this payoff may not be relevant because the avirulent subpopulation is minor as a consequence of skewed switching of *opvAB* toward the OFF state: 3.7×10^{-2} for ON→OFF switching *vs* 6.1×10^{-5} for OFF→ON switching. In other words, only 1/1,000 *S. enterica* cells can be expected to be avirulent in a phage-free environment. The virulence payoff is therefore enforced in the presence of phage only, and its adaptive value may be obvious as it permits survival. On the other hand, the fitness cost of OpvAB-mediated phage resistance can be expected to be temporary only because phase variation permits resuscitation of the virulent $OpvAB^{OFF}$ subpopulation as soon as phage challenge ceases (**Figure C2.3**). Resuscitation may actually be rapid as a consequence of skewed switching towards the $OpvAB^{OFF}$ state.

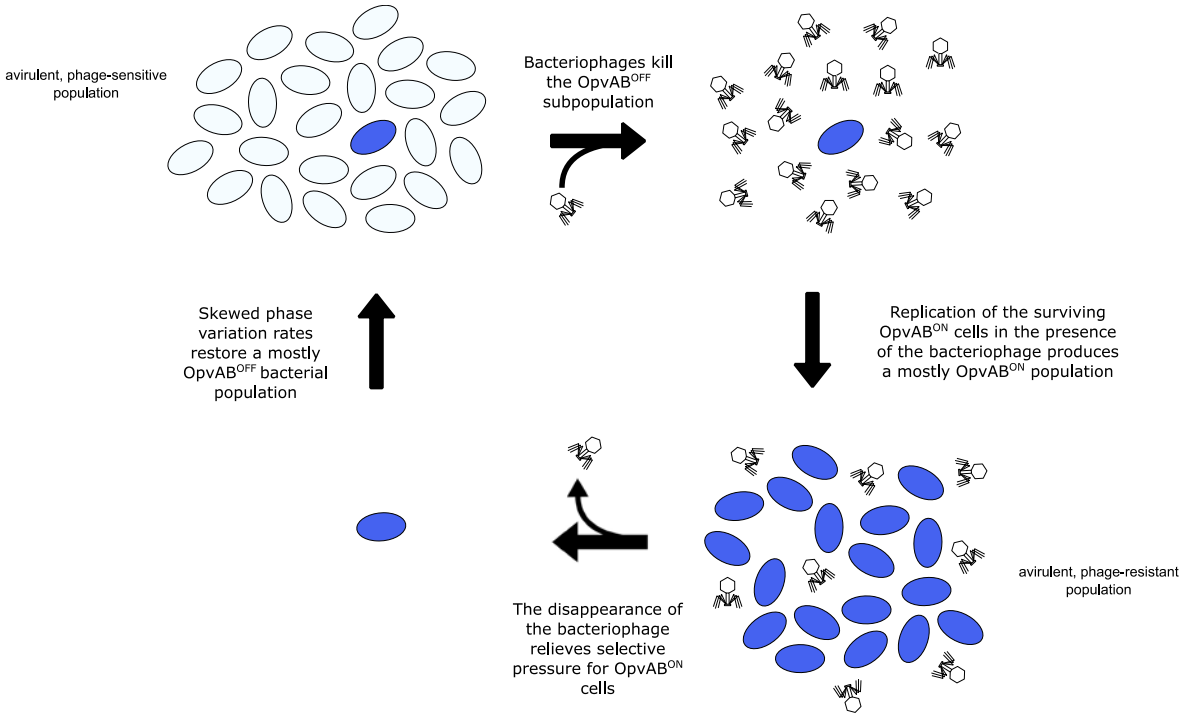

Figure D2. *opvAB* as a reversible bacteriophage resistance mechanism. Diagram for the selection of the OpvAB^{ON} subpopulation in presence of a bacteriophage that uses the O-antigen as receptor. OpvAB^{OFF} cells are represented in white, OpvAB^{ON} cells in blue.

O-antigen alteration may be also the cause of two infection-related traits associated to *opvAB* expression. One is increased sensitivity to serum (**Figure C2.5**), which may be explained by the involvement of O-antigen chain length in serum resistance [45,52,342,344]. Reduced capacity to proliferate in macrophages (**Figure C2.6**) could also be attributed to modification of the structure of LPS [368,369], although the relevance of O-antigen chain length in the *Salmonella*-macrophage interaction has been questioned [41,43]. On the other hand, LPS-containing outer membrane vesicles have been shown to mediate delivery of *Salmonella* virulence effectors to macrophages [370], suggesting that constitutive synthesis of OpvA and OpvB might impair the secretion process. Current evidence suggests that diversity in the structure and distribution of O-antigen length permits a balance between resistance to antimicrobial compounds and the ability to interact with different cell types [43].

The fact that OpvAB confers bacteriophage resistance at the expense of reducing virulence is an example of a bet-hedging strategy, which is based on a tradeoff. A

tradeoff is established whenever the adaptive capacity of an organism is increased at the expense of lowering the fitness conferred by specific phenotypic traits [371]. Tradeoffs have been mainly studied in sexually reproducing organisms but they occur also in microbes [372–375]. In pathogens, for instance, acquisition of mutational resistance to antimicrobial compounds often affects fitness [376,377], and may require loss of virulence as a payoff [378]. Bacteriophage resistance has been also shown to impair virulence in a variety of bacterial pathogens [379]. Expression of *opvAB* constitutes an unusual case of a tradeoff because phage resistance is not mutational but epigenetic, and because the phage-resistant, avirulent phenotype is reversible.

Phase variation systems that contribute to bacteriophage resistance have been described previously. For instance, certain restriction-modification systems show phase-variable expression [222]. However, protection by restriction-modification systems can be expected to be incomplete as only a fraction of infecting phage genomes are modified [380]. Phase variation can also confer phage resistance by preventing infection, and an interesting example is the *gtr* cluster which protects *S. enterica* against the T5-like phage SPC35 [219]. Although the receptor of SPC35 is the BtuB vitamin transporter, Gtr-mediated glycosylation of the LPS O-antigen may reduce SPC35 adsorption by an indirect mechanism [219]. In *Haemophilus influenzae*, phase-variable resistance to bacteriophage HP1c1 may involve changes in LPS [220]. Because these studies did not investigate the impact of phase variation on bacterial fitness, it remains unknown whether the tradeoff associated with *opvAB* phase variation is unusual or commonplace. However, if one considers that envelope structures play multiple roles in bacterial physiology aside from serving as phage receptors, it is tempting to predict that phase-variable bacteriophage resistance may frequently involve fitness costs. Whatever the payoff, however, phase-variable resistance may have a crucial advantage over mutation by creating phenotypic heterogeneity in a reversible manner.

Phase variation of *opvAB* depends on a regulatory region upstream of the *opvAB* promoter, depicted in **Figures C1.7, C3.2, and D2**. This region contains 4 half-sites for binding of OxyR (OBS_{A-D}), and 4 methylatable GATC motifs ($GATC_{1-4}$). As already stated, OxyR is a LysR-type transcriptional regulator that also acts as a sensor of oxidative stress, but its function in *opvAB* regulation is unrelated to oxidative damage and independent of its own oxidation state. The same is true for other OxyR-dependent

phase variation systems such as *agn43* [96] and *gtr* [93]. OxyR binds DNA as a tetramer [90].

SMRT sequencing data show that *S. enterica* $OpvAB^{OFF}$ and $OpvAB^{ON}$ bacterial subpopulations differ in their pattern of Dam methylation at the *opvAB* regulatory region (**Table C3.1**). The patterns found are actually opposite: in the $OpvAB^{OFF}$ state, $GATC_1$ and $GATC_3$ are nonmethylated, whereas $GATC_2$ and $GATC_4$ are methylated; in the $OpvAB^{ON}$ state, $GATC_2$ and $GATC_4$ are nonmethylated, whereas $GATC_1$ and $GATC_3$ are methylated. We provide evidence that DNA methylation patterns at the *opvAB* control region are generated by OxyR binding (**Figure C3.5**). Combinations of methylated and nonmethylated GATC sites have been previously described in other phase variation loci including *pap* and *gtr* [93,353]. In these loci, GATC nonmethylation is the consequence of DNA methylation hindrance upon protein binding. The methylation blocking factor active in the *pap* operon is Lrp [216,353], while in *gtr* it is, like in this study, OxyR [93].

The higher stability of the $OpvAB^{OFF}$ lineage is in agreement with the fact that the protected OxyR binding sites (OBS_A and OBS_C) are identical to the consensus sequence for OxyR binding. In contrast, OBS_B and OBS_D share 8/10 and 7/10 nucleotides with the consensus, respectively. The relevance of the nucleotide sequence of OxyR binding sites for *opvAB* regulation is illustrated by the observation that a single nucleotide change in OBS_B locks the system in the ON state (**Figure C3.6**). A mutation in OBS_D also yields an $OpvAB^{ON}$ lineage even though increase in expression is lower (**Figure C3.6**). It has been suggested that RNA polymerase may contact OxyR and other LysR-type transcription factors within the DNA region occupied by the regulator [381]. Because OBS_D is located immediately upstream of the -35 module, mutation of OBS_D might impair the interaction between OxyR and the RNA polymerase. In support of this view, the mutation in OBS_D is epistatic over the mutation in OBS_B (**Figure C3.6**). In *gtr*, another phase variation system controlled by OxyR and Dam methylation, the sites bound by OxyR in the OFF and ON lineages have identical number of nucleotides in common with the consensus sequence [93], which may explain why the *gtr* locus has similar ON→OFF and OFF→ON transition rates.

Preferential methylation of $GATC_4$ might be an additional factor contributing to the stability of the $OpvAB^{OFF}$ lineage. The DNA sequences that flank $GATC_1$, $GATC_2$ and

$GATC_3$ are predicted to be relatively poor Dam methylation substrates compared with the flanking sequences of $GATC_4$ [111]. Rapid methylation of $GATC_4$ might thus contribute to perpetuation of the $OpvAB^{OFF}$ state.

Our tentative model is based on a combination of experimental data and information from the literature (and including some speculation as well), and proposes that the predominant OFF state involves binding of an OxyR tetramer to the OBS_{AC} binding site, which protects $GATC_1$ and $GATC_3$ from methylation (**Table C3.1 and Figure C3.5**). In this configuration, $GATC_2$ and $GATC_4$ are unprotected and therefore are methylated by Dam. In the ON state, two OxyR tetramers are bound to two adjacent pairs of OxyR binding half-sites, one to OBS_{AB} and the other to OBS_{CD}. In this way, $GATC_2$ and $GATC_4$ are protected from methylation and remain nonmethylated, whereas $GATC_1$ and $GATC_3$ are unprotected and are methylated (**Table C3.1**). In the latter configuration, RNA polymerase is successfully recruited to the *opvAB* promoter and transcription of *opvAB* takes place. OxyR has been shown to recruit RNA polymerase by direct contact with the C-terminal domain of the α subunit [73,382], and the inverse is also true: RNA polymerase can recruit OxyR [73], which might contribute to maintenance of the $OpvAB^{ON}$ state. OxyR has been shown to bind alternative pairs of half-sites in *gtr* [93], and *opvAB* may constitute another example of the same phenomenon albeit with a different genomic architecture.

DNA bending, which is commonly induced by OxyR [90], specifically by the reduced tetramer structure [72], and by other LysR-type regulators [80,383–385] may further contribute to interaction between the OxyR tetramers and the RNA polymerase. A DNA bend is induced by OxyR in *agn43* [96,386], another phase variation locus regulated by Dam methylation and OxyR. The occurrence of bending might help to understand why $GATC_1$ and $GATC_3$ are protected from methylation in the $OpvAB^{OFF}$ configuration (**Table C3.1 and Figure C3.5**) despite their location outside OBS_A and OBS_c (**Figure D3**).

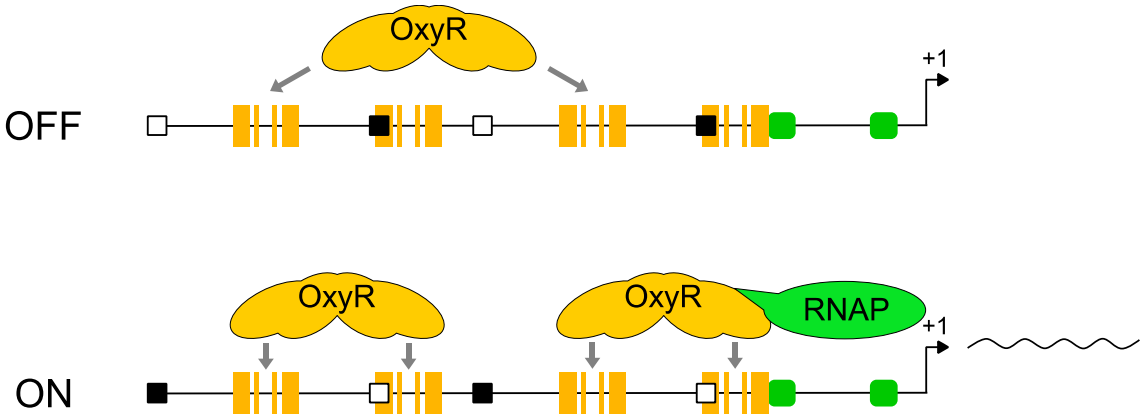

Figure D3. Model of *opvAB* phase variation. The diagram shows the Dam methylation states found in $OpvAB^{OFF}$ and $OpvAB^{ON}$ cell lineages and the hypothetical patterns of OxyR binding to cognate sites. Black and white squares represent methylated and nonmethylated GATC sites, respectively.

Another factor that might contribute to methylation hindrance in $GATC_1$ and $GATC_3$ might be DNA wrapping, which has been proposed for other transcriptional regulators whose footprints extend outside the binding sites. Examples include the NtrC [348], RcnR [349] and NorR [350,351] transcription factors from *Escherichia coli*. CarP, also called PepA, an *E. coli* transcription factor, specifically prevents methylation of a GATC site which is not included in the binding footprint [387]. $GATC_1$ and $GATC_3$, which lie in the extended OxyR-bound region, may be protected from Dam methylation in an analogous fashion.

Additional factors involved in the formation of OpvAB cell lineages are the GATC-binding protein SeqA and the nucleoid protein HU. SeqA contributes to the stability of the $OpvAB^{OFF}$ lineage, acting as a repressor of the OFF→ON transition (**Figure C3.7**). SeqA action seems to be exerted mostly on $GATC_3$ and $GATC_4$ (**Figure C3.8**). Because SeqA binds hemimethylated GATC sites [140], a tentative speculation is that it might favor DNA methylation over OxyR binding during DNA replication, as previously suggested for *agn43* [154]. In turn, HU contributes to formation of the $OpvAB^{ON}$ lineage (**Figure C3.9**). Tentative interpretations may be that HU contributes to the establishment of the $OpvAB^{ON}$ state either by inducing DNA bending or by stabilizing OxyR-mediated bending. The latter possibility may be more likely as HU often stabilizes bent DNA rather than bend DNA itself [183], and HU is not essential in

OpvAB^{ON}-locked backgrounds (**Figure C3.9**). On the other hand, AT-rich DNA, such as that found in the *opvAB* regulatory region (which is 23% G+C only) is intrinsically prone to DNA bending [388,389].

If our model is correct, two OxyR tetramers may be required to maintain the ON state but only one tetramer may be necessary to maintain the OFF state. This difference may contribute to explain the high ON→OFF transition rate. Upon passage of the DNA replication fork, the local concentration of OxyR will be halved, therefore facilitating the transition from ON (depending on two OxyR tetramers) to OFF (depending on one tetramer only).

A caveat of our model is that, to our knowledge, OxyR has not been described to bind non-consecutive half-sites. However, such binding pattern is consistent with the evidence that only OBS_A and OBS_C are fully protected in the footprinting assay (**Figure 4B**) and with the fact that OxyR has been always described to bind DNA as a tetramer [73,90]. An alternative hypothesis is that OxyR dimers may bind independently to OBS_A and OBS_C.

CONCLUSIONS

1. Expression of *opvAB* is subject to phase variation: *Salmonella enterica* populations are composed of a major $OpvAB^{OFF}$ subpopulation and a minor $OpvAB^{ON}$ subpopulation.

2. $OpvAB^{OFF}$ and $OpvAB^{ON}$ subpopulations show opposite DNA methylation patterns in the *opvAB* regulatory region. Such patterns are formed upon OxyR binding and Dam methylase hindrance.

3. OpvAB activity modifies the lipopolysaccharide O-antigen, conferring a preferred modal length of 3-8 O-antigen repeat units.

4. OpvAB-mediated modification of the LPS confers resistance to bacteriophages that use the O-antigen as receptor.

5. Because OpvAB-mediated modification of the LPS decreases the virulence of *Salmonella*, *opvAB* phase variation may be considered an evolutionary tradeoff between bacteriophage resistance and virulence.

REFERENCES

1. Tindall BJ, Grimont PAD, Garrity GM, Euzéby JP. Nomenclature and taxonomy of the genus *Salmonella*. Int J Syst Evol Microbiol. 2005;55: 521–4.

2. Grimont PAD, Weill F-X. Antigenic formulae of the Salmonellae serovars. WHO Collab Cent Ref Res *Salmonella*. 2007;9th ed Ins.

3. Popoff MY, Le Minor L. Antigenic formulas of the *Salmonella* serovars. 8th revision. WHO Collab Cent Ref Res *Salmonella* Paris, Inst Pasteur. 2001;

4. McQuiston JR, Parrenas R, Ortiz-Rivera M, Gheesling L, Brenner F, Fields PI. Sequencing and comparative analysis of flagellin genes *fliC*, *fljB*, and *flpA* from *Salmonella*. J Clin Microbiol. 2004;42: 1923–1932.

5. Popoff MY, Bockemuhl J, Gheesling LL, Bockemühl J, Gheesling LL. Supplement 2002 (no. 46) to the Kauffmann-White scheme. Res Microbiol. 2004;155: 568–570.

6. McClelland M, Sanderson KE, Spieth J, Clifton SW, Latreille P, Courtney L, *et al*. Complete genome sequence of *Salmonella enterica* serovar Typhimurium LT2. Nature. 2001;413: 852–856.

7. Baumler AJ, Tsolis RM, Ficht TA, Adams LG. Evolution of host adaptation in *Salmonella enterica*. Infect Immun. 1998;66: 4579–4587.

8. Baumler A, Fang FC. Host specificity of bacterial pathogens. Cold Spring Harb Perspect Med. 2013;3: a010041.

9. Velge P, Wiedemann A, Rosselin M, Abed N, Boumart Z, Chausse AM, *et al*. Multiplicity of *Salmonella* entry mechanisms, a new paradigm for *Salmonella* pathogenesis. Microbiologyopen. 2012;1: 243–258.

10. Santos RL, Zhang S, Tsolis RM, Kingsley RA, Adams LG, Baumler AJ. Animal models of *Salmonella* infections: enteritis versus typhoid fever. Microbes Infect. 2001;3: 1335–1344.

11. Jarvik T, Smillie C, Groisman EA, Ochman H. Short-term signatures of evolutionary change in the *Salmonella enterica* serovar Typhimurium 14028 genome. J Bacteriol. 2010;192: 560–567.

12. Ochman H, Wilson AC. Evolution in bacteria: evidence for a universal substitution rate in cellular genomes. J Mol Evol. 1987;26: 74–86.

13. Porwollik S, McClelland M. Lateral gene transfer in *Salmonella*. Microbes Infect. 2003;5: 977–989.

14. Groisman EA, Ochman H. How *Salmonella* became a pathogen. Trends Microbiol. 1997;5: 343–349.

15. Kelly BG, Vespermann A, Bolton DJ. The role of horizontal gene transfer in the evolution of selected foodborne bacterial pathogens. Food Chem Toxicol. 2009;47: 951–968.

16. Hensel M. Evolution of pathogenicity islands of *Salmonella enterica*. Int J Med Microbiol. 2004;294: 95–102.

17. Ellermeier CD, Slauch JM. The genus *Salmonella*. The prokaryotes. 2006. pp. 123–158.

18. Que F, Wu S, Huang R. *Salmonella* pathogenicity island 1(SPI-1) at work. Curr Microbiol. 2013;66: 582–587.

19. Ochman H, Soncini FC, Solomon F, Groisman EA. Identification of a pathogenicity island required for *Salmonella* survival in host cells. Proc Natl Acad Sci U S A. 1996;93: 7800–7804.

20. Humphries AD, Townsend SM, Kingsley R a, Nicholson TL, Tsolis M, Ba AJ. Role of fimbriae as antigens and intestinal colonization factors of *Salmonella* serovars. 2001;201: 121–125.

21. Tennant SM, Hartland EL, Phumoonna T, Lyras D, Rood JI, Robins-Browne RM, *et al*. Influence of gastric acid on susceptibility to infection with ingested bacterial pathogens. Infect Immun. 2008;76: 639–645.

22. Foster JW, Hall HK. Adaptive acidification tolerance response of *Salmonella typhimurium*. J Bacteriol. 1990;172: 771–778.

23. Lee IS, Slonczewski JL, Foster JW. A low-pH-inducible, stationary-phase acid tolerance response in *Salmonella typhimurium*. J Bacteriol. 1994;176: 1422–1426.

24. Gunn JS. Mechanisms of bacterial resistance and response to bile. Microbes Infect. 2000;2: 907–913.

25. Prieto AI, Ramos-Morales F, Casadesus J, Casadesús J. Bile-induced DNA damage in *Salmonella enterica*. Genetics. 2004;168: 1787–1794.

26. Hernandez SB, Cota I, Ducret A, Aussel L, Casadesus J. Adaptation and preadaptation of *Salmonella enterica* to Bile. PLoS Genet. 2012;8: e1002459.

27. Hernandez SB, Cava F, Pucciarelli MG, Garcia-Del Portillo F, de Pedro MA, Casadesus J. Bile-induced peptidoglycan remodelling in *Salmonella enterica*. Env Microbiol. 2015;17: 1081–1089.

28. Sansonetti PJ. War and peace at mucosal surfaces. Nat Rev Immunol. 2004;4: 953–964.

29. Wagner C, Hensel M. Adhesive mechanisms of *Salmonella enterica*. Adv Exp Med Biol. 2011;715: 17–34.

30. Finlay BB, Brumell JH. *Salmonella* interactions with host cells: *in vitro* to *in vivo*. Philos Trans R Soc L B Biol Sci. 2000;355: 623–631.

31. Walter M, Fiedler C, Grassl R, Biebl M, Rachel R, Hermo-Parrado XL, *et al*. Structure of the receptor-binding protein of bacteriophage Det7: a podoviral tail spike in a myovirus. J Virol. 2008;82: 2265–2273.

32. Zhou D, Galan J. *Salmonella* entry into host cells: the work in concert of type III secreted effector proteins. Microbes Infect. 2001;3: 1293–1298.

33. Watson KG, Holden DW. Dynamics of growth and dissemination of *Salmonella in vivo*. Cell Microbiol. 2010;12: 1389–1397.

34. Santos RL, Tsolis RM, Zhang S, Ficht TA, Baumler AJ, Adams LG. *Salmonella*-induced cell death is not required for enteritis in calves. Infect Immun. 2001;69: 4610–4617.

35. Nunes JS, Lawhon SD, Rossetti CA, Khare S, Figueiredo JF, Gull T, *et al*. Morphologic and cytokine profile characterization of *Salmonella enterica* serovar Typhimurium infection in calves with bovine leukocyte adhesion deficiency. Vet Pathol. 2010;47: 322–333.

36. Winter SE, Thiennimitr P, Winter MG, Butler BP, Huseby DL, Crawford RW, *et al*. Gut inflammation provides a respiratory electron acceptor for *Salmonella*. Nature. 2010;467: 426–429.

37. Baumler AJ, Winter SE, Thiennimitr P, Casadesus J, Bäumler AJ, Winter SE, *et al*. Intestinal and chronic infections: *Salmonella* lifestyles in hostile environments. Env Microbiol Rep. 2011;3: 508–517.

38. Silhavy TJ, Kahne D, Walker S. The bacterial cell envelope. Cold Spring Harb Perspect Biol. 2010;2: a000414.

39. Toguchi A, Siano M, Burkart M, Harshey RM. Genetics of swarming motility in *Salmonella enterica* serovar Typhimurium: critical role for lipopolysaccharide. J Bacteriol. 2000;182: 6308–6321.

40. Nevola JJ, Laux DC, Cohen PS. In vivo colonization of the mouse large intestine and *in vitro* penetration of intestinal mucus by an avirulent smooth strain of *Salmonella typhimurium* and its lipopolysaccharide-deficient mutant. Infect Immun. 1987;55: 2884–2890.

41. Murray GL, Attridge SR, Morona R. Altering the length of the lipopolysaccharide O antigen has an impact on the interaction of *Salmonella enterica* serovar Typhimurium with macrophages and complement. J Bacteriol. 2006;188: 2735–2739.

42. Nagy G, Danino V, Dobrindt U, Pallen M, Chaudhuri R, Emody L, *et al*. Down-regulation of key virulence factors makes the *Salmonella enterica* serovar

Typhimurium *rfaH* mutant a promising live-attenuated vaccine candidate. Infect Immun. 2006;74: 5914–5925.

43. Hölzer SU, Schlumberger MC, Jäckel D, Hensel M, Holzer SU, Schlumberger MC, *et al*. Effect of the O-antigen length of lipopolysaccharide on the functions of Type III secretion systems in *Salmonella enterica*. Infect Immun. 2009;77: 5458–5470.

44. Shaio MF, Rowland H. Bactericidal and opsonizing effects of normal serum on mutant strains of *Salmonella typhimurium*. Infect Immun. 1985;49: 647–653.

45. Murray GL, Attridge SR, Morona R. Inducible serum resistance in *Salmonella typhimurium* is dependent on *wzz*fepE-regulated very long O antigen chains. Microbes Infect. 2005;7: 1296–1304.

46. Crawford RW, Keestra a. M, Winter SE, Xavier MN, Tsolis RM, Tolstikov V, *et al*. Very long O-antigen chains enhance fitness during *Salmonella*-induced colitis by increasing bile resistance. PLoS Pathog. 2012;8: e1002918.

47. Lindberg AA. Bacteriophage receptors. Annu Rev Microbiol. 1973;27: 205–241.

48. Lerouge I, Vanderleyden J. O-antigen structural variation : mechanisms and possible roles in animal / plant - microbe interactions. FEMS Microbiol Rev. 2001;26.

49. Raetz CRH, Whitfield C. Lipopolysaccharide endotoxins. Annu Rev Biochem. 2002;71: 635–700.

50. Islam ST, Lam JS. Synthesis of bacterial polysaccharides via the Wzy-dependent pathway. 2014;716: 697–716.

51. Islam ST, Huszczynski SM, Nugent T, Gold AC, Lam JS. Conserved-residue mutations in Wzy affect O-antigen polymerization and Wzz-mediated chain-length regulation in *Pseudomonas aeruginosa* PAO1. Sci Rep. 2013;3: 3441.

52. Murray GL, Attridge SR, Morona R. Regulation of *Salmonella typhimurium* lipopolysaccharide O antigen chain length is required for virulence; identification of FepE as a second Wzz. Mol Microbiol. 2003;47: 1395–1406.

53. Batchelor R a., Alifano P, Biffali E, Hull SI, Hull R a. Nucleotide sequences of the genes regulating O-polysaccharide antigen chain length (*rol*) from *Escherichia coli* and *Salmonella typhimurium*: protein homology and functional complementation. J Bacteriol. 1992;174: 5228–5236.

54. Morona R, Van den Bosch L, Daniels C. Evaluation of Wzz/MPA1/MPA2 proteins based on the presence of coiled-coil regions. Microbiology. 2000;146 (Pt 1: 1–4.

55. Tocilj A, Munger C, Proteau A, Morona R, Purins L, Ajamian E, *et al*. Bacterial polysaccharide co-polymerases share a common framework for control of polymer length. Nat Struct Mol Biol. 2008;15: 130–138.

56. Morona R, Purins L, Tocilj A, Matte A, Cygler M. Sequence-structure relationships in polysaccharide co-polymerase (PCP) proteins. Trends Biochem Sci. 2008;34: 78–84.

57. Bastin DA, Stevenson G, Brown PK, Haase A, Reeves PR. Repeat unit polysaccharides of bacteria: a model for polymerization resembling that of ribosomes and fatty acid synthetase, with a novel mechanism for determining chain length. Mol Microbiol. 1993;7: 725–734.

58. Morona R, van den Bosch L, Manning PA. Molecular, genetic, and topological characterization of O-antigen chain length regulation in *Shigella flexneri*. J Bacteriol. 1995;177: 1059–1068.

59. Kintz EN, Goldberg JB. Site-directed mutagenesis reveals key residue for O antigen chain length regulation and protein stability in *Pseudomonas aeruginosa* Wzz2. J Biol Chem. 2011;286: 44277–44284.

60. Kalynych S, Valvano M a., Cygler M. Polysaccharide co-polymerases: The enigmatic conductors of the O-antigen assembly orchestra. Protein Eng Des Sel. 2012;25: 797–802.

61. Mühlradt PF, Menzel J, Golecki JR, Speth V, Muhlradt PF, Menzel J, *et al*. Outer membrane of *Salmonella*. Sites of export of newly synthesised lipopolysaccharide on the bacterial surface. Eur J Biochem. 1973;35: 471–481.

62. Muhlradt PF, Menzel J, Golecki JR, Speth V, Mühlradt PF, Menzel J, *et al*. Lateral mobility and surface density of lipopolysaccharide in the outer membrane of *Salmonella typhimurium*. Eur J Biochem. 1974;43: 533–539.

63. Ghosh AS, Young KD. Helical disposition of proteins and lipopolysaccharide in the outer membrane of *Escherichia coli*. J Bacteriol. 2005;187: 1913–1922.

64. Takeuchi Y, Nikaido H. Persistence of segregated phospholipid domains in phospholipid--lipopolysaccharide mixed bilayers: studies with spin-labeled phospholipids. Biochemistry. 1981;20: 523–529.

65. Nikaido H. Molecular basis of bacterial outer membrane permeability revisited. Microbiol Mol Biol Rev. 2003;67: 593–656.

66. Wang Y, Hollingsworth RI. An NMR spectroscopy and molecular mechanics study of the molecular basis for the supramolecular structure of lipopolysaccharides. Biochemistry. 1996;35: 5647–5654.

67. Kastowsky M, Gutberlet T, Bradaczek H. Molecular modelling of the three-dimensional structure and conformational flexibility of bacterial lipopolysaccharide. J Bacteriol. 1992;174: 4798–4806.

68. Ursell TS, Trepagnier EH, Huang KC, Theriot J a. Analysis of surface protein expression reveals the growth pattern of the gram-negative outer membrane. PLoS Comput Biol. 2012;8: e1002680.

69. Christman MF, Storz G, Ames BN. OxyR, a positive regulator of hydrogen peroxide-inducible genes in *Escherichia coli* and *Salmonella typhimurium*, is homologous to a family of bacterial regulatory proteins. Proc Natl Acad Sci U S A. 1989;86: 3484–3488.

70. Maddocks SE, Oyston PCF. Structure and function of the LysR-type transcriptional regulator (LTTR) family proteins. Microbiology. 2008;154: 3609–3623.

71. Schell MA. Molecular biology of the LysR family of transcriptional regulators. Annu Rev Microbiol. 1993;47: 597–626.

72. Choi HJ, Kim SJ, Mukhopadhyay P, Cho S, Woo JR, Storz G, *et al*. Structural basis of the redox switch in the OxyR transcription factor. Cell. 2001;105: 103–113.

73. Kullik I, Stevens J, Toledano MB, Storz G. Mutational analysis of the redox-sensitive transcriptional regulator OxyR: regions important for DNA binding and multimerization. J Bacteriol. 1995;177: 1285–1291.

74. Schell MA, Brown PH, Raju S. Use of saturation mutagenesis to localize probable functional domains in the NahR protein, a LysR-type transcription activator. J Biol Chem. 1990;265: 3844–3850.

75. Muraoka S, Okumura R, Ogawa N, Nonaka T, Miyashita K, Senda T. Crystal structure of a full-length LysR-type transcriptional regulator, CbnR: unusual combination of two subunit forms and molecular bases for causing and changing DNA bend. J Mol Biol. 2003;328: 555–566.

76. Smirnova IA, Dian C, Leonard GA, McSweeney S, Birse D, Brzezinski P. Development of a bacterial biosensor for nitrotoluenes: the crystal structure of the transcriptional regulator DntR. J Mol Biol. 2004;340: 405–418.

77. Zhou X, Lou Z, Fu S, Yang A, Shen H, Li Z, *et al*. Crystal structure of ArgP from Mycobacterium tuberculosis confirms two distinct conformations of full-length LysR transcriptional regulators and reveals its function in DNA binding and transcriptional regulation. J Mol Biol. 2010;396: 1012–1024.

78. Guadarrama C, Medrano-Lopez A, Oropeza R, Hernandez-Lucas I, Calva E. The *Salmonella enterica* serovar Typhi LeuO global regulator forms tetramers: residues involved in oligomerization, DNA binding, and transcriptional regulation. J Bacteriol. 2014;196: 2143–2154.

79. Maxon ME, Wigboldus J, Brot N, Weissbach H. Structure-function studies on *Escherichia coli* MetR protein, a putative prokaryotic leucine zipper protein. Proc Natl Acad Sci U S A. 1990;87: 7076–7079.

80. Fisher RF, Long SR. Interactions of NodD at the nod Box: NodD binds to two distinct sites on the same face of the helix and induces a bend in the DNA. J Mol Biol. 1993;233: 336–348.

81. Sainsbury S, Lane L a., Ren J, Gilbert RJ, Saunders NJ, Robinson C V., *et al*. The structure of CrgA from *Neisseria meningitidis* reveals a new octameric assembly state for LysR transcriptional regulators. Nucleic Acids Res. 2009;37: 4545–4558.

82. Gong W, Xiong G, Maser E. Oligomerization and negative autoregulation of the LysR-type transcriptional regulator HsdR from *Comamonas testosteroni*. J Steroid Biochem Mol Biol. 2012;132: 203–211.

83. Chiang SM, Schellhorn HE. Regulators of oxidative stress response genes in *Escherichia coli* and their functional conservation in bacteria. Arch Biochem Biophys. Elsevier Inc.; 2012;525: 161–169.

84. Storz G, Tartaglia LA, Ames BN. The OxyR regulon. Antonie Van Leeuwenhoek. 1990;58: 157–161.

85. Christman MF, Morgan RW, Jacobson FS, Ames BN. Positive control of a regulon for defenses against oxidative stress and some heat-shock proteins in *Salmonella typhimurium*. Cell. 1985;41: 753–62.

86. Kramer GF, Ames BN. Oxidative mechanisms of toxicity of low-intensity near-UV light in *Salmonella typhimurium*. J Bacteriol. 1987;169: 2259–2266.

87. Kim SY, Kim EJ, Park JW. Control of singlet oxygen-induced oxidative damage in *Escherichia coli*. J Biochem Mol Biol. 2002;35: 353–357.

88. Yoon SJ, Park JE, Yang JH, Park JW. OxyR regulon controls lipid peroxidation-mediated oxidative stress in *Escherichia coli*. J Biochem Mol Biol. 2002;35: 297–301.

89. Staudinger BJ, Oberdoerster MA, Lewis PJ, Rosen H. mRNA expression profiles for *Escherichia coli* ingested by normal and phagocyte oxidase-deficient human neutrophils. J Clin Invest. 2002;110: 1151–1163.

90. Toledano MB, Kullik I, Trinh F, Baird PT, Schneider TD, Storz G. Redox-dependent shift of OxyR-DNA contacts along an extended DNA-binding site: a mechanism for differential promoter selection. Cell. 1994;78: 897–909.

91. Kullik I, Toledano MB, Tartaglia L a., Storz G. Mutational analysis of the redox-sensitive transcriptional regulator OxyR: regions important for oxidation and transcriptional activation. J Bacteriol. 1995;177: 1275–1284.

92. Zheng M, Aslund F, Storz G. Activation of the OxyR transcription factor by reversible disulfide bond formation. Science (80-). 1998;279: 1718–1721.

93. Broadbent SE, Davies MR, Van Der Woude MW. Phase variation controls expression of *Salmonella* lipopolysaccharide modification genes by a DNA methylation-dependent mechanism. Mol Microbiol. 2010;77: 337–353.

94. Goethals K, Van Montagu M, Holsters M. Conserved motifs in a divergent *nod* box of *Azorhizobium caulinodans* ORS571 reveal a common structure in promoters regulated by LysR-type proteins. Proc Natl Acad Sci U S A. 1992;89: 1646–1650.

95. Hattman S, Sun W. *Escherichia coli* OxyR modulation of bacteriophage Mu *mom* expression in dam+ cells can be attributed to its ability to bind hemimethylated P*mom* promoter DNA. Nucleic Acids Res. 1997;25: 4385–4388.

96. Wallecha A, Correnti J, Munster V, Woude M Van Der. Phase Variation of Ag43 Is Independent of the Oxidation State of OxyR. 2003;185.

97. Barbeyron T, Kean K, Forterre P. DNA adenine methylation of GATC sequences appeared recently in the *Escherichia coli* lineage. J Bacteriol. 1984;160: 586–590.

98. Cheng X. Structure and function of DNA methyltransferases. Annu Rev Biophys Biomol Struct. 1995;24: 293–318.

99. Jeltsch A. Beyond Watson and Crick: DNA methylation and molecular enzymology of DNA methyltransferases. Chembiochem. 2002;3: 274–293.

100. Wion D, Casadesus J. N6-methyl-adenine: an epigenetic signal for DNA-protein interactions. Nat Rev Microbiol. 2006;4: 183–192.

101. Engel JD, von Hippel PH. Effects of methylation on the stability of nucleic acid conformations. Studies at the polymer level. J Biol Chem. 1978;253: 927–934.

102. Diekmann S. DNA methylation can enhance or induce DNA curvature. EMBO J. 1987;6: 4213–4217.

103. Bickle TA, Kruger DH. Biology of DNA restriction. Microbiol Rev. 1993;57: 434–450.

104. Loenen WA, Dryden DT, Raleigh EA, Wilson GG, Murray NE. Highlights of the DNA cutters: a short history of the restriction enzymes. Nucleic Acids Res. 2014;42: 3–19.

105. Løbner-Olesen A, Skovgaard O, Marinus MG, Lobner-Olesen A, Skovgaard O, Marinus MG. Dam methylation: coordinating cellular processes. Curr Opin Microbiol. 2005;8: 154–160.

106. Julio SM, Heithoff DM, Provenzano D, Klose KE, Sinsheimer RL, Low DA, *et al*. DNA adenine methylase is essential for viability and plays a role in the pathogenesis of *Yersinia pseudotuberculosis* and *Vibrio cholerae*. Infect Immun. 2001;69: 7610–7615.

107. Marinus MG. Methylation of DNA. In: al. FCN et, editor. *Escherichia coli* and *Salmonella*: cellular and molecular biology. Washington, D.C.: ASM Press; 1996. pp. 782–791.

108. Torreblanca J, Casadesus J. DNA adenine methylase mutants of *Salmonella typhimurium* and a novel dam-regulated locus. Genetics. 1996;144: 15–26.

109. Low DA, Weyand NJ, Mahan MJ. Roles of DNA adenine methylation in regulating bacterial gene expression and virulence. Infect Immun. 2001;69: 7197–7204.

110. Urig S, Gowher H, Hermann A, Beck C, Fatemi M, Humeny A, *et al*. The *Escherichia coli* dam DNA methyltransferase modifies DNA in a highly processive reaction. J Mol Biol. 2002;319: 1085–1096.

111. Peterson SN, Reich NO. GATC flanking sequences regulate Dam activity: evidence for how Dam specificity may influence pap expression. J Mol Biol. 2006;355: 459–472.

112. Reisenauer A, Kahng LS, McCollum S, Shapiro L. Bacterial DNA methylation: a cell cycle regulator? J Bacteriol. 1999;181: 5135–5139.

113. Hsieh P. Molecular mechanisms of DNA mismatch repair. Mutat Res. 2001;486: 71–87.

114. Friedhoff P, Thomas E, Pingoud A. Tyr212: a key residue involved in strand discrimination by the DNA mismatch repair endonuclease MutH. J Mol Biol. 2003;325: 285–297.

115. Boye E, Løbner-Olesen A, Skarstad K. Limiting DNA replication to once and only once. EMBO Rep. 2000;1: 479–83.

116. Zyskind JW, Smith DW. DNA replication, the bacterial cell cycle, and cell growth. Cell. 1992;69: 5–8.

117. Taghbalout A, Landoulsi A, Kern R, Yamazoe M, Hiraga S, Holland B, *et al*. Competition between the replication initiator DnaA and the sequestration factor SeqA for binding to the hemimethylated chromosomal origin of E. coli in vitro. Genes Cells. 2000;5: 873–884.

118. Han JS, Kang S, Lee H, Kim HK, Hwang DS. Sequential binding of SeqA to paired hemi-methylated GATC sequences mediates formation of higher order complexes. J Biol Chem. 2003;278: 34983–34989.

119. Guarné A, Brendler T, Zhao Q, Ghirlando R, Austin S, Yang W, *et al*. Crystal structure of a SeqA-N filament: implications for DNA replication and chromosome organization. EMBO J. 2005;24: 1502–1511.

120. Badie G, Heithoff DM, Sinsheimer RL, Mahan MJ. Altered levels of *Salmonella* DNA adenine methylase are associated with defects in gene expression, motility,

flagellar synthesis, and bile resistance in the pathogenic strain 14028 but not in the laboratory strain LT2. J Bacteriol. 2007;189: 1556–1564.

121. García-Del Portillo F, Pucciarelli MG, Casadesús J, Garcia-Del Portillo F, Pucciarelli MG, Casadesus J. DNA adenine methylase mutants of *Salmonella typhimurium* show defects in protein secretion, cell invasion, and M cell cytotoxicity. Proc Natl Acad Sci U S A. 1999;96: 11578–11583.

122. Marinus MG, Casadesus J. Roles of DNA adenine methylation in host-pathogen interactions: mismatch repair, transcriptional regulation, and more. FEMS Microbiol Rev. 2009;33: 488–503.

123. Sarnacki SH, Marolda CL, Noto Llana M, Giacomodonato MN, Valvano M a., Cerquetti MC, *et al*. Dam methylation controls O-antigen chain length in *Salmonella enterica* serovar Enteritidis by regulating the expression of Wzz protein. J Bacteriol. 2009;191: 6694–6700.

124. López-Garrido J, Casadesús J. Regulation of *Salmonella enterica* pathogenicity island 1 by DNA adenine methylation. Genetics. 2010;184: 637–649.

125. Low DA, Casadesús J. Clocks and switches: bacterial gene regulation by DNA adenine methylation. Curr Opin Microbiol. 2008;11: 106–112.

126. Roberts D, Hoopes BC, McClure WR, Kleckner N. IS10 transposition is regulated by DNA adenine methylation. Cell. 1985;43: 117–130.

127. Camacho EM, Casadesus J. Regulation of *traJ* transcription in the *Salmonella* virulence plasmid by strand-specific DNA adenine hemimethylation. Mol Microbiol. 2005;57: 1700–1718.

128. Kucherer C, Lother H, Kolling R, Schauzu MA, Messer W. Regulation of transcription of the chromosomal *dnaA* gene of *Escherichia coli*. Mol Gen Genet. 1986;205: 115–121.

129. Van der Woude MW. Phase variation: how to create and coordinate population diversity. Curr Opin Microbiol. Elsevier Ltd; 2011;14: 205–211.

130. Casadesús J, Low D. Epigenetic gene regulation in the bacterial world. Microbiol Mol Biol Rev. 2006;70: 830–856.

131. Hiraga S, Ichinose C, Onogi T, Niki H, Yamazoe M. Bidirectional migration of SeqA-bound hemimethylated DNA clusters and pairing of *oriC* copies in *Escherichia coli*. Genes Cells. 2000;5: 327–341.

132. Lu M, Campbell JL, Boye E, Kleckner N. SeqA: a negative modulator of replication initiation in *E. coli*. Cell. 1994;77: 413–426.

133. Campbell JL, Kleckner N. *E. coli oriC* and the *dnaA* gene promoter are sequestered from Dam methyltransferase following the passage of the chromosomal replication fork. Cell. 1990;62: 967–979.

134. Lee H, Kang S, Bae SH, Choi BS, Hwang DS. SeqA protein aggregation is necessary for SeqA function. J Biol Chem. 2001;276: 34600–34606.

135. Kang S, Han JS, Kim KP, Yang HY, Lee KY, Hong CB, *et al*. Dimeric configuration of SeqA protein bound to a pair of hemi-methylated GATC sequences. Nucleic Acids Res. 2005;33: 1524–1531.

136. Brendler T, Sawitzke J, Sergueev K, Austin S. A case for sliding SeqA tracts at anchored replication forks during *Escherichia coli* chromosome replication and segregation. EMBO J. 2000;19: 6249–6258.

137. Han JS, Kang S, Kim SH, Ko MJ, Hwang DS. Binding of SeqA protein to hemi-methylated GATC sequences enhances their interaction and aggregation properties. J Biol Chem. 2004;279: 30236–30243.

138. Brendler T, Abeles A, Austin S. A protein that binds to the P1 origin core and the *oriC* 13mer region in a methylation-specific fashion is the product of the host *seqA* gene. EMBO J. 1995;14: 4083–4089.

139. Slater S, Wold S, Lu M, Boye E, Skarstad K, Kleckner N. *E. coli* SeqA protein binds *oriC* in two different methyl-modulated reactions appropriate to its roles in DNA replication initiation and origin sequestration. Cell. 1995;82: 927–936.

140. Kang S, Lee H, Han JS, Hwang DS. Interaction of SeqA and Dam methylase on the hemimethylated origin of *Escherichia coli* chromosomal DNA replication. J Biol Chem. 1999;274: 11463–11468.

141. Skarstad K, Lueder G, Lurz R, Speck C, Messer W. The *Escherichia coli* SeqA protein binds specifically and co-operatively to two sites in hemimethylated and fully methylated *oriC*. Mol Microbiol. 2000;36: 1319–1326.

142. Skarstad K, Boye E. The initiator protein DnaA: evolution, properties and function. Biochim Biophys Acta. 1994;1217: 111–130.

143. Boye E, Stokke T, Kleckner N, Skarstad K. Coordinating DNA replication initiation with cell growth: differential roles for DnaA and SeqA proteins. Proc Natl Acad Sci U S A. 1996;93: 12206–12211.

144. Torheim NK, Skarstad K. *Escherichia coli* SeqA protein affects DNA topology and inhibits open complex formation at oriC. EMBO J. 1999;18: 4882–4888.

145. Katayama T. Feedback controls restrain the initiation of *Escherichia coli* chromosomal replication. Mol Microbiol. 2001;41: 9–17.

146. Hansen FG, Atlung T, Braun RE, Wright A, Hughes P, Kohiyama M. Initiator (DnaA) protein concentration as a function of growth rate in *Escherichia coli* and *Salmonella typhimurium*. J Bacteriol. 1991;173: 5194–5199.

147. Bogan JA, Helmstetter CE. DNA sequestration and transcription in the *oriC* region of *Escherichia coli*. Mol Microbiol. 1997;26: 889–896.

148. Brendler T, Austin S. Binding of SeqA protein to DNA requires interaction between two or more complexes bound to separate hemimethylated GATC sequences. EMBO J. 1999;18: 2304–2310.

149. Fossum S, Soreide S, Skarstad K. Lack of SeqA focus formation, specific DNA binding and proper protein multimerization in the *Escherichia coli* sequestration mutant *seqA2*. Mol Microbiol. 2003;47: 619–632.

150. Helgesen E, Fossum-Raunehaug S, Saetre F, Schink KO, Skarstad K. Dynamic *Escherichia coli* SeqA complexes organize the newly replicated DNA at a considerable distance from the replisome. Nucleic Acids Res. 2015;43: 2730–2743.

151. Molina F, Skarstad K. Replication fork and SeqA focus distributions in *Escherichia coli* suggest a replication hyperstructure dependent on nucleotide metabolism. Mol Microbiol. 2004;52: 1597–1612.

152. Fossum S, Crooke E, Skarstad K. Organization of sister origins and replisomes during multifork DNA replication in *Escherichia coli*. EMBO J. 2007;26: 4514–4522.

153. Lobner-Olesen A, Marinus MG, Hansen FG. Role of SeqA and Dam in *Escherichia coli* gene expression: a global/microarray analysis. Proc Natl Acad Sci U S A. 2003;100: 4672–4677.

154. Correnti J, Munster V, Chan T, Woude M, Van der Woude M. Dam-dependent phase variation of Ag43 in *Escherichia coli* is altered in a *seqA* mutant. Mol Microbiol. 2002;44: 521–532.

155. Jakomin M, Chessa D, Bäumler AJ, Casadesús J. Regulation of the *Salmonella enterica std* fimbrial operon by DNA adenine methylation, SeqA, and HdfR. J Bacteriol. 2008;190: 7406–7413.

156. Browning DF, Grainger DC, Busby SJ. Effects of nucleoid-associated proteins on bacterial chromosome structure and gene expression. Curr Opin Microbiol. 2010;13: 773–780.

157. Haselkorn R, Rouviere-Yaniv J. Cyanobacterial DNA-binding protein related to *Escherichia coli* HU. Proc Natl Acad Sci U S A. 1976;73: 1917–1920.

158. Oberto J, Drlica K, Rouviere-Yaniv J. Histones, HMG, HU, IHF: Meme combat. Biochimie. 1994;76: 901–908.

159. Guo F, Adhya S. Spiral structure of *Escherichia coli* HUalphabeta provides foundation for DNA supercoiling. Proc Natl Acad Sci U S A. 2007;104: 4309–4314.

160. Claret L, Rouviere-Yaniv J. Variation in HU composition during growth of *Escherichia coli*: the heterodimer is required for long term survival. J Mol Biol. 1997;273: 93–104.

161. Giangrossi M, Giuliodori AM, Gualerzi CO, Pon CL. Selective expression of the beta-subunit of nucleoid-associated protein HU during cold shock in *Escherichia coli*. Mol Microbiol. 2002;44: 205–216.

162. Huisman O, Faelen M, Girard D, Jaffe A, Toussaint A, Rouviere-Yaniv J. Multiple defects in *Escherichia coli* mutants lacking HU protein. J Bacteriol. 1989;171: 3704–3712.

163. Mangan MW, Lucchini S, T OC, Fitzgerald S, Hinton JCD, Dorman CJ, *et al*. Nucleoid-associated protein HU controls three regulons that coordinate virulence, response to stress and general physiology in *Salmonella enterica* serovar Typhimurium. Microbiology. 2011;157: 1075–1087.

164. Fernandez S, Rojo F, Alonso JC. The *Bacillus subtilis* chromatin-associated protein Hbsu is involved in DNA repair and recombination. Mol Microbiol. 1997;23: 1169–1179.

165. Pinson V, Takahashi M, Rouviere-Yaniv J. Differential binding of the *Escherichia coli* HU, homodimeric forms and heterodimeric form to linear, gapped and cruciform DNA. J Mol Biol. 1999;287: 485–497.

166. Krylov AS, Zasedateleva OA, Prokopenko D V, Rouviere-Yaniv J, Mirzabekov AD. Massive parallel analysis of the binding specificity of histone-like protein HU to single- and double-stranded DNA with generic oligodeoxyribonucleotide microchips. Nucleic Acids Res. 2001;29: 2654–2660.

167. Prieto AI, Kahramanoglou C, Ali RM, Fraser GM, Seshasayee ASN, Luscombe NM. Genomic analysis of DNA binding and gene regulation by homologous nucleoid-associated proteins IHF and HU in *Escherichia coli* K12. Nucleic Acids Res. 2012;40: 3524–3537.

168. Pontiggia A, Negri A, Beltrame M, Bianchi ME. Protein HU binds specifically to kinked DNA. Mol Microbiol. 1993;7: 343–350.

169. Bianchi ME. Prokaryotic HU and eukaryotic HMG1: a kinked relationship. Mol Microbiol. 1994;14: 1–5.

170. Nash HA. The HU and IHF Proteins: Accessory Factors for Complex Protein-DNA Assemblies. In: Lin, E.C.C., Lynch AS, editor. Regulation of Gene Expression in *Escherichia coli*. Springer; 1996. pp. 149–179.

171. Kamashev D, Balandina A, Rouviere-Yaniv J. The binding motif recognized by HU on both nicked and cruciform DNA. EMBO J. 1999;18: 5434–5444.

172. Boubrik F, Rouviere-Yaniv J. Increased sensitivity to gamma irradiation in bacteria lacking protein HU. Proc Natl Acad Sci U S A. 1995;92: 3958–3962.

173. Li S, Waters R. *Escherichia coli* strains lacking protein HU are UV sensitive due to a role for HU in homologous recombination. J Bacteriol. 1998;180: 3750–3756.

174. Hashimoto M, Imhoff B, Ali MM, Kow YW. HU protein of *Escherichia coli* has a role in the repair of closely opposed lesions in DNA. J Biol Chem. 2003;278: 28501–28507.

175. Drlica K, Rouviere-Yaniv J. Histonelike proteins of bacteria. Microbiol Rev. 1987;51: 301–319.

176. Dillon SC, Dorman CJ. Bacterial nucleoid-associated proteins, nucleoid structure and gene expression. Nat Rev Microbiol. 2010;8: 185–195.

177. Broyles SS, Pettijohn DE. Interaction of the *Escherichia coli* HU protein with DNA. Evidence for formation of nucleosome-like structures with altered DNA helical pitch. J Mol Biol. 1986;187: 47–60.

178. Seong GH, Kobatake E, Miura K, Nakazawa A, Aizawa M. Direct atomic force microscopy visualization of integration host factor-induced DNA bending structure of the promoter regulatory region on the Pseudomonas TOL plasmid. Biochem Biophys Res Commun. 2002;291: 361–366.

179. Lia G, Bensimon D, Croquette V, Allemand JF, Dunlap D, Lewis DE, *et al*. Supercoiling and denaturation in Gal repressor/heat unstable nucleoid protein (HU)-mediated DNA looping. Proc Natl Acad Sci U S A. 2003;100: 11373–11377.

180. Dame RT, Goosen N. HU: promoting or counteracting DNA compaction? FEBS Lett. 2002;529: 151–156.

181. Wojtuszewski K, Hawkins ME, Cole JL, Mukerji I. HU binding to DNA: evidence for multiple complex formation and DNA bending. Biochemistry. 2001;40: 2588–2598.

182. Wojtuszewski K, Mukerji I. HU binding to bent DNA: a fluorescence resonance energy transfer and anisotropy study. Biochemistry. 2003;42: 3096–3104.

183. Swinger KK, Rice PA. IHF and HU: flexible architects of bent DNA. Curr Opin Struct Biol. 2004;14: 28–35.

184. Oberto J, Nabti S, Jooste V, Mignot H, Rouviere-Yaniv J. The HU regulon is composed of genes responding to anaerobiosis, acid stress, high osmolarity and SOS induction. PLoS One. 2009;4: e4367.

185. Devaraj A, Justice SS, Bakaletz LO, Goodman SD. DNABII proteins play a central role in UPEC biofilm structure. Mol Microbiol. 2015;96: 1119–1135.

186. Semsey S, Geanacopoulos M, Lewis DE a, Adhya S. Operator-bound GalR dimers close DNA loops by direct interaction: tetramerization and inducer binding. EMBO J. 2002;21: 4349–4356.

187. Kar S, Adhya S. Recruitment of HU by piggyback: a special role of GalR in repressosome assembly. Genes Dev. 2001;15: 2273–2281.

188. Aki T, Adhya S. Repressor induced site-specific binding of HU for transcriptional regulation. EMBO J. 1997;16: 3666–3674.

189. Shapiro L. Differentiation in the *Caulobacter* cell cycle. Annu Rev Microbiol. 1976;30: 377–407.

190. Kaiser D. Control of multicellular development: *Dictyostelium* and *Myxococcus*. Annu Rev Genet. 1986;20: 539–566.

191. Stragier P, Losick R. Molecular genetics of sporulation in *Bacillus subtilis*. Annu Rev Genet. 1996;30: 241–297.

192. Andrewes FW. Studies in group agglutination. I. *Salmonella* group and its antigenic structure. . J Path Bact. 1922; 505–525.

193. Legroux R, Magrou J. Etat organizé des colonies bactériennes. Ann Inst Pasteur (Paris). 1920;34: 417–433.

194. Shapiro JA, Higgins NP. Differential activity of a transposable element in *Escherichia coli* colonies. J Bacteriol. 1989;171: 5975–5986.

195. Shapiro JA. Thinking about bacterial populations as multicellular organisms. Annu Rev Microbiol. 1998;52: 81–104.

196. Zgur-Bertok D. Phenotypic heterogeneity in bacterial populations. Acta Agric Slov. 2007; 17–24.

197. Dhar N, McKinney JD. Microbial phenotypic heterogeneity and antibiotic tolerance. Curr Opin Microbiol. 2007;10: 30–38.

198. Davidson CJ, Surette MG. Individuality in bacteria. Annu Rev Genet. 2008;42: 253–268.

199. Veening J-WW, Smits WK, Kuipers OP. Bistability, epigenetics, and bet-hedging in bacteria. Annu Rev Microbiol. 2008;62: 193–210.

200. Casadesús J, Low DA. Programmed heterogeneity: epigenetic mechanisms in bacteria. J Biol Chem. 2013;288: 13929–13935.

201. Thattai M, van Oudenaarden A. Stochastic gene expression in fluctuating environments. Genetics. 2004;167: 523–530.

202. Kussell E, Leibler S. Phenotypic diversity, population growth, and information in fluctuating environments. Science (80-). 2005;309: 2075–2078.

203. Wolf DM, Vazirani V V, Arkin AP. Diversity in times of adversity: probabilistic strategies in microbial survival games. J Theor Biol. 2005;234: 227–253.

204. Ni M, Decrulle AL, Fontaine F, Demarez A, Taddei F, Lindner AB. Predisposition and epigenetics govern variation in bacterial survival upon stress. PLoS Genet. 2012;8: e1003148.

205. Sánchez-Romero MA, Casadesús J. Contribution of phenotypic heterogeneity to adaptive antibiotic resistance. Proc Natl Acad Sci U S A. 2014;111: 355–360.

206. Ackermann M. Microbial individuality in the natural environment. ISME J. Nature Publishing Group; 2013;7: 465–467.

207. Lambert G, Kussell E. Memory and fitness optimization of bacteria under fluctuating environments. PLoS Genet. 2014;10: e1004556.

208. Silverman M, Zieg J, Hilmen M, Simon M. Phase variation in *Salmonella*: genetic analysis of a recombinational switch. Proc Natl Acad Sci U S A. 1979;76: 391–395.

209. Moxon ER, Rainey PB, Nowak MA, Lenski RE. Adaptive evolution of highly mutable loci in pathogenic bacteria. Curr Biol. 1994;4: 24–33.

210. Moxon R, Bayliss C, Hood D. Bacterial contingency loci: the role of simple sequence DNA repeats in bacterial adaptation. Annu Rev Genet. 2006;40: 307–333.

211. Dubnau D, Losick R. Bistability in bacteria. Mol Microbiol. 2006;61: 564–572.

212. Elowitz MB, Levine AJ, Siggia ED, Swain PS. Stochastic gene expression in a single cell. Science (80-). 2002;297: 1183–1186.

213. Ozbudak EM, Thattai M, Kurtser I, Grossman AD, van Oudenaarden A. Regulation of noise in the expression of a single gene. Nat Genet. 2002;31: 69–73.

214. Swain PS, Elowitz MB, Siggia ED. Intrinsic and extrinsic contributions to stochasticity in gene expression. Proc Natl Acad Sci U S A. 2002;99: 12795–12800.

215. Smits WK, Kuipers OP, Veening J-WW. Phenotypic variation in bacteria: the role of feedback regulation. Nat Rev Microbiol. 2006;4: 259–271.

216. Hernday A, Krabbe M, Braaten B, Low D. Self-perpetuating epigenetic pili switches in bacteria. Proc Natl Acad Sci U S A. 2002;99 Suppl 4: 16470–16476.

217. Woude MW Van Der, Bäumler AJ. Phase and Antigenic Variation in Bacteria. Clin Microbiol Rev. 2004;17: 581–611.

218. Van der Woude MW. Re-examining the role and random nature of phase variation. FEMS Microbiol Lett. 2006;254: 190–197.

219. Kim M, Ryu S. Spontaneous and transient defence against bacteriophage by phase-variable glucosylation of O-antigen in *Salmonella enterica* serovar Typhimurium. Mol Microbiol. 2012;86: 411–425.

220. Zaleski P, Wojciechowski M, Piekarowicz A. The role of Dam methylation in phase variation of *Haemophilus influenzae* genes involved in defence against phage infection. Microbiology. 2005;151: 3361–3369.

221. Srikhanta YN, Maguire TL, Stacey KJ, Grimmond SM, Jennings MP. The phasevarion: a genetic system controlling coordinated, random switching of expression of multiple genes. Proc Natl Acad Sci U S A. 2005;102: 5547–5551.

222. Hoskisson PA, Smith MC. Hypervariation and phase variation in the bacteriophage "resistome". Curr Opin Microbiol. 2007;10: 396–400.

223. Sanchez-Romero MA, Cota I, Casadesus J. DNA methylation in bacteria: from the methyl group to the methylome. Curr Opin Microbiol. 2015;25: 9–16.

224. Hernday A, Braaten B, Low D. The intricate workings of a bacterial epigenetic switch. Adv Exp Med Biol. 2004;547: 83–89.

225. Blyn LB, Braaten BA, Low DA. Regulation of *pap* pilin phase variation by a mechanism involving differential Dam methylation states. EMBO J. 1990;9: 4045–4054.

226. Kaltenbach LS, Braaten BA, Low DA. Specific binding of PapI to Lrp-*pap* DNA complexes. J Bacteriol. 1995;177: 6449–6455.

227. Forsman K, Goransson M, Uhlin BE. Autoregulation and multiple DNA interactions by a transcriptional regulatory protein in *E. coli* pili biogenesis. EMBO J. 1989;8: 1271–1277.

228. Xia Y, Forsman K, Jass J, Uhlin BE. Oligomeric interaction of the PapB transcriptional regulator with the upstream activating region of pili adhesin gene promoters in *Escherichia coli*. Mol Microbiol. 1998;30: 513–523.

229. Dautin N, Bernstein HD. Protein secretion in gram-negative bacteria via the autotransporter pathway. Annu Rev Microbiol. 2007;61: 89–112.

230. Diderichsen B. *flu*, a metastable gene controlling surface properties of *Escherichia coli*. J Bacteriol. 1980;141: 858–867.

231. Danese PN, Pratt LA, Dove SL, Kolter R. The outer membrane protein, antigen 43, mediates cell-to-cell interactions within *Escherichia coli* biofilms. Mol Microbiol. 2000;37: 424–432.

232. Zalewska-Piatek B, Zalewska-Piatek R, Olszewski M, Kur J. Identification of antigen Ag43 in uropathogenic *Escherichia coli* Dr+ strains and defining its role in the pathogenesis of urinary tract infections. Microbiology. 2015;161: 1034–1049.

233. Ulett GC, Valle J, Beloin C, Sherlock O, Ghigo JM, Schembri MA. Functional analysis of antigen 43 in uropathogenic *Escherichia coli* reveals a role in long-term persistence in the urinary tract. Infect Immun. 2007;75: 3233–3244.

234. Lüthje P, Brauner A. Ag43 promotes persistence of uropathogenic *Escherichia coli* isolates in the urinary tract. J Clin Microbiol. 2010;48: 2316–2317.

235. Fexby S, Bjarnsholt T, Jensen PO, Roos V, Hoiby N, Givskov M, *et al*. Biological Trojan horse: Antigen 43 provides specific bacterial uptake and survival in human neutrophils. Infect Immun. 2007;75: 30–34.

236. Henderson IR, Meehan M, Owen P. Antigen 43, a phase-variable bipartite outer membrane protein denermines colony morphology and antoaggregation in *E. coli* k12.pdf. 1997;149.

237. Henderson IR, Owen P. The major phase-variable outer membrane protein of *Escherichia coli* structurally resembles the immunoglobulin A1 protease class of exported protein and is regulated by a novel mechanism involving Dam and OxyR. J Bacteriol. 1999;181: 2132–2141.

238. Wallecha A, Munster V, Correnti J, Chan T, van der Woude M. Dam- and OxyR-dependent phase variation of *agn43*: essential elements and evidence for a new role of DNA methylation. J Bacteriol. 2002;184: 3338–3347.

239. Haagmans W, Van Der Woude M. Phase variation of Ag43 in *Escherichia coli*: Dam-dependent methylation abrogates OxyR binding and OxyR-mediated repression of transcription. Mol Microbiol. 2000;35: 877–887.

240. Waldron DE, Owen P, Dorman CJ. Competitive interaction of the OxyR DNA-binding protein and the Dam methylase at the antigen 43 gene regulatory region in *Escherichia coli*. Mol Microbiol. 2002;44: 509–520.

241. Van der Woude MW, Henderson IR. Regulation and function of Ag43 (*flu*). Annu Rev Microbiol. 2008;62: 153–169.

242. Henderson IR, Owen P, Nataro JP. Molecular switches--the ON and OFF of bacterial phase variation. Mol Microbiol. 1999;33: 919–932.

243. Kaminska R, Van Der Woude MW. Establishing and maintaining sequestration of Dam target sites for phase variation of *agn43* in *Escherichia coli*. J Bacteriol. 2010;192: 1937–1945.

244. Bogomolnaya LM, Santiviago C a., Yang HJ, Baumler AJ, Andrews-Polymenis HL. “Form variation” of the O12 antigen is critical for persistence of *Salmonella* Typhimurium in the murine intestine. Mol Microbiol. 2008;70: 1105–1119.

245. Villafane R, Zayas M, Gilcrease EB, Kropinski AM, Casjens SR. Genomic analysis of bacteriophage epsilon 34 of *Salmonella enterica* serovar Anatum (15+). BMC Microbiol. 2008;8: 227.

246. Davies MR, Broadbent SE, Harris SR, Thomson NR, van der Woude MW. Horizontally acquired glycosyltransferase operons drive salmonellae lipopolysaccharide diversity. PLoS Genet. 2013;9: e1003568.

247. Allison GE, Verma NK. Serotype-converting bacteriophages and O-antigen modification in *Shigella flexneri*. Trends Microbiol. 2000;8: 17–23.

248. Fukazawa Y, Hartman PE. A P22 Bacteriophage Mutant Defective in Antigen Conversion. Virology. 1964;23: 279–283.

249. Fauquet CM, Mayo MA, Maniloff J, Desselberger U, Ball LA. Virus Taxonomy, Eighth Report of the International Committee on Taxonomy of Viruses. London, UK: Elsevier/Academic Press; 2005.

250. Ackermann HW. Classification of bacteriophages. In: Calendar R, editor. The Bacteriophages. New York, USA: Oxford University Press; 2006. pp. 8–16.

251. Bergh O, Borsheim KY, Bratbak G, Heldal M. High abundance of viruses found in aquatic environments. Nature. 1989;340: 467–468.

252. Fuhrman JA. Marine viruses and their biogeochemical and ecological effects. Nature. 1999;399: 541–548.

253. Wommack KE, Colwell RR. Virioplankton: viruses in aquatic ecosystems. Microbiol Mol Biol Rev. 2000;64: 69–114.

254. Hambly E, Suttle CA. The viriosphere, diversity, and genetic exchange within phage communities. Curr Opin Microbiol. 2005;8: 444–450.

255. Bohannan BJM, Lenski RE. Linking genetic change to community evolution: insights from studies of bacteria and bacteriophage. Ecol Lett. 2000;3: 362–377.

256. Joo J, Gunny M, Cases M, Hudson P, Albert R, Harvill E. Bacteriophage-mediated competition in *Bordetella* bacteria. Proc Biol Sci. 2006;273: 1843–1848.

257. Buckling A, Rainey PB. The role of parasites in sympatric and allopatric host diversification. Nature. 2002;420: 496–499.

258. Harcombe WR, Bull JJ. Impact of phages on two-species bacterial communities. Appl Env Microbiol. 2005;71: 5254–5259.

259. Kidambi SP, Ripp S, Miller R V. Evidence for phage-mediated gene transfer among *Pseudomonas aeruginosa* strains on the phylloplane. Appl Env Microbiol. 1994;60: 496–500.

260. Canchaya C, Fournous G, Chibani-Chennoufi S, Dillmann ML, Brussow H. Phage as agents of lateral gene transfer. Curr Opin Microbiol. 2003;6: 417–424.

261. TF T, Lignell R. Theoretical models for the control of bacterial growth rate, abundance, diversity and carbon demand . Aquat Microb Ecol. 1997;13: 19–27.

262. Chaturongakul S, Ounjai P. Phage-host interplay: examples from tailed phages and Gram-negative bacteria. 2014;5: 1–8.

263. Hendrix RW. Evolution: the long evolutionary reach of viruses. Curr Biol. 1999;9: R914–7.

264. Stern A, Sorek R. The phage-host arms race: shaping the evolution of microbes. Bioessays. 2011;33: 43–51.

265. Braun V, Hantke K. Bacterial receptors for phages and colicins as constituents of specific transport systems. Microb Interact Recept Recognition. 1997;3: 101–137.

266. Israel V, Rosen H, Levine M. Binding of bacteriophage P22 tail parts to cells. J Virol. 1972;10: 1152–1158.

267. Kruger DH, Schroeder C. Bacteriophage T3 and bacteriophage T7 virus-host cell interactions. Microbiol Rev. 1981;45: 9–51.

268. Chang JT, Schmid MF, Haase-Pettingell C, Weigele PR, King JA, Chiu W. Visualizing the structural changes of bacteriophage Epsilon15 and its *Salmonella* host during infection. J Mol Biol. 2010;402: 731–740.

269. Shin H, Lee JH, Lim JA, Kim H, Ryu S. Complete genome sequence of *Salmonella enterica* serovar Typhimurium bacteriophage SPN1S. J Virol. 2012;86: 1284–1285.

270. Kagawa H, Ono N, Enomoto M, Komeda Y. Bacteriophage chi sensitivity and motility of *Escherichia coli* K-12 and *Salmonella* typhimurium Fla- mutants possessing the hook structure. J Bacteriol. 1984;157: 649–654.

271. Shin H, Lee JH, Kim H, Choi Y, Heu S, Ryu S. Receptor diversity and host interaction of bacteriophages infecting *Salmonella enterica* serovar Typhimurium. PLoS One. 2012;7: e43392.

272. Choi Y, Shin H, Lee JH, Ryu S. Identification and characterization of a novel flagellum-dependent *Salmonella*-infecting bacteriophage, iEPS5. Appl Env Microbiol. 2013;79: 4829–4837.

273. Hong J, Kim KP, Heu S, Lee SJ, Adhya S, Ryu S. Identification of host receptor and receptor-binding module of a newly sequenced T5-like phage EPS7. FEMS Microbiol Lett. 2008;289: 202–209.

274. Kim M, Ryu S. Characterization of a T5-like coliphage, SPC35, and differential development of resistance to SPC35 in *Salmonella enterica* serovar Typhimurium and *Escherichia coli*. Appl Env Microbiol. 2011;77: 2042–2050.

275. Ho TD, Slauch JM. OmpC is the receptor for Gifsy-1 and Gifsy-2 bacteriophages of *Salmonella*. J Bacteriol. 2001;183: 1495–1498.

276. Marti R, Zurfluh K, Hagens S, Pianezzi J, Klumpp J, Loessner MJ. Long tail fibres of the novel broad-host-range T-even bacteriophage S16 specifically recognize *Salmonella* OmpC. Mol Microbiol. 2013;87: 818–834.

277. Ricci V, Piddock LJ. Exploiting the role of TolC in pathogenicity: identification of a bacteriophage for eradication of *Salmonella* serovars from poultry. Appl Env Microbiol. 2010;76: 1704–1706.

278. Casjens SR, Gilcrease EB, Winn-Stapley DA, Schicklmaier P, Schmieger H, Pedulla ML, *et al*. The generalized transducing *Salmonella* bacteriophage ES18: complete genome sequence and DNA packaging strategy. J Bacteriol. 2005;187: 1091–1104.

279. Pickard D, Toribio AL, Petty NK, van Tonder A, Yu L, Goulding D, *et al*. A conserved acetyl esterase domain targets diverse bacteriophages to the Vi capsular receptor of *Salmonella enterica* serovar Typhi. J Bacteriol. 2010;192: 5746–5754.

280. Andres D, Roske Y, Doering C, Heinemann U, Seckler R, Barbirz S. Tail morphology controls DNA release in two *Salmonella* phages with one lipopolysaccharide receptor recognition system. Mol Microbiol. 2012;83: 1244–1253.

281. Sun S, Rao VB, Rossmann MG. Genome packaging in viruses. Curr Opin Struct Biol. 2010;20: 114–120.

282. Herskowitz I, Hagen D. The lysis-lysogeny decision of phage lambda: explicit programming and responsiveness. Annu Rev Genet. 1980;14: 399–445.

283. Wikipedia contributors. Caudovirales [Internet]. Wikipedia, The Free Encyclopedia. 2015.

284. Grose JH, Casjens SR. Understanding the enormous diversity of bacteriophages: the tailed phages that infect the bacterial family Enterobacteriaceae. Virology. Elsevier; 2014;468-470: 421–443.

285. Lawrence JG, Hatfull GF, Hendrix RW. Imbroglios of viral taxonomy: genetic exchange and failings of phenetic approaches. J Bacteriol. 2002;184: 4891–4905.

286. Casjens SR. Comparative genomics and evolution of the tailed-bacteriophages. Curr Opin Microbiol. 2005;8: 451–458.

287. Smith HO, Levine M. Two Sequential Repressions of DNA Synthesis in the Establishment of Lysogeny by Phage P22 and Its Mutants. Proc Natl Acad Sci U S A. 1964;52: 356–363.

288. Casjens SR, Leavitt JC, Hatfull GF, Hendrix W, Hendrix RW. Genome Sequence of *Salmonella* Phage 9NA. Genome Announc. 2014;2: 2009–2010.

289. Casjens SR, Jacobs-Sera D, Hatfull GF, Hendrix RW, Hendrix W. Genome Sequence of *Salmonella enterica* Phage Det7. Genome Announc. 2015;3: 2046.

290. Adriaenssens EM, Ackermann HW, Anany H, Blasdel B, Connerton IF, Goulding D, *et al*. A suggested new bacteriophage genus: "Viunalikevirus." Arch Virol. 2012;157: 2035–2046.

291. Labrie SJ, Samson JE, Moineau S. Bacteriophage resistance mechanisms. Nat Rev Microbiol. 2010;8: 317–327.

292. Heller KJ. Molecular interaction between bacteriophage and the gram-negative cell envelope. Arch Microbiol. 1992;158: 235–248.

293. Buckling A, Wei Y, Massey RC, Brockhurst MA, Hochberg ME. Antagonistic coevolution with parasites increases the cost of host deleterious mutations. Proc Biol Sci. 2006;273: 45–49.

294. Middelboe M, Holmfeldt K, Riemann L, Nybroe O, Haaber J. Bacteriophages drive strain diversification in a marine *Flavobacterium*: implications for phage resistance and physiological properties. Env Microbiol. 2009;11: 1971–1982.

295. Brockhurst MA, Buckling A, Rainey PB. The effect of a bacteriophage on diversification of the opportunistic bacterial pathogen, *Pseudomonas aeruginosa*. Proc Biol Sci. 2005;272: 1385–1391.

296. Avrani S, Wurtzel O, Sharon I, Sorek R, Lindell D. Genomic island variability facilitates Prochlorococcus-virus coexistence. Nature. 2011;474: 604–608.

297. Filippov AA, Sergueev K V., He Y, Huang XZ, Gnade BT, Mueller AJ, *et al*. Bacteriophage-resistant mutants in *Yersinia pestis*: identification of phage receptors and attenuation for mice. PLoS One. 2011;6: e25486.

298. León M, Bastías R. Virulence reduction in bacteriophage resistant bacteria. Front Microbiol. 2015;06: 1–7.

299. Sumby P, Smith MCM. Phase variation in the phage growth limitation system of *Streptomyces coelicolor* A3(2). J Bacteriol. 2003;185: 4558–63.

300. Balbontín R, Rowley G, Pucciarelli MG, López-Garrido J, Wormstone Y, Lucchini S, *et al*. DNA adenine methylation regulates virulence gene expression in *Salmonella enterica* serovar Typhimurium. J Bacteriol. 2006;188: 8160–8168.

301. Chan RK, Botstein D, Watanabe T, Ogata Y. Specialized transduction of tetracycline resistance by phage P22 in *Salmonella typhimurium*. II. Properties of a high-frequency-transducing lysate. Virology. 1972;50: 883–98.

302. Torreblanca J, Marqués S, Casadesus J. Synthesis of FinP RNA by plasmids F and pSLT is regulated by DNA adenine methylation. Genetics. 1999;152: 31–45.

303. Datsenko KA, Wanner BL. One-step inactivation of chromosomal genes in *Escherichia coli* K-12 using PCR products. Proc Natl Acad Sci U S A. 2000;97: 6640–6645.

304. Ellermeier CD, Janakiraman A, Slauch JM. Construction of targeted single copy *lac* fusions using λ Red and FLP-mediated site-specific recombination in bacteria. Gene. 2002;290: 153–161.

305. Uzzau S, Figueroa-Bossi N, Rubino S, Bossi L. Epitope tagging of chromosomal genes in *Salmonella*. Proc Natl Acad Sci U S A. 2001;98: 15264–15269.

306. Lee DJ, Bingle LEH, Heurlier K, Pallen MJ, Penn CW, Busby SJW, *et al*. Gene doctoring: a method for recombineering in laboratory and pathogenic Escherichia coli strains. BMC Microbiol. 2009;9: 252.

307. HHautefort I, Proenca MJ, Jose M, Hinton JCD. Single-Copy Green Fluorescent Protein Gene Fusions Allow Accurate Measurement of *Salmonella* gene expression *in vitro* and during infection of mammalian cells . Appl Environ Microbiol. 2003 Dec;69(12):7480-91

308. Schmieger H. Phage P22-mutants with increased or decreased transduction abilities. MGG Mol Gen Genet. 1972;119: 75–88.

309. Garzon A, Cano DA, Casadesus J. Role of Erf recombinase in P22-mediated plasmid transduction. Genetics. 1995;140: 427–434.

310. Marinus MG, Poteete A, Arraj JA. Correlation of DNA adenine methylase activity with spontaneous mutability in *Escherichia coli* K-12. Gene. 1984;28: 123–125.

311. Wilkinson RG, Gemski P, Stocker BA. Non-smooth mutants of *Salmonella typhimurium*: differentiation by phage sensitivity and genetic mapping. J Gen Microbiol. 1972;70: 527–54.

312. Miller JH. Experiments in molecular genetics. Cold Spring Harbor Laboratory; 1972.

313. Pucciarelli MG, Prieto AI, Casadesús J, García-del Portillo F. Envelope instability in DNA adenine methylase mutants of *Salmonella enterica*. Microbiology. 2002;148: 1171–1182.

314. Marques S, Ramos JL, Timmis KN. Analysis of the mRNA structure of the *Pseudomonas putida* TOL meta fission pathway operon around the transcription initiation point, the *xylTE* and the *xylFJ* regions. Biochim Biophys Acta - Gene Struct Expr. 1993;1216: 227–236.

315. Gabig M, Herman-Antosiewicz A, Kwiatkowska M, Los M, Thomas MS, Węgrzyn G. The cell surface protein Ag43 facilitates phage infection of *Escherichia coli* in the presence of bile salts and carborhydrates. Microbiology. 2002;148: 1533–1542.

316. Buendía-Clavería AM, Moussaid A, Ollero FJ, Vinardell JM, Torres A, Moreno J, *et al*. A *purL* mutant of *Sinorhizobium fredii* HH103 is symbiotically defective and altered in its lipopolysaccharide. Microbiology. 2003;149: 1807–1818.

317. Eisenstein 1981 - Phase variation of type 1 fimbriae in *Escherichia coli* is under transcriptional control.

318. Rang C, Alix E, Felix C, Heitz A, Tasse L, Blanc-Potard AB. Dual role of the MgtC virulence factor in host and non-host environments. Mol Microbiol. 2007;63: 605–622.

319. Karimova G, Pidoux J, Ullmann A, Ladant D. A bacterial two-hybrid system based on a reconstituted signal transduction pathway. Proc Natl Acad Sci U S A. 1998;95: 5752–5756.

320. Beuzón CR, Holden DW. Use of mixed infections with *Salmonella* strains to study virulence genes and their interactions in vivo. Microbes Infect. 3: 1345–52.

321. Segura I, Casadesús J, Ramos-Morales F. Use of mixed infections to study cell invasion and intracellular proliferation of *Salmonella enterica* in eukaryotic cell cultures. J Microbiol Methods. 2004;56: 83–91.

322. Dillon SC, Espinosa E, Hokamp K, Ussery DW, Casadesús J, Dorman CJ. LeuO is a global regulator of gene expression in *Salmonella enterica* serovar Typhimurium. Mol Microbiol. 2012;85: 1072–1089.

323. Cameron ADS, Dorman CJ. A fundamental regulatory mechanism operating through OmpR and DNA topology controls expression of *Salmonella* pathogenicity islands SPI-1 and SPI-2. PLoS Genet. 2012;8: e1002615.

324. Liu JY, Miller PF, Willard J, Olson ER. Membranes and Bioenergetics : Functional and Biochemical Characterization of *Escherichia coli* Sugar Efflux Transporters Functional and Biochemical Characterization of Escherichia coli Sugar Efflux Transporters. 1999.

325. Altschul S, Madden T, Schaffer A, Zhang J, Zhang Z, Miller W, *et al*. Gapped BLAST and PSI- BLAST: a new generation of protein database search programs. Nucleic acids Res. 1997;25: 3389–3402.

326. Navarre WW, Porwollik S, Wang Y, McClelland M, Rosen H, Libby SJ, *et al*. Selective silencing of foreign DNA with low GC content by the H-NS protein in *Salmonella*. Science. 2006;313: 236–238.

327. Médigue C, Rouxel T, Vigier P, Hénaut A, Danchin A. Evidence for horizontal gene transfer in *Escherichia coli* speciation. J Mol Biol. 1991;222: 851–856.

328. Daubin V, Ochman H. Start-up entities in the origin of new genes. Curr Opin Genet Dev. 2004;14: 616–619.

329. Krogh a, Larsson B, von Heijne G, Sonnhammer EL. Predicting transmembrane protein topology with a hidden Markov model: application to complete genomes. J Mol Biol. 2001;305: 567–580.

330. Marchler-Bauer A, Lu S, Anderson JB, Chitsaz F, Derbyshire MK, DeWeese-Scott C, *et al*. CDD: A Conserved Domain Database for the functional annotation of proteins. Nucleic Acids Res. 2011;39: 225–229.

331. Huerta AM, Collado-Vides J. Sigma70 promoters in *Escherichia coli*: Specific transcription in dense regions of overlapping promoter-like signals. J Mol Biol. 2003;333: 261–278.

332. Rappleye C a., Roth JR. A Tn10 derivative (T-POP) for isolation of insertions with conditional (tetracycline-dependent) phenotypes. J Bacteriol. 1997;179: 5827–5834.

333. Hassett DJ, Alsabbagh E, Parvatiyar K, Howell ML, Wilmott RW, Ochsner U a. A protease-resistant catalase, KatA, released upon cell lysis during stationary phase is essential for aerobic survival of a *Pseudomonas aeruginosa oxyR* mutant at low cell densities. J Bacteriol. 2000;182: 4557–4563.

334. Alix E, Blanc-Potard AB. Hydrophobic peptides: Novel regulators within bacterial membrane. Mol Microbiol. 2009;72: 5–11.

335. Storz G, Wolf YI, Ramamurthi KS. Small Proteins Can No Longer Be Ignored. Annu Rev Biochem. 2014;83: 753–777.

336. Karimova G, Dautin N, Ladant D. Interaction Network among Escherichia coli Membrane Proteins Involved in Cell Division as Revealed by Bacterial Two-Hybrid Analysis Interaction Network among Escherichia coli Membrane Proteins Involved in Cell Division as Revealed by Bacterial Two-Hybrid. J Bacteriol. 2005;187: 2233–2243.

337. Wright A, Kanegasaki S. Molecular aspects of lipopolysaccharides. Physiol Rev. 1971;51: 748–84.

338. Wu T, McCandlish AC, Gronenberg LS, Chng S-S, Silhavy TJ, Kahne D. Identification of a protein complex that assembles lipopolysaccharide in the outer membrane of *Escherichia coli*. Proc Natl Acad Sci U S A. 2006;103: 11754–11759.

339. Peterson a a, McGroarty EJ. High molecular weight components in lipopolysaccharides of *Salmonella typhimurium*, *Salmonella minnesota*, and *Escherichia coli*. J Bact. 1985;162: 738–745.

340. Goldman RC, Hunt F. Mechanism of O-antigen distribution in lipopolysaccharide. J Bacteriol. 1990;172: 5352–9.

341. Daniels C, Morona R. Analysis of *Shigella flexneri* Wzz (Rol) function by mutagenesis and cross-linking: Wzz is able to oligomerize. Mol Microbiol. 1999;34: 181–194.

342. Grossman N, Schmetz M a., Foulds J, Klima EN, Jimenez-Lucho VE, Leive LL, *et al*. Lipopolysaccharide size and distribution determine serum resistance in *Salmonella montevideo*. J Bacteriol. 1987;169: 856–863.

343. Ciurana B, Tomas JM. Role of lipopolysaccharide and complement in susceptibility of *Klebsiella pneumoniae* to nonimmune serum. Infect Immun. 1987;55: 2741–2746.

344. Bravo D, Silva C, Carter J a., Hoare A, Álvarez S a., Blondel CJ, *et al*. Growth-phase regulation of lipopolysaccharide O-antigen chain length influences serum resistance in serovars of *Salmonella*. J Med Microbiol. 2008;57: 938–946.

345. Pescaretti MDLM, López FE, Morero RD, Delgado MA. The PmrA/PmrB regulatory system controls the expression of the *wzz*fepE gene involved in the O-antigen synthesis of *Salmonella enterica* serovar Typhimurium. Microbiology. 2011;157: 2515–2521.

346. Camacho EM, Casadesús J. Conjugal transfer of the virulence plasmid of *Salmonella enterica* is regulated by the leucine-responsive regulatory protein and DNA adenine methylation. Mol Microbiol. 2002;44: 1589–98.

347. Wang JC. Helical repeat of DNA in solution. Proc Natl Acad Sci U S A. 1979;76: 200–3.

348. Lilja AE, Jenssen JR, Kahn JD. Geometric and dynamic requirements for DNA looping, wrapping and unwrapping in the activation of E. coli *glnA*p2 transcription by NtrC. J Mol Biol. 2004;342: 467–478.

349. Iwig JS, Chivers PT. DNA Recognition and Wrapping by *Escherichia coli* RcnR. J Mol Biol. Elsevier Ltd; 2009;393: 514–526.

350. Tucker NP, Ghosh T, Bush M, Zhang X, Dixon R. Essential roles of three enhancer sites in σ54-dependent transcription by the nitric oxide sensing regulatory protein NorR. Nucleic Acids Res. 2009;38: 1182–1194.

351. Bush M, Ghosh T, Tucker N, Zhang X, Dixon R. Transcriptional regulation by the dedicated nitric oxide sensor, NorR: a route towards NO detoxification. Biochem Soc Trans. 2011;39: 289–293.

352. Flusberg BA, Webster DR, Lee JH, Travers KJ, Olivares EC, Clark TA, *et al*. Direct detection of DNA methylation during single-molecule, real-time sequencing. Nat Methods. 2010;7: 461–5.

353. Van Der Woude M, Braaten B, Low D. Epigenetic phase variation of the *pap* operon in Escherichia coli. Trends Microbiol. 1996;4: 5–9.

354. Waldminghaus T, Skarstad K. The *Escherichia coli* SeqA protein. Plasmid. Elsevier Inc.; 2009;61: 141–150.

355. Dorman CJ. Genome architecture and global gene regulation in bacteria: making progress towards a unified model? Nat Rev Microbiol. 2013;11: 349–55.

356. Ghosh AS, Young KD. Helical Disposition of Proteins and Lipopolysaccharide in the Outer Membrane of *Escherichia coli* Helical Disposition of Proteins and Lipopolysaccharide in the Outer Membrane of *Escherichia coli*. 2005;187.

357. Taylor 2013 - The D3 bacteriophage α-Polymerase inhibitor (Iap) peptide disrupts O-antigen biosynthesis through mimicry of the chain length regulator Wzz in *P. aeruginosa*.

358. Dawson JP, Weinger JS, Engelman DM. Motifs of serine and threonine can drive association of transmembrane helices. J Mol Biol. 2002;316: 799–805.

359. Senes A, Engel DE, Degrado WF. Folding of helical membrane proteins: The role of polar, GxxxG-like and proline motifs. Curr Opin Struct Biol. 2004;14: 465–479.

360. Walters RFS, DeGrado WF. Helix-packing motifs in membrane proteins. Proc Natl Acad Sci U S A. 2006;103: 13658–13663.

361. Nou X, Braaten B, Kaltenbach L, Low D a. Differential binding of Lrp to two sets of pap DNA binding sites mediated by Pap I regulates Pap phase variation in *Escherichia coli*. EMBO J. 1995;14: 5785–5797.

362. Holden NJ, Uhlin BE, Gally DL. PapB paralogues and their effect on the phase variation of type 1 fimbriae in *Escherichia coli*. Mol Microbiol. 2001;42: 319–330.

363. Båga M, Göransson M, Normark S, Uhlin BE. Transcriptional activation of a *pap* pilus virulence operon from uropathogenic *Escherichia coli*. EMBO J. 1985;4: 3887–3893.

364. White-Ziegler CA, Angus Hill ML, Braaten BA, Van Der Woude MW, Low DA. Thermoregulation of *Escherichia coli* pap transcription: H-NS is a temperature-dependent DNA methylation blocking factor. Mol Microbiol. 1998;28: 1121–1137.

365. Hung DL, Raivio TL, Jones CH, Silhavy TJ, Hultgren SJ. Cpx signaling pathway monitors biogenesis and affects assembly and expression of P pili. EMBO J. 2001;20: 1508–1518.

366. Susskind MM, Botstein D. Molecular genetics of bacteriophage P22. Microbiol Rev. 1978;42: 385–413.

367. Whitfield C, Trent MS. Biosynthesis and export of bacterial lipopolysaccharides. Annu Rev Biochem. 2014;83: 99–128.

368. Piao 2010 - Immunological responses induced by *asd* and *wzy asd* mutant strains of *Salmonella enterica* serovar Typhimurium in BALBc mice.pdf.

369. Paixão T a., Roux CM, Den Hartigh AB, Sankaran-Walters S, Dandekar S, Santos RL, *et al*. Establishment of systemic *Brucella melitensis* infection through the digestive tract requires urease, the type IV secretion system, and lipopolysaccharide O antigen. Infect Immun. 2009;77: 4197–4208.

370. Yoon H, Ansong C, Adkins JN, Heffron F. Discovery of *Salmonella* virulence factors translocated via outer membrane vesicles to murine macrophages. Infect Immun. 2011;79: 2182–2192.

371. Williams GC. Natural Selection, the Costs of Reproduction, and a Refinement of Lack's Principle. Am Nat. 1966;100: 687.

372. Nyström T. Growth versus maintenance: a trade-off dictated by RNA polymerase availability and sigma factor competition? Mol Microbiol. 2004;54: 855–62.

373. Shoval O, Sheftel H, Shinar G, Hart Y, Ramote O, Mayo A, *et al*. Evolutionary trade-offs, Pareto optimality, and the geometry of phenotype space. Science. 2012;336: 1157–60.

374. Bailly-Bechet M, Benecke A, Hardt WD, Lanza V, Sturm A, Zecchina R. An externally modulated, noise-driven switch for the regulation of SPI1 in *Salmonella enterica* serovar Typhimurium. J Math Biol. 2011;63: 637–62.

375. Ferenci T, Spira B. Variation in stress responses within a bacterial species and the indirect costs of stress resistance. Ann N Y Acad Sci. 2007;1113: 105–13.

376. Andersson DI, Hughes D. Antibiotic resistance and its cost: is it possible to reverse resistance? Nat Rev Microbiol. 2010;8: 260–71.

377. De Paepe M, Gaboriau-Routhiau V, Rainteau D, Rakotobe S, Taddei F, Cerf-Bensussan N. Trade-off between bile resistance and nutritional competence drives *Escherichia coli* diversification in the mouse gut. PLoS Genet. 2011;7: e1002107.

378. Vincent BM, Lancaster AK, Scherz-Shouval R, Whitesell L, Lindquist S. Fitness trade-offs restrict the evolution of resistance to amphotericin B. PLoS Biol. 2013;11: e1001692.

379. Leon M, Bastias R. Virulence reduction in bacteriophage resistant bacteria. Front Microbiol. 2015;6: 343.

380. Wilson GG, Murray NE. Restriction and modification systems. Annu Rev Genet. 1991;25: 585–627.

381. Zaim J, Kierzek AM. The structure of full-length LysR-type transcriptional regulators. Modeling of the full-length OxyR transcription factor dimer. Nucleic Acids Res. 2003;31: 1444–1454.

382. Tao K, Fujita N, Ishihama A. Involvement of the RNA polymerase alpha subunit C-terminal region in co-operative interaction and transcriptional activation with OxyR protein. Mol Microbiol. 1993;7: 859–64.

383. Hryniewicz MM, Kredich NM. The *cysP* promoter of *Salmonella typhimurium*: characterization of two binding sites for CysB protein, studies of in vivo transcription initiation, and demonstration of the anti-inducer effects of thiosulfate. J Bacteriol. 1991;173: 5876–86.

384. Wang L, Helmann JD, Winans SC. The *A. tumefaciens* transcriptional activator OccR causes a bend at a target promoter, which is partially relaxed by a plant tumor metabolite. Cell. 1992;69: 659–667.

385. Keulen G Van, Ridder ANJ a, Dijkhuizen L, Meijer WG. Analysis of DNA Binding and Transcriptional Activation by the LysR-Type Transcriptional Regulator CbbR of *Xanthobacter flavus* Analysis of DNA Binding and Transcriptional Activation by the LysR-Type Transcriptional Regulator CbbR of *Xanthobacter flavus*. 2003;185: 1245–1252.

386. Lim HN, van Oudenaarden A. A multistep epigenetic switch enables the stable inheritance of DNA methylation states. Nat Genet. 2007;39: 269–275.

387. Charlier D, Hassanzadeh G, Kholti A, Gigot D, Piérard A, Glansdorff N. *carP*, involved in pyrimidine regulation of the *Escherichia coli* carbamoylphosphate synthetase operon encodes a sequence-specific DNA-binding protein identical to XerB and PepA, also required for resolution of ColEI multimers. J Mol Biol. 1995;250: 392–406.

388. Carrera P, Azorín F. Structural characterization of intrinsically curved AT-rich DNA sequences. Nucleic Acids Res. 1994;22: 3671–3680.

389. Hizver J, Rozenberg H, Frolow F, Rabinovich D, Shakked Z. DNA bending by an adenine--thymine tract and its role in gene regulation. Proc Natl Acad Sci U S A. 2001;98: 8490–8495.